**DEPARTMENT OF ELECTRICAL AND COMPUTER ENGINEERING**

# Multi-bacteria, Multi-antibiotic, Testing Using Surface Enhanced Raman Spectroscopy (SERS) for Urinary Tract Infection (UTI) Diagnosis

**DOCTOR OF PHILOSOPHY DISSERTATION**

**KATERINA HADJIGEORGIOU**

**2020**

**DEPARTMENT OF ELECTRICAL AND COMPUTER ENGINEERING**

# Multi-bacteria, Multi-antibiotic, Testing Using Surface Enhanced Raman Spectroscopy (SERS) for Urinary Tract Infection (UTI) Diagnosis

**KATERINA HADJIGEORGIOU**

**A dissertation submitted to the University of Cyprus in partial fulfillment of the requirements for the degree of Doctor of Philosophy**

**May 2020**

# VALIDATION PAGE

## Doctoral Candidate: Katerina Hadjigeorgiou

## Doctoral Dissertation Title: Multi-bacteria, Multi-antibiotic, Testing Using Surface Enhanced Raman Spectroscopy (SERS) for Urinary Tract Infection (UTI) Diagnosis

*The present Doctoral Dissertation was submitted in partial fulfillment of the requirements for the degree of Doctor of Philosophy at the* ***Department of*** *Electrical and Computer Engineering and was approved on the 8th of May 2020, by the members of the* ***Examination Committee.***

**Examination Committee:**

**Research Supervisor:** _____
(Costas Pitris, Professor)

**Committee Member:** _____
(Stavros Iezekiel, Professor)

**Committee Member:** _____
(Chrysafis Andreou, Lecturer)

**Committee Member:** _____
(Constantinos Pattichis, Professor)

**Committee Member:** _____
(Evdokia Kastanos, Professor)

# DECLARATION OF DOCTORAL CANDIDATE

The present doctoral dissertation was submitted in partial fulfillment of the requirements for the degree of Doctor of Philosophy of the University of Cyprus. It is a product of original work of my own, unless otherwise mentioned through references, notes, or any other statements.

Katerina Hadjigeorgiou

……...

# ΠΕΡΙΛΗΨΗ

Ο σκοπός της παρούσας έρευνας ήταν η ανάπτυξη μίας γρήγορης και αξιόπιστης μεθόδου, βασισμένης στην Ενισχυμένη Φασματοσκοπία Ράμαν, η οποία (i) θα προσδιορίζει αν ένα δείγμα είναι "θετικό" ή "αρνητικό" για ουρολοίμωξη, (ii) θα κατηγοριοποιεί τα βακτήρια που βρίσκονται στο "θετικό δείγμα" ανάλογα με το είδος τους, και (iii) θα καθορίζει την ευαισθησία των βακτηρίων σε διάφορα αντιβιοτικά, σε σύντομο χρονικό διάστημα. Θα παρέχει επίσης την ικανότητα κατηγοριοποίησης των βακτηρίων που προέρχονται απευθείας από δείγματα ούρων, ανάλογα με το είδος τους.

Η ουρολοίμωξη είναι μια βακτηριακή λοίμωξη που εντοπίζεται οπουδήποτε στο ουροποιητικό σύστημα και είναι ένας από τους πιο συνήθεις τύπους λοιμώξεων. Περισσότερο από το 50% των γυναικών ανά το παγκόσμιο θα εκδηλώσουν ουρολοίμωξη κατά τη διάρκεια της ζωής τους. Επίσης, ευάλωτοι στις ουρολοιμώξεις είναι οι χρόνιοι ασθενείς και τα παιδιά κάτω των δύο ετών. Οι παρούσες μέθοδοι διάγνωσης απαιτούν 24 ώρες για την ταυτοποίηση των βακτηρίων που προκαλούν τις ουρολοιμώξεις, όπως επίσης ακόμα 24 ώρες για τον καθορισμό του πιο αποτελεσματικού αντιβιοτικού. Αυτές οι συμβατικές μέθοδοι διάγνωσης είναι χρονοβόρες, με αποτέλεσμα οι γιατροί να συνταγογραφούν ένα αντιβιοτικό ευρέος φάσματος μέχρι να γνωστοποιηθούν τα επίσημα αποτελέσματα της διάγνωσης. Αναπόφευκτα, η χρήση μη βέλτιστων, ως προς το είδος της ουρολοίμωξης, αντιβιοτικών οδηγεί σε αναποτελεσματικές θεραπείες, επανερχόμενες λοιμώξεις, αυξημένο οικονομικό κόστος στα εθνικά συστήματα υγείας και ευθύνεται για ανάπτυξη αντίστασης των βακτηρίων στα αντιβιοτικά. Ως εκ τούτου μία μέθοδος που θα μειώσει κατά πολύ τον χρόνο που χρειάζεται για τη διάγνωση ουρολοίμωξης και την δημιουργία αντιβιογράμματος, θα είχε σημαντικά οφέλη στη διαχείριση των ουρολοιμόξεων.

Η βάση αυτής της πειραματικής μελέτης είναι η Φασματοσκοπία Ράμαν. Η φασματοσκοπία Ράμαν είναι μια οπτική τεχνική η οποία χρησιμοποιεί μονοχρωματική δέσμη φωτός (λέιζερ) και συλλέγει φάσματα τα οποία περιέχουν κορυφές που αντιστοιχούν στη χημική σύνθεση και τη μοριακή δομή μίας ουσίας. Αυτή η πληροφορία είναι μοναδική και χαρακτηριστική για κάθε δείγμα. Ένα μειονέκτημα της φασματοσκοπίας Ράμαν είναι το πολύ αδύνατο σήμα της. Για να αυξηθεί η ένταση του σήματος Ράμαν, μεταλλικά νανοσωματίδια προστίθενται στο δείγμα. Αυτή η τεχνική ονομάζεται Ενισχυμένη Φασματοσκοπία Ράμαν. Επίσης, για αυτή τη μελέτη χρησιμοποιήθηκαν πέντε είδη βακτηρίων τα οποία συναντιόνται συχνότερα σε μια ουρολοίμωξη: *Citrobacter*, *Proteus*,

*Klebsiella* sp., *Escherichia coli* και *Enterobacteur*. Όλα τα στελέχη των βακτηρίων συλλέχθηκαν από ασθενείς με ουρολοίμωξη. Επιπρόσθετα, για τον καθορισμό της ευαισθησίας των βακτηρίων, εξετάστηκαν οκτώ αντιβιοτικά που έχουν διαφορετικούς μηχανισμούς δράσης: amoxil, augmentin, cefaclor, cefuroxime, ciprofloxacin, ceftriaxone, cefazolin και amikacin.

Η επεξεργασία των δεδομένων έγινε με αλγόριθμους που αναπτύχθηκαν στη MATLAB. Αρχικά, τα δείγματα προ-επεξεργάστηκαν για να αφαιρεθεί ο θόρυβος και να ελαχιστοποιηθεί η διαφορά ανάμεσα στα φάσματα. Ακολούθως, δημιουργήθηκαν διανύσματα χαρακτηριστικών (feature vectors) από τα δεδομένα των φασμάτων. Ακολούθησε Ανάλυση Κύριων Συνιστωσών (Principal Component Analysis) για να μειωθεί η διάσταση των δεδομέων. Με τη χρήση Linear Discriminant Analysis τα δεδομένα κατηγοριοποιήθηκαν με τεχνική διασταυρούμενης επικύρωσης εξόδου-εξόδου (Leave-One Out Cross Validation). Η πολυπαραγοντική ανάλυση διακύμανσης (MANOVA) χρησιμοποιήθηκε για αξιολόγηση και οπτικοποίηση των αποτελεσμάτων της κατηγοριοποίησης.

Τα αποτελέσματα αυτού του ερευνητικού έργου είναι πολύ ελπιδοφόρα. Χρησιμοποιώντας Ενισχυμένη Φασματοσκοπία Ράμαν είναι δυνατό (i) να εντοπιστεί η συγκέντρωση βακτηρίων σε κάθε δείγμα, σε συγκεντρώσεις ακόμα και $10^3$ βακτήρια/ml, και να καθοριστεί η παρουσία ουρολοίμωξης, (ii) να κατηγοριοποιηθεί σωστά το είδος των βακτηρίων με ακρίβεια 93.75%, και (iii) να ταυτοποιηθεί η ευαισθησία στα αντιβιοτικά μέσα σε 2 ως 4 ώρες έκθεσης, με ακρίβεια 81.25 ως 100%. Αυτά τα προκαταρκτικά αποτελέσματα θα μπορούσαν να αποτελέσουν σημείο αφετηρίας για ανάπτυξη ενός καινοτόμου εργαλείου, το οποίο θα παρέχει διάγνωση και αντιβιόγραμμα ουρολοίμωξης εντός της ίδιας μέρας, επιτρέποντας πιο αποτελεσματική θεραπεία.

# ABSTRACT

The aim of this research was to develop of a fast and accurate method, based on Surface Enhanced Raman Spectroscopy (SERS), that could (i) detect if a sample is "positive" or "negative" for a Urinary Tract Infection (UTI); (ii) classify the causative bacteria, found in the "positive sample", according to their species; and (iii) determine bacterial susceptibility to various antibiotics in a short period of time. It should also allow correct classification of bacterial species coming directly from urine samples.

UTI is a bacterial infection, anywhere in the urinary tract, and is one of the most common types of infections. More than 50% of women globally will develop UTIs in their lifetime. Also, vulnerable το UTIs are chronically ill patients and children younger than two years old. Current diagnostic methods require 24 hours for the identification of the causative bacteria as well as another 24 hours for the determination of the most effective antibiotic. These conventional diagnostic methods are time consuming and lead doctors to prescribe broad spectrum antibiotics until the official results of the diagnosis are known. The use of a broad-spectrum antibiotics inevitably leads to ineffective treatments, recurrent infections, significant burden to national healthcare systems and is responsible for antibiotic resistance. A method that will reduce the time needed for UTI diagnosis and antibiogram could significantly benefit the management of UTIs.

This experimental study will be based on Raman Spectroscopy. Raman Spectroscopy is an optical technique that utilizes a monochromatic laser source to collect spectra that contain peaks corresponding to the chemical composition and the molecular structure of a substance. This information is unique and characteristic for any sample. A disadvantage of the Raman technique is that it produces a very weak signal. In order to increase the intensity of the Raman signal, metal nanoparticles are introduced in the sample. This technique is called Surface Enhanced Raman Spectroscopy (SERS). Furthermore, for this study included five bacteria species that are most commonly present in UTI: *Citrobacter*, *Proteus*, *Klebsiella* sp., *Escherichia coli* and *Enterobacteur*. All bacteria strains have been collected from patients with UTI. Additionally, for determining bacterial susceptibility eight antibiotics, with different action mechanisms, were examined: amoxil, augmentin, cefaclor, cefuroxime, ciprofloxacin, ceftriaxone, cefazolin and amikacin.

The data were processed using algorithms developed in MATLAB. Initially, the samples were preprocessed in order to remove the noise and eliminate the variance between

the spectra. Afterwards, feature vectors were created from the Raman spectra data. The implementation of Principal Component Analysis (PCA), to reduce the dimensionality of the feature vectors, followed. Using Linear Discriminant Analysis (LDA) the data were classified with Leave-One Out Cross Validation (LOOCV). MANOVA was used for the evaluation and visualization of the results.

The results of this research project are very promising. They provide a clear indication that, utilizing SERS, it is feasible to (i) detect the concentration of bacteria per sample, down to levels of $10^3$ bacteria/ml, and determine the presence of a UTI; (ii) classify correctly the bacterial species with an acuracy of 93.75%; and (iii) identify antibiotic susceptibility within two to four hours of exposure with correct classification ranging from 81.25 to 100%. These preliminary results can serve as the starting point for developing an innovative tool that will provide same day diagnosis and antibiogram for UTI, leading to more effective treatment.

# ACKNOWLEDGMENTS

This research project was performed under the supervision of Dr. Costas Pitris, Professor at the Department of Electrical and Computer Engineering of the University of Cyprus. There are a number of people that I would like to thank for making, each in their own way, this project a reality. First and foremost, I would like to express my deepest gratitude to my advisors, Prof. Pitris and Prof. Kastanos for the step-by step guidance and support into a new and exciting world that combines engineering and biochemical sciences. During this journey, I also met Alexandros Kyriakides who was an invaluable member of the team.

Additionally, I would like to express my gratitude to the University of Nicosia (UNIC) for hosting me and allowing me to use their laboratory facilities. Special thanks for their support go to Maria Leigh, Maria Mastorikou and Elena Violari, the lovely staff of UNIC biological department. I would also like to thank Kian Sharifi and Evanthia Sotiriou, undergraduate students at that time at UNIC, for their thoughts and insights when we were experimenting together at the topic. Furthermore, I would like to thanks KIOS Research and Innovation Center of Excellence, and the Youth Board of Cyprus for the partial funding of the project.

A special thanks also to all members of the Optical Diagnostics Lab and especially Christos Photiou and Louiza Sophocleous for the very effective collaboration. Furthermore, I would like to express my sincere gratitude to Dr. Chrysafis Andreou who embedded me in his team, allowing me to deepen my knowledge on the subject and broaden my horizons. Moreover, I would like to thank my colleagues Elina Panteli.

Above all, I would like to thank my mother, my father, and my grandmother Eleni for all the financial and psychological support throughout my studies. Last but not least, I would like to thank my sisters Styliana and Eleni for believing in me and for their great help during the long procedure for the completion of my PhD.

At this point I would like to thank once again Dr. Pitris for giving me this great opportunity to be a part of this high perspectives project and, in whole, for this learning experience. Special thanks to Dr. Stavros Iezekiel, Dr. Chrysafis Andreou, Dr. Constantinos Pattichis, and Dr. Evdokia Kastanos for their participation in the committee and the time and effort that they spent to review and improve the quality of this dissertation.

# TABLE OF CONTENTS

# LIST OF TABLES

# LIST OF FIGURES

# Chapter 1
# PhD Thesis Summary

## 1.1 Problem Statement

Urinary tract infections (UTIs) are infections of any part of the urinary tract, including the kidneys, ureters, bladder and urethra. The rate of UTI depends on age and gender. Children and infants, women and patients who are hospitalized for a long time are most susceptible. Statistically, UTIs are the most common bacterial infections in children who are younger than two years old. Additionally, more than 50% of women will develop a UTI at some point in their life and women of all ages have a higher probability to suffer a UTI than men. Furthermore, the elderly, over 65 years old, and chronically ill patients are more prone to UTIs. It is reported that UTIs are the most common source of nosocomial infection [1].

Statistically, most UTIs are considered uncomplicated and are easily treated. However, if they are not addressed swiftly, the infection may spread from the bladder and ureters to the kidneys. A kidney infection is more dangerous and can lead to permanent kidney damage. In some cases, an untreated UTI may spread to the bloodstream and cause sepsis, which can be life-threatening [2]. In 2011, there were approximately 400 000 hospitalizations for UTIs in the United States with an estimated cost of $2.8 billion. Additionally, it was reported that UTI incidences have increased by 52% between 1998 and 2011 [3]. UTIs are usually caused by *Escherichia Coli*, a type of bacteria that is commonly found in the gastrointestinal tract [4]. Other bacteria that can be responsible for UTIs are *Klebsiella* sp., *Pseudomonas aeruginosa*, *Enterococcus*, *Proteus*, *Enterobacter*, *Citrobacter*, *Staphylococcus* and *Acinobacter*.

Currently, the procedures leading to a UTI diagnosis are urinalysis, urine culture, antibiotic susceptibility testing and imaging scans. However, these procedures require forty-eight hours in order to provide results [5]. In order to treat the UTIs expeditiously, physicians do not usually wait but, instead, empirically prescribe broad-spectrum antibiotics, like fluoroquinolones, amoxicillin-clavulanate and aminoglycosides [6]. Unfortunately, this tendency of physicians to prescribe broad spectrum antibiotics causes recurrent infections due to ineffective treatments and, more importantly, microbial resistance to antibiotics.

According to the Centre for Disease Prevention and Control of the European Union, the present state of microbial resistance development is alarming. Data taken from surveillance reports of European Antimicrobial Resistance Surveillance Network (EARS-Net), indicates that bacteria are developing resistance to most antibiotics. In Cyprus, the combined resistance to antibiotics reached 14.6% in 2018, a number that is not as high as in other countries which is very worrisome. However, this percentage has increased by 58% in the last decade. The only antibiotics to which the majority of bacteria are still sensitive belong to the carbapenem group. The higher level of resistance to carbapenem group in European Union was reported in Cyprus where it reached 2% in 2018 [7].

Challenges in UTI diagnosis and treatment include the increasing trend of antimicrobial resistance, the fact that few new antibiotics are expected to be developed in the next five to ten years, and the predisposition for recurrent infections that are caused by ineffective treatments. The development of novel methods for rapid, accurate and effective UTI diagnosis and treatment could lead to significant improvement and in the effectiveness and efficiency of the management of UTIs [7].

## 1.2 Aim and Objectives

The aim of this PhD study was to contribute to the development of an accurate method for diagnosis and treatment of Urinary Tract Infections (UTIs). The ultimate goal was to design a novel diagnosis and antibiogram method that would provide results in four hours or less, with minimal sample preparation, rapidly and inexpensively. Hence, the main objectives of this PhD thesis were:

1. Identification of a sample as "positive" or "negative" for a UTI (midstream urine samples, containing over $10^5$ cfu/ml (colony forming units) bacterial counts, are considered as "positive" while midstream urine containing less than $10^4$ cfu/ml are considered as "negative" for a UTI).

2. Classification and identification of the causative bacterial species in positive samples (bacterial strains from the species *Citrobacter spp*, *Proteus*, *Klebsiella* sp., *Escherichia coli* and *Enterobacter* cause more than 95% of possible UTIs).

3. Determination of bacteria sensitivity or resistance to antibiotics (common antibiotics include amoxicillin, amoxicillin/clavulanic acid, cefaclor, cefazolin, ceftriaxone, cefuroxime and ciprofloxacin).

4. Implementation of the above procedure on urine samples.

## 1.3 Hypothesis

The research question investigated by this project was whether it is feasible to develop a method that within a few hours would detect if a urine sample is infected by bacteria (patient suffers from UTI) and prescribe the most effective antibiotic to treat the infection using Surface Enhanced Raman Spectroscopy (SERS). The aspects investigated in order to verify this hypothesis were:

1. Identification of the sample as "positive" or "negative" for UTI: A sample was considered "positive" for UTI if the concentration of bacteria in a sample was over $10^5$ cfu/ml (colony forming units per ml) while a sample was "negative" for UTI indicates when that bacteria concentration was less than $10^4$ cfu/ml. The research question was whether the proposed approach could identify if a sample was negative or positive using the Raman data.

2. Classification of the causative bacteria: The research question was whether the proposed approach was able to classify the bacteria causing most of the UTIs into species classes, using the Raman spectra.

3. Determination of bacteria sensitivity to antibiotics in less than four hours: The issue to be resolved here was whether the proposed method was able to classify the most common bacteria causing UTIs as sensitive or resistant to the most common antibiotics.

4. Direct data collection from urine samples: The research here aimed to investigate whether the proposed system could identify if a sample was negative or positive for UTI, classify the causative bacteria and determine antimicrobial sensitivity from urine samples. For this purpose, a filtration method had to be developed in order to separate the bacteria from the other constituents of urine.

The expected outcome of this study was the creation of a new method that reduces the time needed for UTI diagnosis and identification of the most effective antibiotic from forty-eight hours to four hours or less.

## 1.4 Thesis outline

The first chapter contains the problem statement, briefly explains the aims and objectives of the project and lists the articles and proceedings that have been published for the dissemination of this work.

The second chapter describes in detail what Urinary Tract Infections (UTIs) are, which bacteria cause these infections, what the mechanism of action of the antibiotics used for treatment is and also what the current diagnostic procedures for UTIs are. The third chapter presents the Raman Spectroscopy theory, the instrumentation required for data collection and concludes with a literature review regarding the application of Raman spectroscopy to bacteria identification. In chapter four, a literature review of the data analysis techniques implemented for the classification of Raman spectroscopy data is presented.

Chapter Five enumerates all the materials required for the experimental procedures and, additionally, describes step by step all the procedures performed to collect and analyze the data. Chapter Six presents the results derived from the experimental procedures of Chapter Five. Finally, Chapter Seven present the conclusions and the future work.

## 1.5 Contributions

The main research contribution of this PhD study was the development of novel methods that enable the classification of bacteria and the identification of bacterial susceptibility to multiple antibiotics utilizing Surface Enhanced Raman Spectroscopy. Despite the well documented use of Raman spectroscopy for bacterial classification reported in the literature, these were the first studies of using Raman for antibiotic-sensitivity testing. The work in this thesis was published in one book chapter, three journal papers and seventeen conference proceedings, resulting in 134 citations and an h-index of 6 (according to Google Scholar as of April 2020).

**List of Publications**

Book Chapter

Kastanos, Evdokia, Alexandros Kyriakides, Katerina Hadjigeorgiou, and Costas Pitris. "Identification and antibiotic sensitivity of UTI pathogens using Raman spectroscopy." *InTech. Urinary Tract Infections* (2011): 207-226.

Articles

1. Kastanos, Evdokia, Alexandros Kyriakides, Katerina Hadjigeorgiou, and Costas Pitris. "A novel method for bacterial UTI diagnosis using Raman spectroscopy." *International Journal of spectroscopy* 2012 (2012).
2. Kyriakides, Alexandros, Evdokia Kastanos, Katerina Hadjigeorgiou, and Costas Pitris. "Classification of Raman spectra using the correlation kernel." *Journal of Raman Spectroscopy* 42, no. 5 (2011): 904-909.
3. Kastanos, Evdokia K., Alexandros Kyriakides, Katerina Hadjigeorgiou, and Costas Pitris. "A novel method for urinary tract infection diagnosis and antibiogram using Raman spectroscopy." *Journal of Raman Spectroscopy* 41, no. 9 (2010): 958-963.

Proceedings

1. Hadjigeorgiou, Katerina, Evdokia Kastanos, and Costas Pitris. "Surface enhanced Raman spectroscopy as a tool for rapid and inexpensive diagnosis and antibiotic susceptibility testing for urinary tract infections." In *2016 IEEE Healthcare Innovation Point-Of-Care Technologies Conference (HI-POCT)*, pp. 158-161. IEEE, 2016.
2. Kastanos, Evdokia, Katerina Hadjigeorgiou, and Costas Pitris. "Rapid identification of bacterial resistance to Ciprofloxacin using surface-enhanced Raman spectroscopy." In *Optical Diagnostics and Sensing XIV: Toward Point-of-Care Diagnostics*, vol. 8951, p. 89510F. International Society for Optics and Photonics, 2014.
3. Hadjigeorgiou, Katerina, Evdokia Kastanos, and Costas Pitris. "Surface Enhanced Raman Spectroscopy (SERS) for Point-Of Care Diagnosis of Urinary Tract Infections", *International Conference on Nanotheranostics (ICoN 2013)*, 26-28 September, 2013, Larnaca, Cyprus.
4. Kyriakides, Alexandros, Evdokia Kastanos, Katerina Hadjigeorgiou, and Costas Pitris. "Rank order kernels for the classification of Raman spectra of bacteria." In *European Conference on Biomedical Optics*, p. 87980M. Optical Society of America, 2013.

5. Hadjigeorgiou, Katerina, Evdokia Kastanos, and Costas Pitris. "Multi-bacteria multi-antibiotic testing using surface enhanced Raman spectroscopy (SERS) for urinary tract infection (UTI) diagnosis." In *European Conference on Biomedical Optics*, p. 87980L. Optical Society of America, 2013.
6. Hadjigeorgiou, Katerina, Evdokia Kastanos, and Costas Pitris. "Urinary tract infection (UTI) multi-bacteria multi-antibiotic testing using surface enhanced Raman spectroscopy (SERS)." In *Optical Diagnostics and Sensing XIII: Toward Point-of-Care Diagnostics*, vol. 8591, p. 85910B. International Society for Optics and Photonics, 2013.
7. Hadjigeorgiou, Katerina, Evdokia Kastanos, Alexandros Kyriakides, and Costas Pitris. "Point-of-care diagnosis of urinary tract infection (UTI) using surface enhanced Raman spectroscopy (SERS)." In *2012 IEEE 12th International Conference on Bioinformatics & Bioengineering (BIBE)*, pp. 333-337. IEEE, 2012.
8. Hadjigeorgiou, Katerina, Evdokia Kastanos, Alexandros Kyriakides, and Costas Pitris. "Complete urinary tract infection (UTI) diagnosis and antibiogram using surface enhanced Raman spectroscopy (SERS)." In *Optical Diagnostics and Sensing XII: Toward Point-of-Care Diagnostics; and Design and Performance Validation of Phantoms Used in Conjunction with Optical Measurement of Tissue IV*, vol. 8229, p. 82290D. International Society for Optics and Photonics, 2012.
9. Kyriakides, Alexandros, Evdokia Kastanos, Katerina Hadjigeorgiou, and Costas Pitris. "Raman spectra classification with Support Vector Machines and a correlation kernel." In *European Conference on Biomedical Optics*, p. 808706. Optical Society of America, 2011.
10. Kyriakides, Alexandros, Evdokia Kastanos, Katerina Hadjigeorgiou, and Costas Pitris. "The correlation kernel and support vector machines for the classification of Raman spectra" In *Proc. SPIE*, 7890, 789047, 2011.
11. Kastanos, Evdokia, Katerina Hadjigeorgiou, Alexandros Kyriakides, and Costas Pitris. "Classification of bacterial samples as negative or positive for a UTI and antibiogram using surface enhanced Raman spectroscopy." In *Plasmonics in Biology and Medicine VIII*, vol. 7911, p. 791107. International Society for Optics and Photonics, 2011.
12. Hadjigeorgiou, Katerina, Evdokia Kastanos, Alexandros Kyriakides, and Costas Pitris. "Surface Enhanced Raman Spectroscopy for Urinary Tract Infection diagnosis and antibiogram" *Nanotheranostics: Fabrication and Safety Concerns, International Conference*, April 27-30, 2010, Ayia Napa, Cyprus
13. Kastanos, Evdokia, Katerina Hadjigeorgiou, Alexandros Kyriakides, and Constantinos Pitris. "Surface enhanced Raman spectroscopy for urinary tract infection diagnosis and

antibiogram." In *Biomedical Vibrational Spectroscopy IV: Advances in Research and Industry*, vol. 7560, p. 75600A. International Society for Optics and Photonics, 2010.

14. Hadjigeorgiou, Katerina, Evdokia Kastanos, Alexandros Kyriakides, and Costas Pitris. "Raman spectroscopy for UTI diagnosis and antibiogram." In *2009 9th International Conference on Information Technology and Applications in Biomedicine*, pp. 1-4. IEEE, 2009.
15. Kyriakides, Alexandros, Evdokia Kastanos, and Constantinos Pitris. "Classification of raman spectra using support vector machines." In *2009 9th International Conference on Information Technology and Applications in Biomedicine*, pp. 1-4. IEEE, 2009.
16. Kastanos, Evdokia, Alexandros Kyriakides, Katerina Hadjigeorgiou, and Costas Pitris. "UTI diagnosis and antibiogram using Raman spectroscopy." In *European Conference on Biomedical Optics*, p. 7368_0U. Optical Society of America, 2009.
17. Kastanos, Evdokia, Alexandros Kyriakides, Katerina Hadjigeorgiou, and Constantinos Pitris. "Urinary tract infection diagnosis and response to antibiotics using Raman spectroscopy." In *Advanced Biomedical and Clinical Diagnostic Systems VII*, vol. 7169, p. 71690I. International Society for Optics and Photonics, 2009.

# Chapter 2
# Urinary Tract Infections (UTIs)

This Chapter focuses on what a Urinary Tract Infections (UTIs), what causes a UTI, what the current UTI diagnostic methods are, and the critical need to develop a technique that could rapidly identify the appropriate antibiotic for UTI treatment.

## 2.1 Urinary Tract Infections

The urinary tract consists of two kidneys, two ureters, the bladder, and the urethra. Urine is produced by the kidneys. The kidneys filter wastes out of the blood into the urine, retain proteins, electrolytes, and other compounds that the body can reuse, and help regulate the amount of water in the body. Urine then flows from the kidneys through the ureters to the bladder and, subsequently, through the urethra out of the body. Urine color is most often yellow and relatively clear, but the color, quantity, concentration, and content of every sample is usually different and can be indicative of the state of health. Substances that are not normally present in the urine like glucose, protein, bilirubin, red blood cells, white blood cells, crystals, and bacteria may indicate the presence of a UTI [5]. Other symptoms of a UTI include dysuria, hematuria, back pain, nocturia and vaginal discharge or irritation [8].

UTIs are divided into two categories based on their frequency of occurrence: uncomplicated and recurrent UTIs. An uncomplicated UTI is less severe and usually presents patients who don't suffer from any structural or functional abnormalities of the urinary tract. It is usually caused by the bacteria *Echerichia coli* in the lower part of the urinary system. Other bacteria that cause uncomplicated UTIs are *Staphylococcus*, *Enterococcus*, *Klebsiella* sp., *Enterobacterand Proteus* [8]. Recurrent UTIs are defined as three or more uncomplicated UTIs in a period of one year. They are relatively common among young, healthy women even though these women generally have anatomically and physiologically normal urinary tracts. Recurrent UTIs result due to reinfection by bacteria or due to bacterial persistence even after two weeks of appropriate antibiotic treatment [8].

The bacterial load of a UTI is measured in colony forming units (cfu) per ml of midstream sample of urine (MSU). A cfu is the unit (usually one bacterium) that forms a colony in culture. MSU is the urine captured midway through micturition (i.e. not the first nor the last part of urine that comes out). There is no individual bacterial count that is

indicative of significant bacteriuria that applies to all UTIs and in all circumstances. The literature recommends the following bacterial counts for possible infections:

- Bacterial count over $10^3$ cfu/ml in a MSU indicates acute uncomplicated cystitis in women.
- Bacterial count over $10^4$ cfu/m in an MSU indicates acute uncomplicated pyelonephritis in women.
- Bacterial count over $10^5$ cfu/ml in an MSU in women, or bacterial count over $10^4$ cfu/ml in an MSU in men, or in straight catheter urine in women, indicates a recurrent UTI.

For this research, bacterial count over $10^5$ cfu/ml in an MSU was considered as positive for UTI and bacterial count less than $10^4$ cfu/ml in an MSU was considered as negative for UTI [9].

## 2.2 Bacterial Resistance to Antibiotics

Antimicrobial resistance in Europe has been studied by the European Antimicrobial Resistance Surveillance Network (EARS-Net) with data collected from invasive isolates reported from thirty European Union (EU) and European Economic Area (EEA) countries in 2018 [7]. The occurrence of antimicrobial resistance depends on three factors:

- The type of microorganism that causes the infection
- The antibiotic group that treats the infection
- The geographical region where the incidence was recorded

The EARS-Net study included a study of the antimicrobial resistance of bacteria *Echerichia coli* and *Klebsiella* sp. bacteria to four antibiotic groups: aminopenicillins, fluoroquinolones, carbapenems and third generation cephalosporins.

Figure 2.1 and Figure 2.2 illustrate the discouraging results of antimicrobial resistance to the antibiotic groups of aminopenicillins and cephalosporins. The resistance to aminopenicillins, as high as 67.6% recorded in Ireland, is probably due to the overuse of the specific category of drugs since the discovery of penicillin in 1928 by Alexander Flemming and its clinical use since 1942 [10]. The exposure of bacteria to the specific group of antibiotics led bacteria to develop mechanisms that prevent its antimicrobial action. Figure 2.3 shows the antimicrobial resistance of bacteria *Echerichia coli* to carbapenems. It is encouraging that for this group of antibiotics the levels of resistance barely reach 2%.

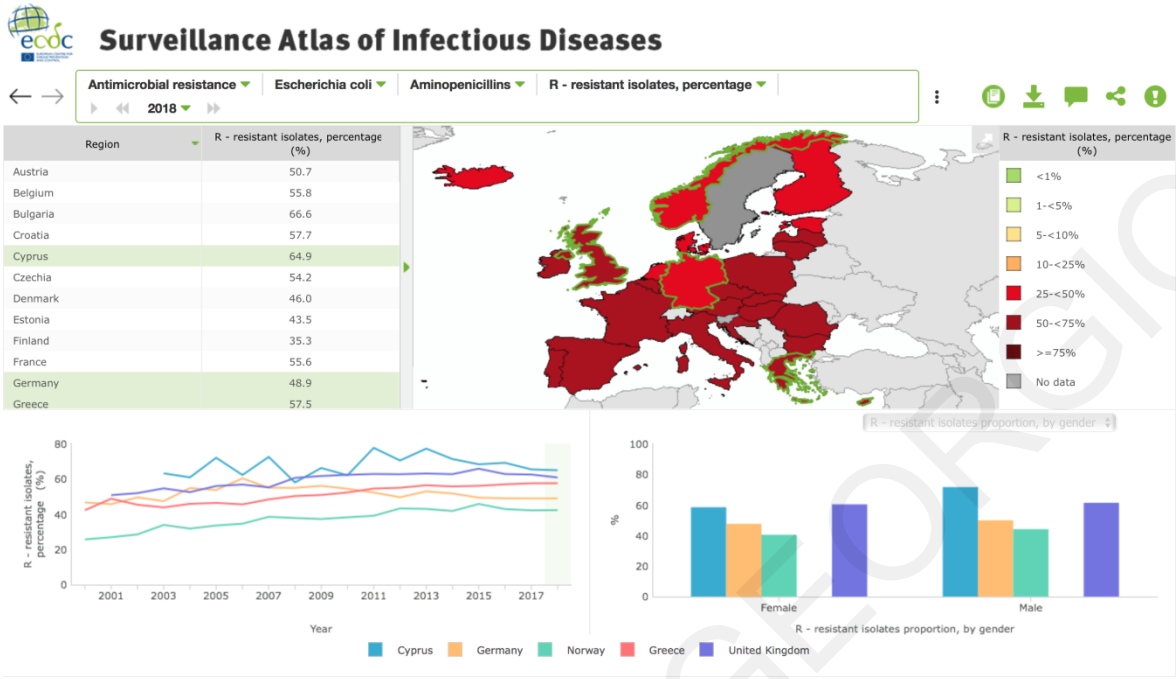


Figure 2.1 Antimicrobial resistance of bacteria *Echerichia coli* to antibiotic group of aminopenicillins

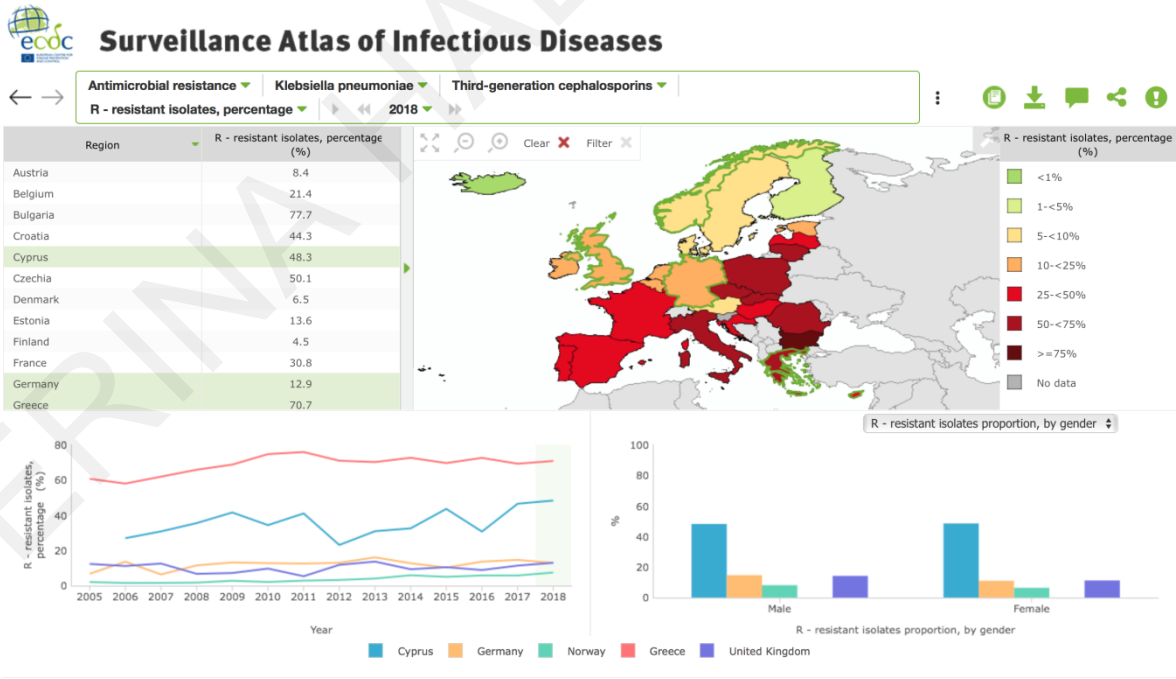


Figure 2.2 Antimicrobial resistance of Bacteria *Klebsiella* sp. to antibiotics group of third generation cephalosporins

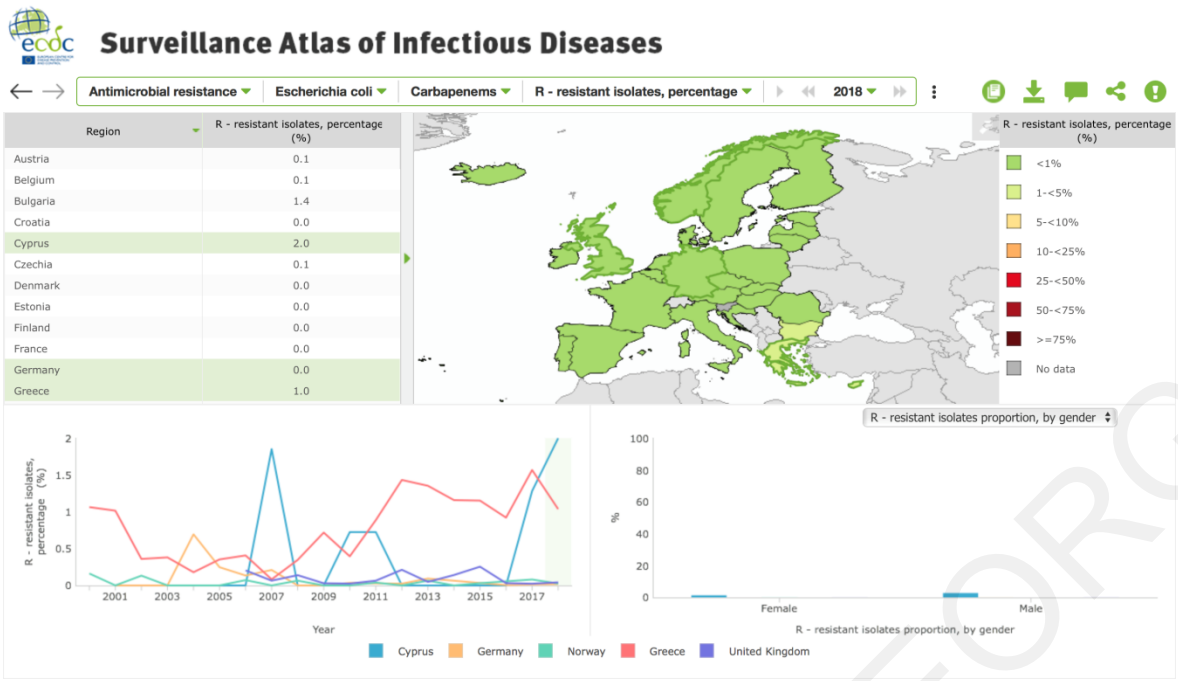


Figure 2.3 Antimicrobial resistance of bacteria *Echerichia coli* to antibiotic group of carbapenems

Aminopenicillins, cephalosporins, and carbapenems have a similar mechanism of action affecting the bacterial cell wall. Due to the fact that these antibiotic groups are the most widely used, bacteria have developed widespread resistance to them. The resistance mechanism is based on the enzyme β-lactamase that is produced by the bacteria. Through hydrolysis, β-lactamase breaks the β-lactam ring of the antibiotic and deactivates the molecule's antibacterial properties [11].

Other types of bacteria, which do not have a cell wall, cannot be treated by antibiotics affecting that part of the cellular structure. For this kind of bacteria, fluoroquinolone antibiotics are used. Fluoroquinolones act by inhibiting two enzymes involved in bacterial DNA synthesis [12]. Figure 2.4 illustrates the antimicrobial resistance of *Echerichia coli* bacteria to the antibiotic group of fluoroquinolones. The resistance varies at moderate levels with the higher percentage, 42.4% recorded in Cyprus for the year 2018.

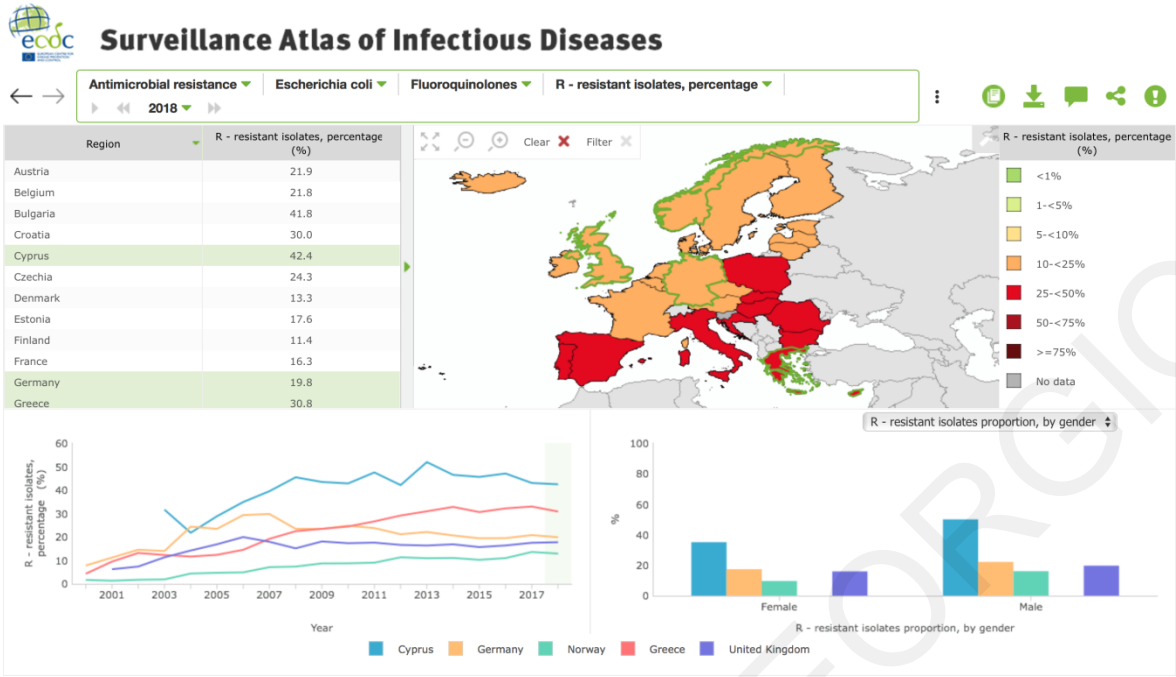


Figure 2.4 Antimicrobial resistance of bacteria *Echerichia coli* to antibiotic group of fluoroquinolones

Figure 2.5 and Figure 2.6 demonstrate that antimicrobial resistance highly depends on bacterial species. Figure 2.5 shows the antimicrobial resistance of *Echerichia coli* bacteria to combined groups of antibiotics, including third generation cephalosporins, fluoroquinolones and aminoglycosides, while Figure 2.6 illustrates the same but for *Klebsiella* sp. bacteria. As the figures indicate, antimicrobial resistance for *Echerichia coli* reached 19.6% in 2018 while for *Klebsiella* sp. it reached 50.4% for the same year. Furthermore, there is geographical variation of antimicrobial resistance. It is evident from the EARS-Net study that southern and eastern European countries suffer from higher resistance percentages compared to northern European countries. Southern and eastern countries often exhibit percentages of over 25% antimicrobial resistance while northern countries usually vary around 5-10%.

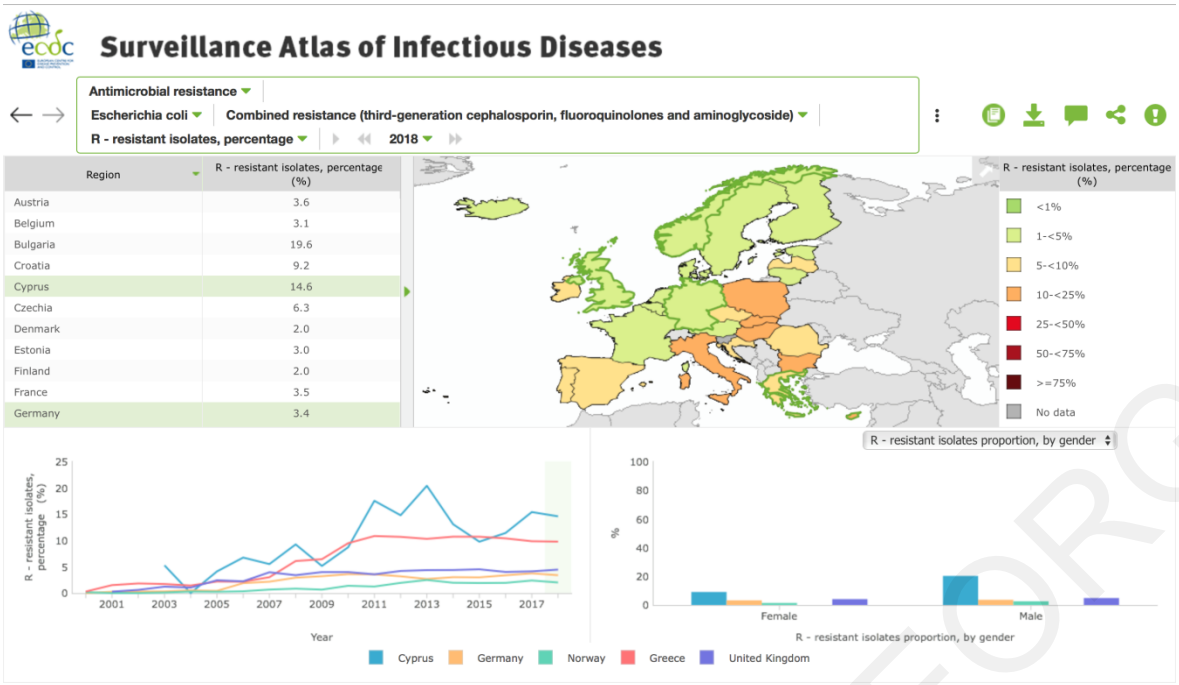


Figure 2.5 Antimicrobial resistance of bacteria *Echerichia coli* to combined groups of antibiotics including third generation cephalosporins, fluoroquinolones and aminoglycosides

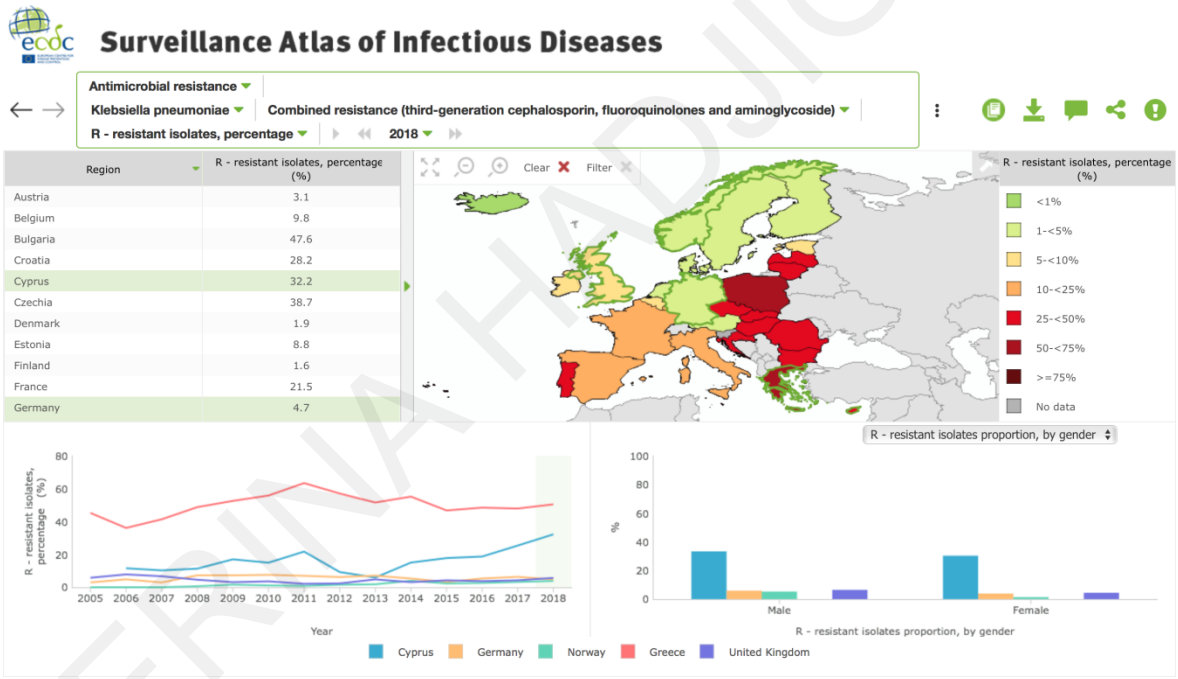


Figure 2.6 Antimicrobial resistance of bacteria *Klebsiella* sp. to combined groups of antibiotics including third generation cephalosporins, fluoroquinolones and aminoglycosides

The increasing resistance to broad-spectrum antibiotics like aminopenicillins, fluoroquinolones and third generation cephalosporins is alarming and these trends force societies to implement and adopt policies and strategies in order to minimize bacterial resistance to antibiotics [13].

## 2.3 Current Diagnostic Methods for Urinary Tract Infections

Most UTIs are, currently, detected by performing a urinalysis. Urinalysis examines for evidence of infection, such as bacteria and white blood cells, in a sample of urine utilizing physical, chemical, and microscopic tests. Initially, visual examination evaluates the urine's color and clarity. It is followed by a chemical examination with a dipstick to test for the presence of various substances and get information about the concentration of urine (Figure 2.7). Finally, a microscopic examination is performed in order to identify and count the types of cells and other components, such as bacteria, that can be presented in urine. A microscopic examination is typically performed when there is an abnormal finding in the visual or chemical examination [5].

Figure 2.7 Urine dipstick and color box instructions [14]

The definitive diagnostic technique for UTIs is urine culture. Urine culture is more common for people who suffer from recurrent urinary tract infections and for those who are hospitalized. Urine culture confirms the results of urinalysis testing. For a urine culture, a small sample of urine is placed on one or more agar plates and is incubated at 37$^{o}$C for 24 to 48 hours (Figure 2.8). A laboratory professional, studies the colonies on the agar plate, counts the total number of colonies that have been grown and determines their type. The size, shape, and color of these colonies help identify which bacteria are present and the number of colonies indicates the quantity of bacteria present in the urine sample. If there is no or little growth on the agar after 24 to 48 hours of incubation, the urine culture is considered negative [5].

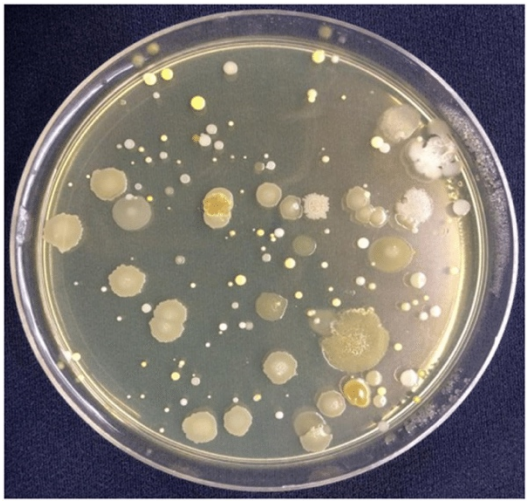

Figure 2.8 Bacterial colonies incubated on agar plate [15]

If bacteria are detected in the urine culture, a susceptibility test is executed to determine which antibiotics are the most effective to inhibit the growth of the bacteria. The results of the susceptibility test enable doctors to prescribe the most appropriate antibiotic that will effectively treat the infection. There are two ways to implement the susceptibility tests. The first method is the solid culture antibiogram where in an agar petri dish bacteria are spread and disks infused with antibiotics are placed on the petri dish. The petri dish with the disks and the bacteria is incubated at 37$^{o}$C for 24 to 48 hours (Figure 2.9). The diameter of the clear zone of inhibition around each antibiotic disk indicates the susceptibility or resistance of bacteria to antibiotics.

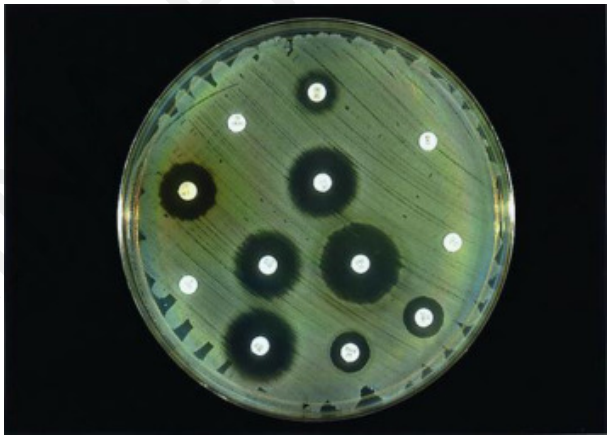

Figure 2.9 Solid culture antibiogram [16]

The second method is the liquid antibiogram where bacteria are diluted in nutrient media with specific concentrations of antibiotics. Antibiotic concentrations are chosen based on their MIC (Minimal Inhibitory Concentration) values. MIC values are the minimum concentrations that kill the bacteria in μgrams per ml. The sample is incubated for 48 hours at 37$^{o}$C (Figure 2.10). If the mixture of bacteria/antibiotic is clear, the bacteria have not

grown and are susceptible to the antibiotic. Otherwise the bacteria are resistant to the antibiotic [5].

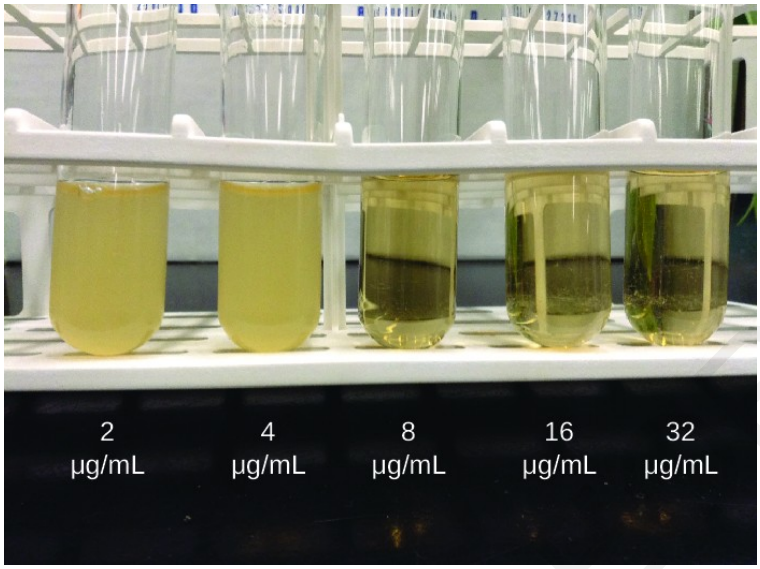


Figure 2.10 Liquid culture antibiogram [17]

Other methods, used in the management of UTIs, include imaging scans (MRI, ultrasound, nuclear, etc.) and specialized X-ray studies. These methods are employed in order to check for anatomical problems or indications of an underlying disease that could be causing recurrent UTIs. Imaging tests are usually performed in children with UTIs, adults suffering from recurrent UTIs and for patients who have blood in their urine. Some of the imaging scan techniques are kidney and bladder ultrasound, voiding cystourethrogram, nuclear scans, cystoscopy and intravenous pyelogram [5].

### 2.3.1 Review of current and emerging technologies for UTI identification and Antibiotic Sensitivity Testing

Currently, various methods are being tested of under development focusing on (i) the isolation and identification of the causative bacteria from an infected sample and (ii) the evaluation of the susceptibility of the bacteria to various antibiotics in order to prescribe of the most effective antibiotic for treatment. Figure 2.11 succinctly summarizes the currently applied methodologies, the emerging technologies that are under development or require FDA approval and the future approaches that aim to penetrate the market in the forthcoming years to minimize the time needed for diagnosis. The technologies currently in use in clinical labs and hospitals are divided into three main categories. The phenotypic methodologies (culture based), molecular techniques and spectroscopic techniques [18].

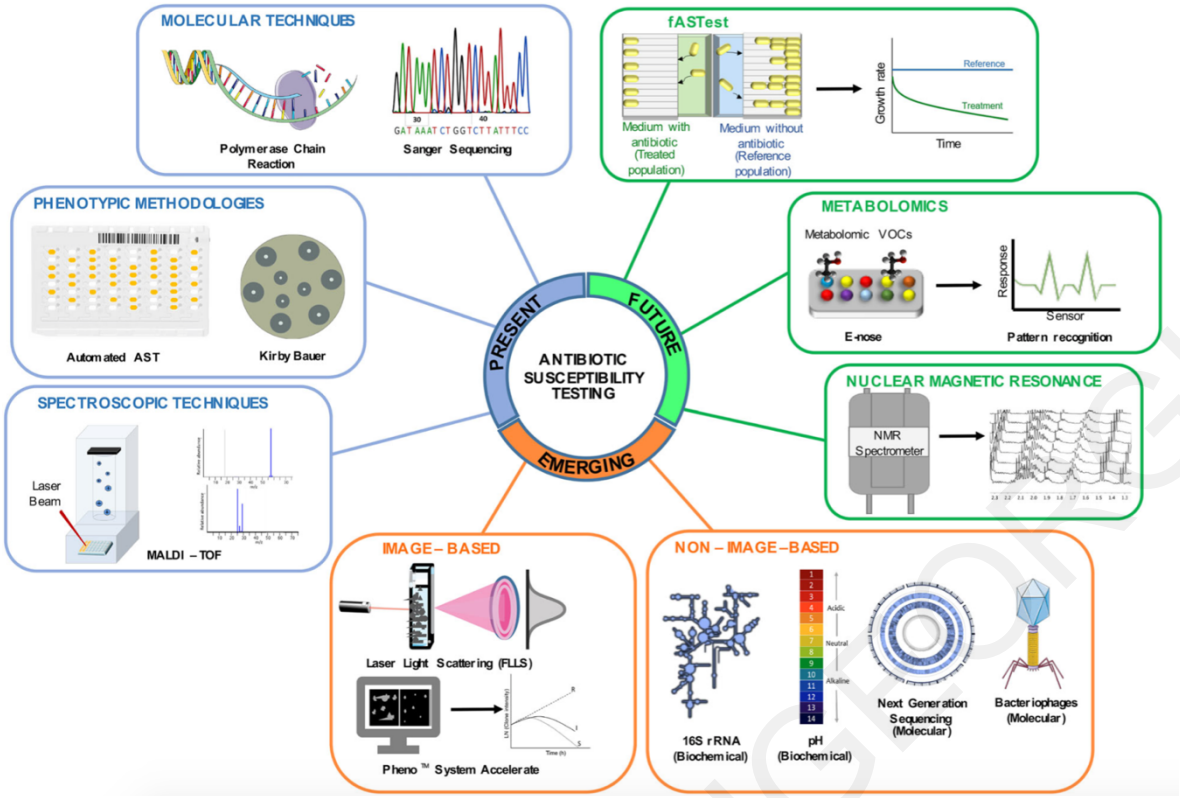


Figure 2.11 Current, emerging and future technologies for bacteria identification and antibiotic sensitivity testing (AST) [1]

Culture-based approaches observe the phenotypic changes, while bacteria are exposed to various antibiotics, and provide data regarding the susceptibility of the bacteria and the MIC values. These approaches are separated into (i) manually performed tests, such as agar dilution, disk diffusion, gradient tests or broth microdilution, and (ii) automated systems.

**Manually performed tests**

A. Dilution assays:

Agar assay: Petri dishes are filled with Mueller-Hinton agar supplemented with the proper antibiotic concentration. Each plate consists of different concentration and can test up to 36 different inocula at the same time. It requires 16-24h to provide results, the cost of the technique is relatively low but require the physical presence of a lab expert.

Broth medium or microdilution technique: 96-well plates are used to test 12 different drugs. The solutions are incubated at 37ºC for 12-24 hours and the development of turbidity or sediment in the wells indicate the growth of organisms and the MICs.

B. Disk diffusion assay: Filter paper disks infused with antibiotics, at known concentrations, are placed in the surface of an agar plate that is already covered with bacteria. The plates are incubated at 37$^{o}$C for 24 hours and the diameter of bacterial growth around each disk indicates if a sample is sensitive or resistant to an antibiotic. The drawback of this technique is that it does not provide information regarding the appropriate concentration of the antibiotics to effectively treat the infection.

C. Gradient tests: A strip containing a gradient of predefined concentrations of antibiotics is placed on the surface of a petri dish that contains bacteria (Figure 2.12). By utilizing these strips, both the susceptibility of a sample to several antibiotics and the MIC values can be determined. The cost of each strip is around 2-3 euros and requires training and expertise which increase the cost of the test. This method also requires16-24h to provide results [18].

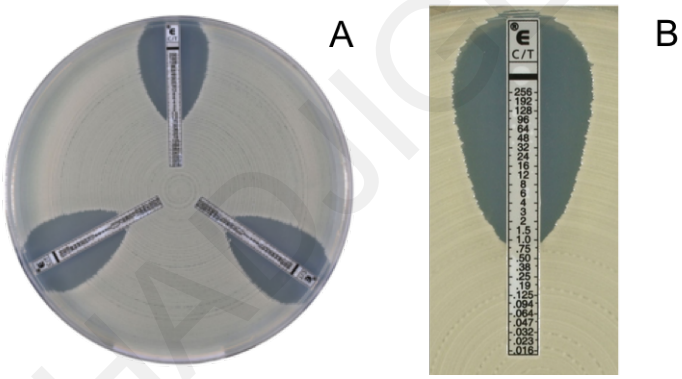


Figure 2.12 Gradient tests containing predefined concentrations of the antibiotic [19], [20]

**Automated systems**

Some automated systems use cassettes (also named panels or cards) with wells where each well contains a different substrate for pathogen identification. Through the use of these substrates the metabolic activity of each strain is examined. Furthermore, in order to examine the susceptibility of bacteria to various antibiotics, the procedure of broth microdilution assay has also been automated, utilizing sensitive optical detection systems that measure the bacterial growth. The drawbacks of these systems are that (i) the number and concentrations of antibiotics tested are limited, (ii) there is a need for a high number of viable cells, (iii) samples that are directly received from patients cannot be process by the instrument, and (iv) a pure culture of the pathogen is required. Moreover, these techniques take several hours for bacteria identification and antibiotic sensitivity testing (AST) including the hours needed for overnight culture. The advantages of these methods include the fact that the processes are

automated and standardized and have the capacity to manage high workloads. Some examples include:

A. MicroScan Walkaway of Beckman Coulter that measures the bacterial growth in the presence of antibiotics by recording the bacterial turbidity using a photometer and requires 4.5-18h to provide results.
B. Vitek bioMérieux by bioMérieux that again measures the bacterial growth in the presence of antibiotics by recording the bacterial turbidity using a photometer and requires 6-11 hours to provide results.
C. BD phoenix by Becton Dickinson that records bacterial growth in the presence of antibiotics by recording bacterial turbidity and colorimetric changes. It requires 9-15 hours to provide results.
D. Sensititre by Thermo Fisher Scientific that record bacterial growth with antibiotics by measuring fluorescence and need 18-24 hours to provide results [18].

Other methodologies that are widely used for bacteria identification and ASTs are based on molecular techniques such as the polymerase chain reaction (PCR) and the quantitative real time PCR (qPCR). These methods provide results through amplifications of specific sequences of nucleic acid. The drawbacks of these techniques are that they require: (i) a DNA extraction step from isolated strains, (ii) a high number of cells to obtain adequate DNA, (iii) previous knowledge on the sequences to amplify and (iv) extensive lab training and expertise. PCR can be either culture independent, thus performed directly on raw samples, or it can be cultured-enriched. These approaches can quantify DNA copies, detect bacterial growth in the presence of different antibiotic concentrations and provide results from isolated colonies in about 6 hours. Some of the instruments utilizing PCR techniques include:

A. SeptiFast test by Roche that is mainly used for bloodstream infections and does not provide any information associated to antimicrobial susceptibility except from methicillin-resistant *Staphylococcus aureus*.
B. Gene Xpert system by Cepheid that utilizes culture-independent qRT-PCR for MRSA and methicillin susceptible *Staphylococcus aureus*, to provide results from a positive blood culture in about 1 hour.
C. AID carbapenemase LPA by Autoimmun Diagnostika which utilizes a Line Probe Assay (LPA) technique (conventional PCR followed by reverse hybridization of PCR amplicons) in order to detect ESβL and carbapenemase resistance genes in the

Enterobacteriaceae family. The test showed 100% sensitivity and 100% specificity when it was used in clinical isolates. The drawback of this technique is that the presence of these resistance genes does not always correlated with the phenotypic resistance since the resistance gene may be present but at very low expression levels. This technique can be applied directly on urine sample.

D. FilmArray by BioFire executes multiplex PCR followed by nested PCR and amplicon melting analysis. It provides results in 1 hour.
E. Verigene by Nanosphere a technique that uses microarrays of oligonucleotide probes which are designed to specifically bind several DNA sequences of different target pathogens. This technique requires around 2.5 hours to provide results. Verigene include two panels for bacterial identification and AST for gram-positive and gram-negative bacteria. For the gram-positive bacteria, a sensitivity of 92.6–100% and specificity of 95.4–100% for identification of bacteria, and sensitivity of 98.6– 100% and specificity of 94.3–100% for detection of resistance markers, have been reported. This system provides a sensitivity of 97.1% and a specificity of 99.5% for gram-negative bacteria [18].

Another technique that is used for bacteria identification is MALDI-TOF MS spectrometry. MALDI-TOF MS utilizes a laser pulse to induce rapid ionization of the bacteria or yeast ribosomal proteins directly from cultured colonies or cell pellets from the clinical sample. The calculated mass of the ions is characteristic of the bacterial or yeast species. The advantages of this system are that (i) it can be used for gram-positive or gram-negative bacteria and yeast, (ii) it does not require specific tests and (iii) it can provide results in a few minutes. The drawbacks of this system include the fact that it needs fresh colonies acquired by an overnight culture (even thought, the number of cells needed can be around $10^4$-$10^6$ indicating that only some hours of culture at 37$^o$C are necessary) and that the instrument cost can be as high as 200 000 euro. Currently, MALDI-TOF MS is used for pathogen identification but there are studies to extend its application to AST. Using this approach bacteria can be identified at the species-level, directly from urine samples, at rates of 91.8%. However, best results are achieved for concentrations higher than $10^5$ and for gram- negative bacteria [18].

An approach that combines spectroscopic and molecular methods is polymerase chain reaction/electrospray ionization mass spectrometry PCR/ESI-MS. A commercial instrument that uses this technique is Iridica by Ibis Biosciences. This system is used for bloodstream infections and sepsis and includes a pre-filled 16-well PCR strip, with 18 primer pairs that

target broadly conserved bacterial and fungal sequences of pathogenic species as well as specific antibiotic resistance markers. PCR/ESI-MS can identify more than 780 bacterial and candida species utilizing a database and software that compares the DNA sample sequence with a sequence library. It can detect concentrations of up to 0.25–128 CFU/mL, and requires around 6 hours to provide results. The IRIDICA system costs £268 000 and the price for a test is £174. The specificity and sensitivity of this system was 84% and 81% respectively as tested on blood culture [18].

Table 2.1 presents an overview of the current technologies that are used for bacteria identification and AST.

**Table 2.1 Current technologies specifications**

| Techno-logy | Method & Example of Manufacturer | ID/AST | Time needed | Sensitivity Specificity Accuracy | Direct from patient sample | Price | General Information |
|---|---|---|---|---|---|---|---|
| Culture based | Agar dilution assay by Oxoid | ID/AST | 16-24h | - | No | - | Bacteria inoculated on agar plates with different concentrations of antibiotics |
| Culture based | Broth dilution assay by Oxoid | AST | 12-24h | - | No | - | Bacteria inoculated in liquid media with different antibiotics to monitor growth |
| Culture based | Disk diffusion by Oxoid | AST | 16-24h | - | No | - | Bacteria inoculated on agar plates with single antibiotic disks |
| Culture based | Gradient test by bioMérieux | AST | 16-24h | - | No | 2-3 euros per strip | Bacteria inoculated on agar plates with graded antibiotic concentration strips |
| Culture based - Automa-ted systems | MicroScan Walkaway by Beckman Coulter | ID/AST | 4.5-18h | - | No | - | Measure bacterial growth in the presence of antibiotics by recording bacterial turbidity using a photometer |
| Culture based - Automa-ted systems | Vitek bioMérieux by bioMérieux | ID/AST | 6-11h | SN=91.1% SP=99.8% [21] | No | - | Measure bacterial growth in the presence of antibiotics by recording bacterial turbidity using a photometer |
| Culture based - Automa- | BD phoenix by Becton Dickinson | ID/AST | 9-15h | SN=100% SP=99.6% [21] | No | - | Record bacterial growth in the presence of |

| | | | | | | | |
|---|---|---|---|---|---|---|---|
| ted systems | | | | | | | antibiotics by recording bacterial turbidity and colorimetric changes |
| Culture based - Automa-ted systems | Sensititre by Thermo Fisher Scientific | ID/AST | 18-24h | - | No | - | Record bacterial growth with antibiotics by measuring fluorescence |
| Molecu-lar based method-logies | SeptiFast test by Roche | ID | 6h | - | Y (Blood) | - | Real-time PCR followed by highly specific melting point analysis using specific hybridization probes (FRET) |
| Molecu-lar based method-logies | Gene Xpert system by Cepheid | ID | >1H | - | No | - | DNA amplification using qRT-PCR to detect methicillin resistance or susceptibility (MRSA/ MSSA) in positive blood culture |
| Molecu-lar based method-logies | AID carbapenemase LPA by Autoimmun Diagnostika | ID/AST | >6h | SN=100% SP=100% | Y (urine) | - | PCR followed by hybridization with DNA probes present on the nitrocellulose strip followed by signal detection of hybridized biotinylated PCR amplicons |
| Molecu-lar based method-logies | FilmArray by BioFire | ID | 1h | - | Y (blood) | - | Double PCR reaction in a row: multiplex PCR followed by nested PCR and amplicon melting analysis |
| Molecu-lar based method-logies | Verigene by Nanosphere | ID/AST | >2h | ID: SN=92.6–100% SP=95.4–100%<br><br>AST: SN=98.6–100% SP=94.3–100% | No | - | Microarray of oligonucleotide probes, designed to specifically bind several DNA sequences of different target pathogens |
| Spectro-metry | MALDI-TOF MS | ID | <5h | - | No | €200 000 | Identification of molecules based on their time of flight though a vacuum tube after laser irradiation of a matrix that is co-crystallized with sample, generating a spectrum that is |

| | | | | | | | |
|---|---|---|---|---|---|---|---|
| | | | | | | | after compared with a reference database |
| Spectro-metry Approa-ches Combi-ned with Molecu-lar Tools | Iridica by Ibis Biosciences | ID | <6h | 80% matching results with state of the art | Y (blood) | £268 000 | Polymerase chain reaction/electrospr ay ionization mass spectrometry PCR/ESI-MS |

Emerging technologies for bacteria identification and AST are separated into image-based technologies, non-image based, biochemical methods and sequencing technologies.

**Imaging-Based technologies**

A. oCelloScope by Philips BioCell is a novel tool which identifies the species of bacteria and performs an AST. Testing has show that this tool provides identification results in just 6 minutes for monoculture infection and 30 minutes for complex samples. Additionally, it provides susceptibility results (in blood cultures) in 1-4.2 hours. oCelloScope performs digital time lapse microscopy scanning of the sample. The images are processed by two algorithms that calculate the pixel histogram summation or contrast segmentation and extraction of surface area to estimate the growth kinetics of the bacteria. The drawbacks of the system are that it does not analyze single cells but populations and has lower resolution than other image-based systems [18] [22]. Figure 2.13 illustrates the oCelloScope instrumentation while Figure 2.14 presents images captured by the system.

Figure 2.13 oCelloScope instrumentation [22]

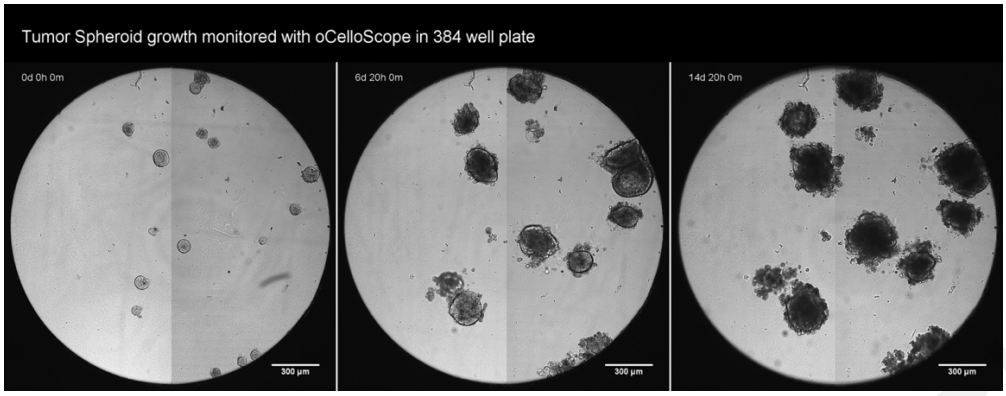


Figure 2.14 oCelloScope can automatically acquire images for hours, days or weeks [22]

B. Multiplexed automated digital microscopy (MADM) is utilized commercially by Accelerate Pheno System by Accelerate Diagnostics. This device allows the diagnosis of mono and polymicrobial infections, directly from the sample, bypassing the need of overnight culture. Currently, this technology has only been tested with blood cultures. It utilizes multichannel test cassettes, high-resolution camera and algorithms with mathematical regression models to achieve real-time observation and measurement of bacterial growth. It provides results in less than 6 hours with sensitivity and specificity of 95.6% and 99.5% for bacteria identification and 95.1% and 95.5% for AST [18][23]. Figure 2.15 shows the Accelerate Pheno System.

Figure 2.15 Accelerate Pheno System

C. Bacterial cytological profiling (BCP) utilizes fluorescent dyes and a microscope to measure the variations in cell length, width, permeability, chromosome number, compactness and shape when the bacteria are exposed to antibiotics. Preliminary evaluation of this method showed 100% accuracy on discrimination between

methicillin-susceptible and methicillin-resistant clinical isolates of *Staphylococcus aureus* within 1-2 h of exposure [18] [24].

D. Single-cell morphological analysis (SCMA) combines microfluidics and imaging. It uses a microscope attached to a true-color CCD camera and observes the bacterial growth from agarose microfluidic channels after antibiotics have been diffused in the device. The images are processed to estimate the antibiotic MIC value. SCMA provides AST results in less than 4 hours with 91.5% categorical agreement and 6.5% minor, 2.6% major and 1.5% very major discrepancies. This system does not perform any identification of bacteria.

**Non-imaging based technologies**

These methods typically detect a specific physical property in order to provide effective AST.

A. BacterioScan measures the angular variation in the intensity of light scattered by a laser beam that passes through a bacterial sample to estimate the concentration of bacteria. It provides information regarding the number and size of bacterial cells, measures bacterial growth and detects concentrations down to $10^3$ CFU/ml. This technique can be applied directly on urine samples and can process up to sixteen samples simultaneously but it can detect only bacteria coming from one species at a time. It provides results in 10 hours. Preliminary results indicate that the sensitivity and specificity of this approach ranged from 68 to 83% and from 80 to 87% respectively [25] .

B. The Lifescale instrument can perform AST directly on blood cultures. This tool measures the bacterial population, using a microcantilever placed inside a microfluidic channel, before and after treatment with an antibiotic in order to measure the MIC value for AST. It can provide results in about 3 hours directly from blood sample. The Lifescale instrument is shown in Figure 2.16.


Figure 2.16 Lifescale instrument

**Biochemical Methods**

These methods utilize several biomarkers, such as quantitative changes in 16S rRNA, NADH, FADH and pH, or emission of light caused by gene insertion in DNA, to detect the bacterial growth. Three techniques that exploit such biochemical approaches are:

A. UtiMax by GeneFluidics provides identification of bacteria and AST. This methodology is based on sandwich hybridization of specific capture and detector probes of bacterial 16S rRNA. The signal from the detector is electrochemically amplified with an enzyme tag, that transduces the molecular hybridization events into quantitative electrical signals. Preliminary results on viable pathogens from urine samples indicated that the signal increase was proportional to the cell number obtained through the conventional culture on agar plates. The Genefluidics instrument was also tested directly in urine samples, providing an accuracy of 94%, compared with the standard AST, within 3.5 hours [18].

B. Stationary nanoliter droplet array (SNDA)–AST system is a tool that uses (i) a microfluidic device to accelerate the detection of flag molecules of active cellular metabolism and (ii) a combination of a Resazurin assay and lyophilized antibiotics that are contained in a well. Resazurin has the property to be reduced by electron acceptors of cellular metabolic activity such as NADH and FADH, and form Resofurin that emits fluorescence. Only viable cells produce NADH and FADH, hence fluorescence emission can be used to measure the efficacy of the antibiotic treatment. The test provides results in less than 6 hours [18].

C. Smarticles by Roche Diagnostics uses bacteriophages to recognize, bind and invade specific bacteria. It provides bacterial identification and AST with little manipulation and preparation at low cost. This tool uses recombinant bacteriophages that carry the

luciferase gene. When the bacteriophages infect the specific bacterial host the luciferase gene is triggered and light is produced by luciferase-associated enzymatic reactions. This signal (light) is proportional to the number of cells in a sample. Recent reports state 91.8% sensitivity and 98.3% specificity for detection of *Staphylococcus aureus* [18].

D. CAPTURE by GeneCapture, Inc uses a combination of specific nucleic acid probes that attach to the DNA sequence of a pathogen and enable the binding of a fluorescent probe. The fluorescent signals are detected through optical scanning of the sample at various wavelengths and a machine-learning algorithm reports the sensitivity or resistance to an antibiotic. The system can identify the causative bacteria in 45 minutes and can perform an AST in less than 2 hours. The instrument is portable and can be easily used for diagnosis in physician's offices or easily carried by health aides during regular home visits, minimizing any delay, inconvenience and additional costs. The overall sensitivity of the CAPTURE assay is 90%, and the specificity is 100% and can detect concentrations between $2x10^4$ to $1x10^8$ CFU/ml [26], [27].

**Sequencing Technologies:**

Currently, there are various commercially available sequencing platforms. Each technology varies regarding read length (from 25 bp to 10 kb), throughput and time-per-run, dominant error type (e.g., indel, substitution and deletion), overall error rate and cost. Their major advantage is their ability to rapidly sequence entire bacterial genomes and analyze the large amounts of data obtained with bioinformatic tools to detect previously described resistance determinants. The disadvantages of these systems are their high cost, the complex workflow, the need for quality control and interfering contamination events. Additionally, sequencing cannot be used when there is a need for detection of novel resistance genes and uncharacterized mechanisms of resistance. Sequencing is not suitable for daily use in clinical microbiology [18].

Table 2.2 presents an overview of the emerging technologies for bacteria identification and AST.

**Table 2.2. Emerging technologies specifications**

| Technology | Method & Example of Manufacturer | ID/AST | Time needed | Sensitivity Specificity Accuracy | Direct from patient sample | General Information |
|---|---|---|---|---|---|---|

| | | | | | | |
|---|---|---|---|---|---|---|
| Imaging | oCelloScope by Philips BioCell | ID/AST | 1-4.2h | 96% [28] | Y (urine, blood, milk) | Digital time lapse microscopy scanning of the sample |
| Imaging | Accelerate pheno system by Accelerate Diagnostics | ID/AST | <6h | ID: SN=95.6% SP=99.5% AST: SN=95.1% SP=95.5% [29] | Y (blood) | Multiplexed automated digital microscopy |
| Imaging | Bacterial cytological profiling | AST | <2h | Preliminary results 100% | No | Fluorescence microscopy to evaluate changes in the shape of bacteria caused by antibiotics |
| Imaging based & microfluidics | Single-cell morphological analysis (SCMA) | AST | <4h | 91.5% categorical agreement | No | Single-cell morphological analysis (performed in microfluidic agarose channels system) |
| Non-imaging-based | BacterioScan by BacterioScan, Inc. | Bacteria concentration | 3-10h | SN=76% SP=84% [25] | Y (urine) | The laser light scattering (FLLS) determines the number and size of bacterial cells suspended in a solution |
| Lab-on-a-chip | LifeScale by Affinity Biosensor | AST | >3h | - | Y (blood) | Resonant mass measurement |
| Lab-on-a-chip | UtiMax by GeneFluidics | ID/AST | <4h | Accuracy= 94% | Y (urine) | Electrochemical measurement of bacterial 16S rRNA |
| Lab-on-a-chip | Nanodroplets/ nanoliter arrays | ID/AST | <6h | - | Y (urine) | Measurement of the metabolically active bacteria |
| Molecular and biochemical based | Smarticles by Roche Diagnostics | ID/AST | - | SN=91.8% SP=98.3% | - | Bacteriophages carrying luciferase gene-infect bacteria producing detectable light signals |
| Molecular and biochemical based | CAPTURE by GeneCapture | ID/AST | ID:45min AST: additional 5-75 min | SN=90% SP=100% | No | Confirms active pathogens through unamplified RNA expression |

## 2.4 Antibiotics

The antibiotics used in this study were selected for their ability to fight bacteria that cause UTIs with a variety of action mechanisms, including affecting the bacterial DNA, RNA or bacterial cell wall. Employing antibiotics with various action mechanisms is necessary to prove the effectiveness of the proposed SERS technique. The research focused on the following specific antibiotics:

1. **Amoxil** or amoxicillin is a penicillin antibiotic. It is used to treat many different types of bacterial infection such as tonsillitis, bronchitis, pneumonia, gonorrhea, and infections of the ear, nose, throat, skin, or urinary tract. The action mechanism of amoxicillin is that it binds to the penicillin-binding protein 1A (PBP-1A) which is located inside the bacterial cell wall and acylates the penicillin-sensitive transpeptidase C-terminal domain by opening its β-lactam ring. This inactivation of the enzyme prevents the formation of a cross-link of two linear peptidoglycan strands, inhibiting the third and last stage of bacterial cell wall synthesis. Cell lysis is then mediated by bacterial cell wall autolytic enzymes such as autolysins. It is possible that amoxicillin also interferes with an autolysin inhibitor [30]. Amoxicillin is, however, susceptible to degradation by β-lactamases, and therefore, the spectrum of activity does not include organisms which produce these enzymes.

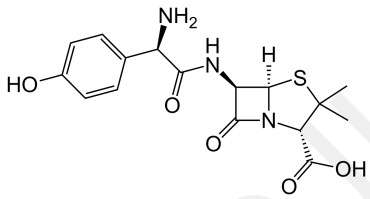


Figure 2.17 Chemical structure of amoxicillin

2. **Augmentin** is an oral antibacterial combination consisting of the semisynthetic antibiotic amoxicillin and the β-lactamase inhibitor, clavulanate potassium (the potassium salt of clavulanic acid). Clavulanic acid is a β-lactam, structurally related to the penicillins, which contains a beta-lactam ring in its structure that binds in an irreversible fashion to beta-lactamases, preventing them from inactivating certain β-lactam antibiotics, with efficacy in treating susceptible gram-positive and gram-negative infections [31]. In particular, it has good activity against the clinically important plasmid-mediated β-lactamases frequently responsible for transferred drug resistance and commonly found in microorganisms resistant to penicillins and cephalosporins. Amoxicillin/clavulanic acid has been shown to be active against most strains of gram-positive aerobes like Staphylococcus aureus, gram-negative aerobes like enterobacter species, *Escherichia coli*, *Haemophilus influenzae*, *Klebsiella species* and *Moraxella catarrhalis*.

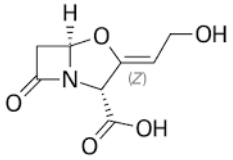

Figure 2.18 Chemical structure of augmentin

3. **Cefaclor** is a semisynthetic, broad-spectrum antibiotic derivative of cephalexin. It is indicated for the treatment of certain infections caused by bacteria such as pneumonia and ear, lung, skin, throat, and urinary tract infections. Cefaclor, like the penicillins, is a β-lactam antibiotic. It binds to specific penicillin-binding proteins (PBPs) located inside the bacterial cell wall and it inhibits cell wall synthesis. Cell lysis is then mediated by bacterial cell wall autolytic enzymes such as autolysins [30].

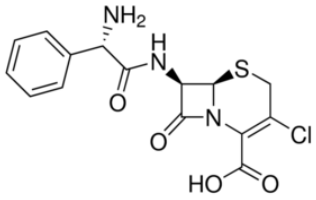


Figure 2.19 Chemical structure of cefaclor

4. **Cefuroxime** is a broad-spectrum cephalosporin antibiotic resistant to β-lactamase. It is indicated for the treatment of many different types of bacterial infections such as bronchitis, sinusitis, tonsillitis, ear infections, skin infections, gonorrhea, and urinary tract infections caused by gram-negative and gram-positive organisms. Cefuroxim's action mechanism is similar to other penicillins [30].

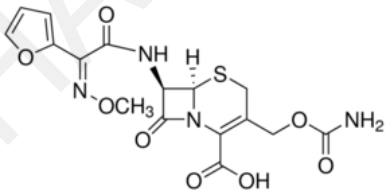


Figure 2.20 Chemical structure of cefuroxime

5. **Ceftriaxone** is a broad-spectrum cephalosporin antibiotic with a very long half-life and high penetrability into the meninges, eyes and inner ears. It is indicated for the treatment of infections caused by *Staphylococcus* sp., *H. influenzae*, *Echerichia coli*, *P. mirabilis* and *Klebsiella* sp.. Ceftriaxone works by inhibiting the mucopeptide synthesis in the bacterial cell wall. The β-lactam moiety of Ceftriaxone binds to carboxypeptidases, endopeptidases, and transpeptidases in the bacterial cytoplasmic membrane. These enzymes are involved in cell-wall synthesis and cell division. By binding to these enzymes, Ceftriaxone results in the formation of defective cell walls and cell death [30].

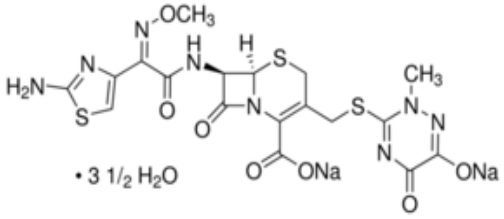

Figure 2.21 Chemical structure of ceftriaxone

6. **Cefazolin** is a semisynthetic cephalosporin analog with broad-spectrum antibiotic action due to inhibition of bacterial cell wall synthesis. It attains high serum levels and is excreted quickly via the urine. Mainly used to treat bacterial infections of the skin. It can also be used to treat moderately severe bacterial infections involving the lungs, bones, joints, blood, heart valve, and urinary tract. The bactericidal action of Cefazolin, like other cephalosporins, results from inhibition of cell wall synthesis [30].

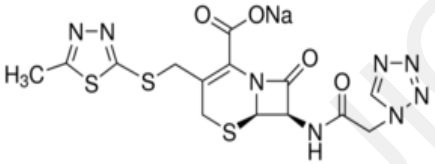

Figure 2.22 Chemical structure of cefazolin

7. **Ciprofloxacin** is a second generation fluoroquinolone. It is formulated for oral, intravenous, intratympanic, ophthalmic, and otic administration for a number of bacterial infections. Ciprofloxacin acts on bacterial topoisomerase II (DNA gyrase) and topoisomerase IV. Targeting the alpha subunits of DNA gyrase prevents it from supercoiling the bacterial DNA which prevents DNA replication [30].

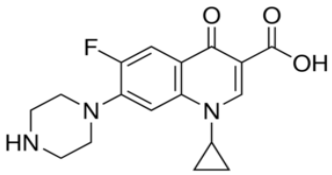

Figure 2.23 Chemical structure of ciprofloxacin

8. **Amikacin** is a semi-synthetic aminoglycoside antibiotic that is derived from kanamycin. Amikacin injection is indicated for the short-term treatment of serious bacterial infections due to susceptible strains of gram-negative bacteria, including *Pseudomonas* species, *Escherichia coli*, *Proteus*, *Providencia species*, *Klebsiella* sp., *Enterobacter*. Clinical studies have shown amikacin to be effective in serious, complicated, and recurrent UTIs. The mechanism of action of amikacin is the same

as that of all aminoglycosides. It binds to bacterial 30S ribosomal subunits and interferes with mRNA binding and tRNA acceptor sites, interfering with bacterial growth. This leads to disruption of normal protein synthesis and production of non-functional or toxic peptides [30].

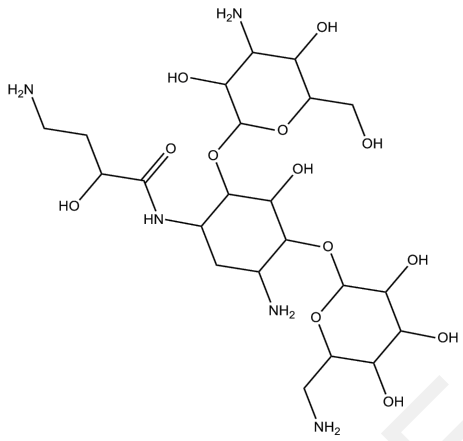

Figure 2.24 Chemical structure of amikacin

### 2.4.1 Solid Culture Antibiogram

Susceptibility-test disks enriched with antibiotics are used for the solid antibiogram. These discs allow semi-quantitative *in vitro* susceptibility testing, using the agar disk diffusion test procedure, for common, rapidly growing and certain fastidious bacterial pathogens. These include the under-study bacteria *Citrobacter spp*, *Proteus*, *Klebsiella* sp., *Escherichia coli* and *Enterobacter*. Agar diffusion methods employing dried filter paper discs impregnated with specific concentrations of antimicrobial agents were developed in the 1940s. The sensitivity or resistance of bacteria to certain antibiotics is determined by the diameter of the clear circle that is created around the susceptibility-test disk. Table 2.1 presents the diameters that would suggest possible resistance, susceptibility or intermediate resistance for the antibiotics that were used for the experimental procedures of this Thesis.

**Table 2.3 Zone diameters for various antibiotics in solid culture antibiograms**

| Zone Diameter Interpretive Chart | | | |
|---|---|---|---|
| **Antımıcrobıal Agent** | **Resıstant** | **Intermedıate** | **Susceptıble** |
| **Amikacin AN-30 30µg** | ≤14 | 15-16 | ≥17 |
| **Amoxicillin/ Clavulanic Acid AmC-30 20/10µg** | ≤13 | 14-17 | ≥18 |
| **Cefaclor CEC-30 30µg** | ≤ 14 | 15-17 | ≥18 |
| **Cefixime CMF-5 5µg** | ≤15 | 16-18 | ≥19 |

| | | | |
|---|---|---|---|
| **Cefuroxime CXM-30 30μg** | ≤14 | 15-17 | ≥18 |
| **Ciprofloxacin CIP-5 5μg** | ≤15 | 16-20 | ≥21 |
| **Norfloxacin NOR-10 10μg** | ≤12 | 13-16 | ≥17 |

### 2.4.2 Liquid Culture Antibiogram

Liquid culture antibiograms specify both the susceptibility but also the appropriate antibiotic concentrations for the treatment. In Table 2.2 the Minimum Inhibitory Concentration (MIC) values of the antibiotics used in this study are presented.

**Table 2.4 MIC Values of Antibiotics**

| Antibiotic/ Interpretation MIC(μg/ml) | Susceptible | Intermediate | Resistant |
|---|---|---|---|
| **Amoxil** | ≤8 μg/ml | - | >8 μg/ml |
| **Augmentin** | ≤18 μg/ml | - | >8 μg/ml |
| **Cefaclor** | ≤8μg/ml | 16 μg/ml | >32 μg/ml |
| **Cefuroxime** | ≤8 μg/ml | - | >8 μg/ml |
| **Ciprofloxacin** | ≤0.5 μg/ml | - | >1 μg/ml |
| **Ceftriaxone** | ≤8 μg/ml | 16-32 μg/ml | >64 μg/ml |
| **Cefazolin** | ≤16 μg/ml | 32 μg/ml | >64μg/ml |
| **Amikacin** | ≤8 μg/ml | - | >16 μg/ml |

## 2.5 Gram-Negative Bacteria

Bacterial cells are extremely small, ranging in size from 0.2μm to 5μm. More specifically, *Escherichia coli* bacteria are ~ 0.5 μm (width) x 2 μm (length). Also, different bacteria have characteristic shapes like cocci, rods and spirals. Bacteria are classified into two main categories based on their cell wall composition: the gram-negative bacteria and the gram-positive bacteria. Gram-positive bacteria have a single cell membrane and a cell wall, composed mostly of a thick layer of peptidoglycan while gram-negative bacteria have an inner membrane a thin layer of peptidoglycan and an outer membrane containing lipopolysaccharide.

Bacterial genera like *Klebsiella* sp., *Proteus* and *Escherichia coli*, that were included in the experimental procedures of this Thesis, belong to the category of gram-negative bacteria. The gram negative cell wall is composed of an outer and an inner cytoplasmic cell membrane. A peptidoglycan layer exists between these two membranes. Moreover, the outer membrane contains, in its outer leaflet, lipopolysaccharides (LPS), which include lipid A, and phospholipids in its inner leaflet. In addition, the gram-negative bacteria cell wall includes porins, periplasm and lipoproteins. Figure 2.15 shows the gram-negative cell wall structure. Furthermore, as it is shown in Figure 2.16, efflux pumps can be found in the outer cell membrane which are sometimes responsible for removing antibiotics from the bacteria and cause resistance [32].

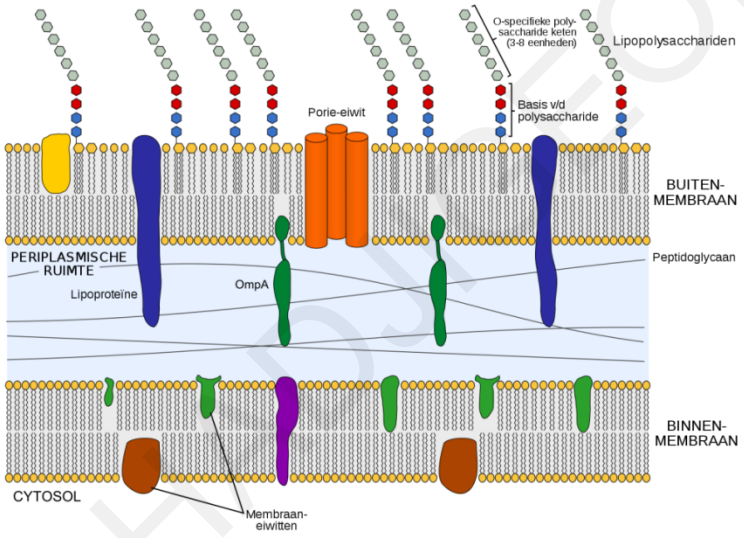


Figure 2.25 Gram-negative cell wall [33]

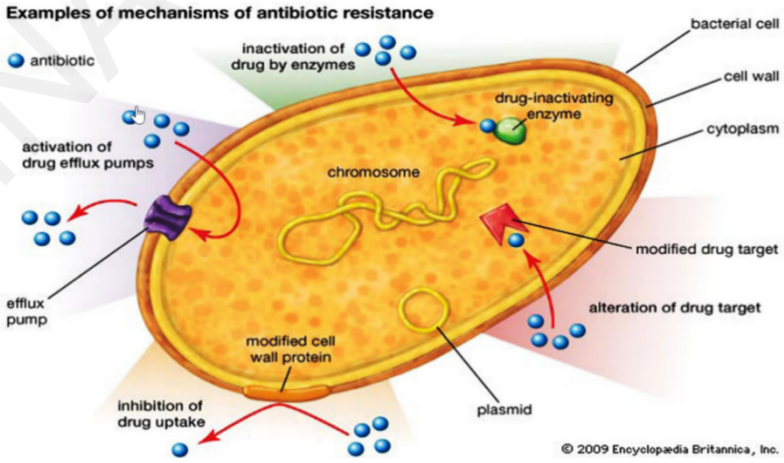


Figure 2.26 Drug efflux pumps can be found in bacterial cell walls

Components of the bacterial cell wall, such as lipids, proteins, carbohydrates, and components of the DNA such as adenine and cytosine, exhibit characteristic peaks in the Raman spectrum (Table 2.3) [34], [35]. This will be further elaborated in the Chapter 6.

**Table 2.5 Bacterial molecules Raman fingerprint peaks**

| Wavenumber ($cm^{-1}$) | Raman Bands |
|---|---|
| 2800–3100 | $CH_3$, $CH_2$ lipids, proteins, olefins |
| 1575–1590 | C–N str proteins, DNA, Amides |
| 1520–1550 | C–H bend |
| 1440–1460 | $CH_2$ lipids, proteins, carbohydrates |
| 1418 | Adenine |
| 1155 | C–N str, amides, DNA, adenine |
| 785–840 | Cytosine, uracil, tyrosine |
| 375 | Guanine |

# Chapter 3
# Raman Spectroscopy

Raman spectroscopy is a spectroscopic technique, based on the interaction of photons with a sample (solid, liquid or gas) which results in scattered radiation at different wavelengths [36]. Raman Spectroscopy is primarily used as a whole organism fingerprinting technique where pathogens are identified based on their unique chemical characteristics.

## 3.1 Raman Spectroscopy Theory

In Raman spectroscopy, a monochromatic light source (i.e. one specific wavelength), such as a laser, is used [36]. When monochromatic radiation is incident on a sample, the incident photons interact with the sample molecules. They will be either reflected, absorbed or scattered. Most of the scattered photons are usually elastically scattered. Hence, they have the same energy, and therefore the same wavelength as well, as the incident photons. This phenomenon is called Rayleigh scattering. A very small proportion (1 in $10^7$) of the incident photons are inelastically scattered. In this case, the scattered photons have lost or gained energy from their interaction with the sample. The wavelength of the reemitted photons is shifted up or down in comparison to the original monochromatic frequency. The energy loss or gain due to inelastic scattering and the energy of the scattered photons is characteristic of the sample material. This phenomenon is called Raman Scattering or Raman Effect [37]. Raman spectroscopy relies on inelastic scattering of monochromatic light, usually from a laser in the near ultraviolet, visible, or near infrared range [38]. There are two kinds of Raman Scattering: Raman Stokes Scattering (less energy, longer wavelength) and Raman Anti-Stokes Scattering (more energy, shorter wavelength).

Raman spectroscopy can be used to study solid, liquid and gaseous samples. The peaks present in the spectrum are characteristic of the sample and depend on the vibrational states of the molecule [39]. Raman Scattering can be explained by the molecular deformations of the electric field. The monochromatic light source can be considered as an oscillating electromagnetic wave with an electrical vector $\bar{E}$. When the light, with frequency $f_0$, interacts with the sample, it excites molecules and transforms them into oscillating dipoles. This action deforms the molecules, with the dipole described by:

$$\bar{P} = a\bar{E}, \qquad \text{Equation 3.1}$$

where:

$\bar{P}$ = electric dipole

$\bar{E}$ = electric field of the laser

$\alpha$ = polarizability.

Due to the periodical deformation, molecules are excited and start vibrating with a characteristic frequency $f_m$. Such oscillating dipoles emit light of three different frequencies (Figure 3.1) when:

1. Rayleigh scattering: The excited molecule returns back to the initial basic vibrational state and emits light with the same frequency $f_0$ as the excitation source [40].

2. Stokes Raman Scattering: Part of the absorbed photon's energy is transferred to the Raman-active mode with frequency $f_m$ and the resulting frequency of scattered light is then reduced to $f_0 - f_m$. This frequency is called Raman Stokes frequency [40] and the scattered photon has less energy than the incident photon. This phenomenon is most commonly observed since most of the molecules are primarily in their ground vibrational state at room temperature [39].

3. Anti-Stokes Raman Scattering: The incident photon is absorbed by a molecule that is already in an excited vibrational state. The excess energy of the excited Raman active mode is released, with the molecule returning to the basic vibrational state, and the resulting scattered photon has an increased frequency $f_0 + f_m$ [40]. In Anti-Stokes Raman Scattering the scattered photon has more energy than the incident photon [39]. It is less probable than Stokes scattering.

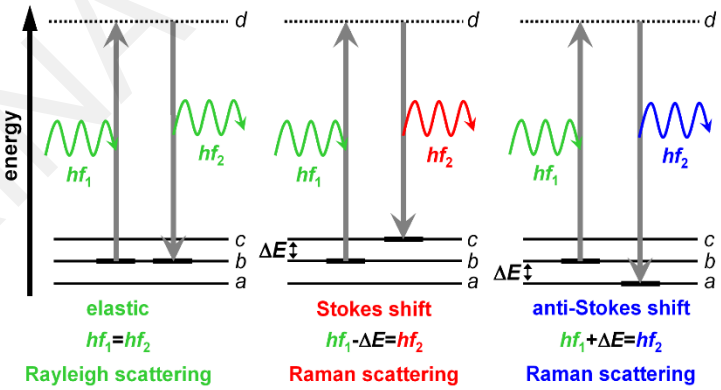


Figure 3.1 Energy level diagram for Raman scattering, Elastic Scattering, Raman Stokes scattering, Raman Anti-Stokes scattering[41]

The Stokes and Anti-Stokes spectra contain the same frequency information. The Anti-Stokes spectrum can be used when the Stokes spectrum is not directly observable, for example, due to poor detector response at lower frequencies [42].

A Raman spectrum is a function of the intensity of scattered photons (y-axis) Vs the vibrational energy difference between the incident photon the scattered photon (x-axis), measured in $cm^{-1}$:

$$\bar{\nu} = \frac{1}{\lambda_{incident}} - \frac{1}{\lambda_{scattered}}$$

Equation 3.2

where:

$\bar{\nu}$ = Raman shift. Vibrational energy difference measured in $cm^{-1}$

$\lambda_{incident}$= incident photon wavelength

$\lambda_{scattered}$= scattered photon wavelength.

These vibrational levels of a molecule are composed of bands representing all possible molecular vibration modes. They depend on the mass of atoms in the molecule, the strength and types of their chemical bonds and the atomic arrangement. Consequently, different molecules have different vibrational spectra and, in other words, different "fingerprints" [42]. Raman spectroscopy is extremely information rich. It is therefore very useful for the chemical identification and characterization of molecular structures [42].

## 3.2 Raman Instrumentation

A Raman system primarily consists of:

1. A light source (A monochromatic excitation source, e.g. a laser).
2. Light focusing optics
3. A spectrograph (wavelength selector)
4. A detector (photodiode array or Charge-Coupled Device (CCD) camera) [43].

A monochromatic excitation source, most commonly a laser, is used, which illuminates the sample. The sample can be excited in the ultraviolet (UV), visible (Vis) or near infrared (NIR) range [40]. The use of a high performance laser source is important for both efficient Raman measurements but also good spectral resolution [39].

The correct selection of the laser wavelength is very important for Raman spectroscopy. For example, many samples, especially those of 'organic' or 'biological' nature are fluorescent species. Exciting those samples with a 532 nm laser (green) can produce significant fluorescence, which can swamp the underlying, weak, Raman spectrum rendering it undetectable. In this scenario, the use of a laser at 633 nm (red) or 785 nm (NIR), may be more appropriate since it will not excite electronic transitions (and hence fluorescence) and so the Raman scattered signal may be easier to detect [39]. However, increasing the

wavelength, from 532 nm to 633 nm or to 785 nm, decreases the scattering efficiency. For this reason, a longer integration time or a higher power laser may be required [39]. Some of the most common lasers used for Raman are CW lasers, such as argon and krypton ion lasers, with a fixed wavelength but also He-Ne lasers which are widely used for micro-Raman Spectroscopy analysis [44].

Light can be delivered to and collected from the sample either directly or via fiber-optic probes [45]. The Rayleigh scattered light, which is much stronger than is Raman counterpart, is blocked by appropriate filters. The Raman scattered signal, which is not filtered out, is directed to a spectrograph where it is analyzed to its constituent wavelengths and projected onto the detector, allowing the latter to acquire a Raman spectrum. The data is collected in raw digital form for further processing on a computer [45]. The detector can be a Photodiode Arrays (PDA) or a CCD camera. In many cases, CCDs are becoming the detector of choice for Raman spectroscopy due to their high quantum efficiency, the extremely low level of thermal noise, when effectively cooled, the low read out noise and the large spectral range available [40]. Additionally, many current dispersive Raman set-ups are now equipped with multichannel two-dimensional CCD detectors. The basic Raman instrumentation is shown in Figure 3.2. Raman systems are commercially available in a variety of sizes and configurations. Depending on the accuracy and sensitivity requirements of the application, the complexity of a Raman system can vary from a simple handheld device to a custom experimental setup [45].

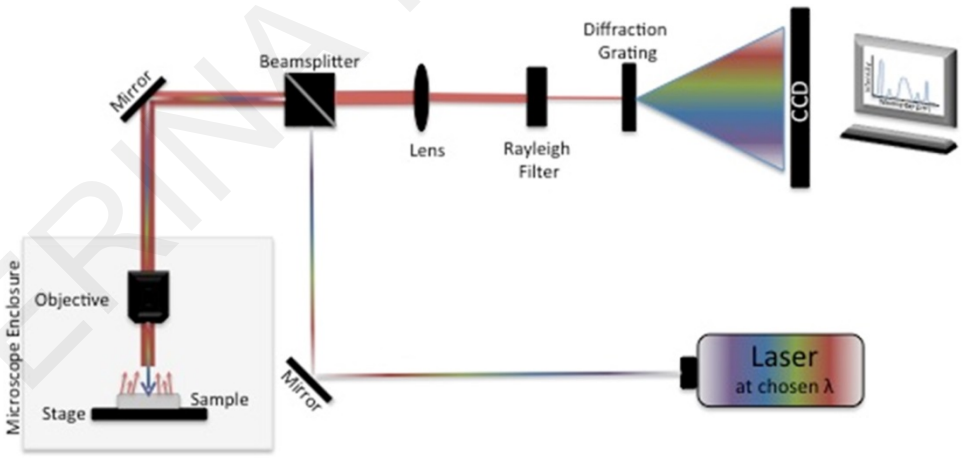


Figure 3.2 Basic Raman instrumentation with a single laser source, fiber-optic delivery probe, spectrograph, CCD, and necessary electronics for power supply and computer interfacing [46]

Raman Spectroscopy has several advantages compared to its main competitor, Fourier-Transform Infra-Red (FT-IR) spectroscopy which also provides vibrational information. Raman provides better spectral and spatial resolution which allows a generation of chemical maps with high spatial resolution and narrow spectral peaks [47]. In addition,

Raman is not affected by the significant absorption of water which exists in the infrared. On the other hand, Raman Spectroscopy has several limitations including the strong fluorescence background and, therefore, suffers from a low dynamic range of measurement. Another limitation of Raman Spectroscopy is the very low efficiency of the Raman Effect itself. This results in extremely weak signals from biological samples. Lastly, Raman often produces highly congested spectra from complicated biological samples, which results in low identification or species selectivity [45].

## 3.3 Enhanced Raman Spectroscopy Techniques

Given the extreme inefficiency of the Raman process, increasing the efficiency of Raman spectroscopy is critical. One of the most effective techniques to enhance the Raman signal is Surface Enhanced Raman Spectroscopy (SERS). SERS was introduced in 1974. When molecules are absorbed onto certain metals (silver, gold and copper), the incident light excites the free electrons in the metal's conduction band and induces plasmon resonance which promotes electronic and chemical interactions between the sample and the SERS substrate, resulting in an enhancement of the Raman signal of up to a theoretical $10^{11}$ [48], [49].

The total enhancement of the SERS effect is a result of an electromagnetic enhancement and a charge-transfer mechanism also referred to as chemical enhancement. SERS enhancement mostly arises from the electromagnetic effect. Electromagnetic enhancement occurs when the incident laser excites surface plasmons (electrons at the metal surface that collectively oscillate upon excitation), thereby creating an electromagnetic field extending up to 10 nm from the metal which enhances the Raman signals of the exposed molecules by an average of $10^4$. Furthermore, single molecule enhancements of $10^{11}$ can occur at nanoparticle junctions where electromagnetic fields overlap. The charge-transfer mechanism, i.e. the transfer of electrons between the molecules under observation and the metal surface, contributes an additional 10-100 times enhancement when the analyte is in direct contact with the metal. Maximum resonance enhancement is possible if the laser wavelength is close to the absorption wavelength of the sample [48], [49]. Another benefit of SERS is the reduction of the fluorescence due to the adsorption of the analyte on to the metal surface [50].

The main disadvantage of SERS is the difficulty of interpreting the spectra. The signal enhancement is so dramatic that Raman bands that are very weak and otherwise unnoticeable in spontaneous Raman, appear strong in SERS. Because of this, some trace

contaminants can also contribute to the Raman spectral shape. In addition, because of chemical interactions with the metal surface, certain peaks, which are strong in conventional Raman might not be present in SERS at all [49].

Overall, as a result of the large enhancement effect, SERS provides both rich spectroscopic information and high sensitivity. These attributes enabled SERS to become the ideal spectroscopic technique for trace analysis. Additionally, due to the fluorescence-quenching effect, SERS is extremely useful in examining microorganisms, which normally exhibit a high fluorescence background under excitation from the visible to the NIR regions [48].

## 3.4 Optical Properties of Nanoparticles

One of the most convenient methods to enhance the Raman signal of an analyte is to bring it in contact with appropriate metal nanoparticles. The optical properties of spherical nanoparticles are highly dependent on the material, shape, diameter and aggregation effect. The absorption peak of the nanoparticle, which defines the resonant wavelength, can be tuned by varying those parameters. For example, it has been shown that spherical nanoparticles have only one absorption peak in the visible region while rod shape nanoparticles exhibit two absorption peaks, in the visible and NIR, due to the different oscillation modes (longitudinal vs. transverse) of the elongated structure. Figure 3.3 illustrates the absorption spectrum of a spherical silver nanoparticle while Figure 3.4 shows the absorption spectrum of a rod shape nanoparticle [51]. In addition, spherical nanoparticles with smaller diameter absorb light and have spectral peaks in the visible region, while larger nanoparticles exhibit broader and more red-shifted peaks as well as increased scattering. This effect is visible in Figure 3.3.

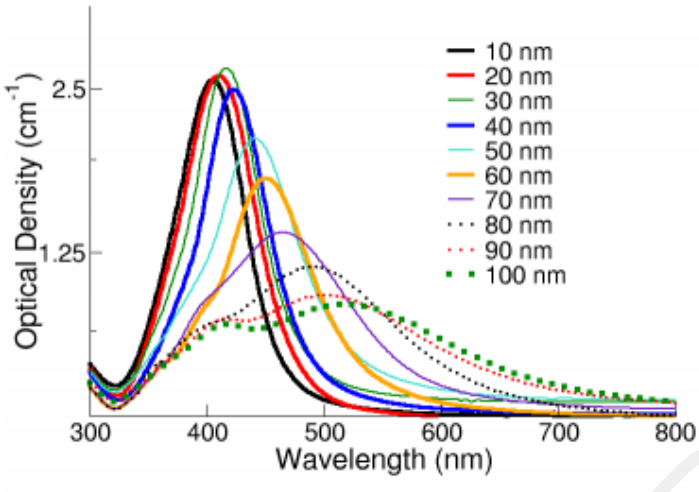


Figure 3.3 Absorption spectrum of Ag spherical nanoparticles [51]

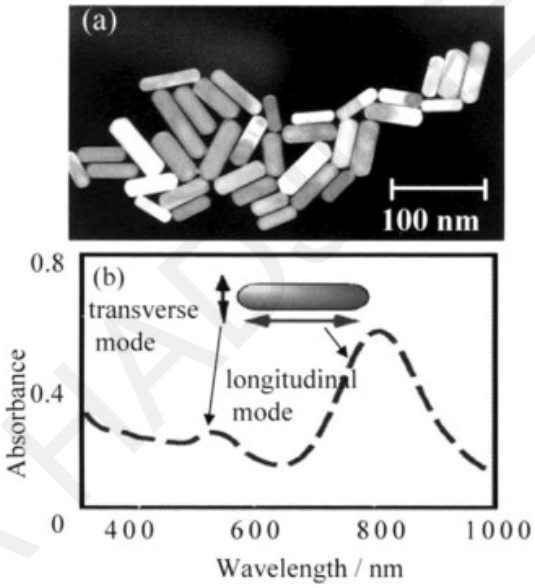


Figure 3.4 (a) Transmission electron microscopic (TEM) image of Au nanorods (b) and their absorption spectrum [51]

Another factor that affects the absorption spectrum is nanoparticle aggregation. When particles aggregate, the surface plasmon resonance shifts to lower energies because the conduction electrons near each particle surface are shared amongst aggregated particles. This effect causes the absorption peaks to broaden, shift to longer wavelengths, and have lower intensity. Moreover, a secondary peak may arise at longer wavelengths. To determine the absorption spectrum and characterize the nanoparticle solution UV/Visible spectroscopy is used [52].

## 3.5 Relevant Applications of Raman Spectroscopy

Several applications of Raman Spectroscopy relevant to the subject matter of this thesis have been reported. They include identification, detection, differentiation-discrimination and quantification of bacteria as well as research studies into the biochemistry of bacteria.

Many bacterial strains have been examined with Raman during the last few decades, including *Escherichia coli*, *Acinetobacter calcoaceticus*, *Pseudomonas aeruginosa*, *Bacillus megaterium*, *Salmonella typhimurium*, *Bacillus cereus*, *Bacillus thuringiensis*, *Bacillus anthracis*, *Bacillus subtilis*, *Brevibacillus*, *Staphylococcus cohnii*, *Staphylococcus warneri*, *Staphylococcus epidermidis*, *Enterobacter aerogenes*, *Streptococcus pyrogenes*, *Enterococcus faecalis*, *Streptococcus salivarius*, *Pseudomonas aeruginosa*, *Lactobacillus acidophilus*, *Bulgaricus*, *Streptococcus thermophiles*, *Mycobacterium smegmatis*, *Mycobacterium fortuitum*, *Shigella sonnei*, *Proteus vulgaris*, *Erwinia amylovara*, *Helicobacter pylori* [53]–[62]. Moreover, Forrester et al., used infrared spectroscopy to identify the exact species of bacteria (*Bacillus cereus*, *Bacillus megaterium*, *Bacillus subtilis*, *Bacillus thuringiensis*) in the sporulated state [63]. In addition, other research groups like Premasiri et al. and Maquelin et al., also studied the ability to obtain single cell level Raman spectra [60], [64]. Xie et al., achieved accurate identification of single bacterial cells in aqueous solution using confocal laser tweezers Raman Spectroscopy [62].

Various Raman systems, with excitation at different wavelengths from UV to the NIR (250-800nm), have been utilized in order to identify the bacteria. Zeiri and Efrima observed the spectral signatures from different biochemical components of *Escherichia coli* while varying between nine laser excitation wavelengths. More precisely, a frequency-doubled argon ion laser exciting at 244 and 257nm, a He-Cd laser at 325 and 442nm, an air-cooled argon ion laser at 457, 488 and 514 nm, a He-Ne laser supplied at 633nm and a diode laser at 785nm were utilized [65]. Furthermore, Schmid et al., identified single bacterial cells by micro-Raman spectroscopy in several strains of bacteria at 532 nm excitation and spectra in the spectral range of 537 $cm^{-1}$ to 3654 $cm^{-1}$ [66].

Lopez-Diez et al., developed UV resonance Raman spectroscopy, with a laser exciting at 244nm, for the reproducible acquisition of information rich Raman fingerprints from endospore-forming bacteria belonging to the genera *Bacillus* and *Brevibacillus* [58]. Gaus et al., also used UV-resonance Raman spectroscopy, with a micro-Raman setup with an Argon-ion laser exciting at 244 nm, in order to identify lactic acid bacteria in yogurt [55].

In the visible range, Harz et al., used a micro-Raman setup, with a frequency doubled Nd:YAG laser at 532nm, to discriminate and classify several bacterial species and strains while Sengupta et al., utilised an argon-ion CW laser operating at 514.5 nm to analyze *Escherichia coli* and *Pseudomonas aeruginosa* that have been diluted in water at concentrations ranging from $10^2$ to $10^5$ cfu/ml [56], [61]. Guicheteau et al., aimed to identify bacterial mixtures of different kinds of bacillus using Raman and surface-enhanced Raman imaging, utilizing a Raman imaging microscope equipped with a 532-nm laser [67]. In the NIR range, Patel et al, performed Surface Enhanced Raman Spectroscopy utilizing a Renishaw Raman microscope exciting at 785 nm in order to identify pathogens such as bacillus. In addition, Xie et al. used a diode laser at 790 nm in order to identify single bacterial cells in aqueous solutions and Cam et al., used an 830 nm diode laser to identify bacteria at species and strain level [53], [59], [62]. Furthermore, Nicolaou et al., performed Fourier Transform Infrared Spectroscopy and Raman spectroscopy with a 785 nm diode laser in order to detect and enumerate *Staphylococcous aureus* in milk, as well as to study the growth interaction between *Staphylococcous aureus* and *Lactococcus lactis ssp. cremoris* [68]. Another research team, Zhu and Berger, utilized longer wavelengths. They aimed to identify oral Streptococci bacteria using Raman with a diode laser at 830nm [69].

In order to enhance the Raman signal, various research groups exploited the plasmon properties of noble metal nanoparticles. One of the first teams to utilize Raman enhancement was Nie and Emory, who in their study performed optical detection and spectroscopy of single molecules and single nanoparticles at room temperature with the use of Surface-Enhanced Raman Spectroscopy (SERS) and silver colloidal nanoparticles [70]. Kneip et al. exploited the extremely large effective cross sections of SERS, to achieve the first observation of single molecule (single crystal violet molecule) at 830 nm [71]. Efrima et al., utilized silver and gold colloids as enhancement media and even produced the colloids in the presence of the bacteria [54], [65], [72]. Premasiri et al., studied the magnitude of the Raman enhancement effect and the reproducibility obtained from gold particle covered $SiO_2$ chips, contrasting the SERS and bulk Raman spectra of *Escherichia coli*, *Salmonella typhimurium* and various strains of Bacillus bacteria [60]. Kudoa et al., performed SERS using Ag nanoparticle aggregates that were directly photo-reduced on the pathogenic bacterium *Helicobacter pylori* [57]. Cam et al. who exposed the bacterial samples to a mixture of Ag nanoparticles of several sizes and shapes with an average diameter of 50 nm [53]. Furthermore, Cheng et al., utilized a gold nanoparticle/polyvinylpyrrolidone/gold substrate

(AuNPs/ PVP/Au), a biomarker for bacterial spores including *Bacillus anthraces*, to perform ultrasensitive detection of dipicolinic acid (DPA), [73].

Among the various factors that affect the Raman spectra of are the growth conditions of the bacteria. Harz et al., studied Raman spectra recorded from single bacteria that were grown under several cultivation conditions with respect to the nutrient medium, incubation temperature and culturing age [56]. Another research group, Hutsebaut et al., investigated the effect of culture conditions on the achievable taxonomic resolution of Raman Spectroscopy [74]. In addition, a study worth mentioning is the research of Sengupta et al., who aimed to detect and identify dilute bacterial samples with SERS. The detection limit of this technique was determined by subtracting the vibrational $H_2O$ background from the SERS spectra of very dilute suspensions of bacteria with concentrations ranging from $10^2$ to $10^5$ cfu/ml [61].

Many research groups conducted experiments in order to classify strains of bacteria. Mello et al., were able to descriminate *Escherichia coli*, *Salmonella choleraesuis* and *Shigella flexneri*, *Staphilococcus aureus*, *Streptococcus pyogenes* and *Neisseria gonorrhoeae* with a low-resolution Raman Spectrometer, coupled to a near-infrared 785 nm multimode diode laser [75], [76]. Preisner et al., assessed FT-IR spectroscopy in the wavenumber range of 4000 $cm^{-1}$-600 $cm^{-1}$, for the identification of *Acinetobacter baumannii*, *Enterococcus faecium*, *Staphylococcus aureus* and *Staphylococcus epidermidis* bacteria [77].

In order to differentiate and discriminate, at strain level, both sporulated and vegetative bacterial samples of five *Bacillus* bacterial strains, Foster et al., used a combined mid-infrared spectroscopic/statistical modelling approach [78]. Furthermore, Willemse-Erix et al., used four different collections of *Staphylococcus aureus* (MSSA) and MRSA isolates in order to demonstrate the effectiveness of a High Performance Raman Spectroscopy Module with 785nm laser light, as a typing tool that could be used in epidemiological surveillance studies [79]. Also, Green et al., investigated the ability to distinguish six different species of *Listeria* with the use of SERS utilizing a semiconductor laser source. Furthermore, Walter et al., used UV resonance Raman to perform a bulk to single-cell classification of the filamentous growing streptomyces bacteria [80], [81]. Additionally, Mobili et al., aimed to rapidly differentiate heterofermentative related *Lactobacilli* [82].

The detection and characterization of UTI with Raman Spectroscopy was studied by Jarvis and Goodacre. Their work suggested SERS could be a rapid whole-organism

fingerprinting method for the characterization of the bacteria associated with UTIs. In their studies, they analyzed closely related groups of bacteria belonging to the genus *Bacillus*. As an enhancement factor they employed aggregated silver colloid substrates. Additionally, their group studied SERS spectra from intracellular and extracellular bacterial locations [47], [83], [84].

Micro-fluidic devices can help to achieve fast, high specificity and reproducible bacterial detection with SERS measurements. Metalized, nanostructured polymer substrates for pathogen detection were also investigated for their applicability to techniques for label-free *in situ* detection of microorganism pathogens and their toxins on a microarray biochip [81], [85]–[87].

Another application of Raman spectroscopy is to extract the biochemical constituents of various bacteria. Schuster et al., performed confocal Raman microspectroscopy (He-Ne laser at 632.8 nm) to assess the heterogeneity within a bacterial cell population by providing spectral information of the chemical composition of single bacterial cells [88]. Furthermore, Ede et al., investigated the structural changes occurring in the cells of various bacteria during their growth curves, utilizing Fourier transform infrared (FT-IR) spectroscopy [89]. Escoriza et al., aimed to identify spectral variations throughout the growth cycle of *Escherichia coli* and *Staphyloccocus epidermidi* using a Raman chemical imaging microscope with a Nd: YV04 laser at 532 nm [90]. De Gelder et al., performed a more detailed interpretation of bacterial Raman spectra in order to extract biochemical information about the cell's metabolism, focusing on relative changes in certain biomolecules during five different stages of growth of *Cupriavidus metallidurans* [91].

Baek et al., was one of the first groups to distinguish live bacteria from bacteria that were killed by heating [92]. Guicheteau et al., aimed to classify live bacillus spores and formalin killed bacillus by SERS [93]. Further, Escoriza et al., applied Raman spectroscopy to study *Escherichia coli* and *Staphylococcus epidermidis* bacteria that were inactivated by different chemical and stress conditions. Utilizing this approach they studied the viability and the metabolic changes of bacteria [94]. In addition, Liu et al., performed analysis of bacterial changes during their growth and studied the bacterial response to antibiotic treatment [95]. Kahraman et al., systematically evaluated the bacteria species of *Bacillus megaterium*, *Escherichia coli*, *Staphylococcus aureus* and *Staphylococcus cohnii* in order to demonstrate the source of the features of bacterial SERS spectra [96]. Worth mentioning is the work of Lopez-Diez et al., who developed UV resonance Raman

spectroscopy to monitor the concentration effect of antibiotics on *Pseudomonas aeruginosa* bacteria [97].

## 3.6 Recent advances in SERS for UTI diagnosis, bacteria identification and Antibiotic Sensitivity Testing (AST)

Ting-Ting Liu et al. have demonstrated that: (i) SERS profiles are indicative of the chemical features of the bacterial envelope, since silver nanoparticles aggregate mostly at the outer surfaces of the bacteria, and, therefore, subtle structural alterations in the cell morphology might contribute to the SERS changes observed; (ii) the different components and architecture between gram-positive and gram-negative bacteria envelopes can be detected with SERS; and (iii) gram-negative bacteria in different growth phases exhibit discernibly different SERS spectral profiles, due to changes in the bacterial envelope as the bacteria divide at different rates. Figure 3.5 illustrates these SERS changes, which are present only in gram-negative (at the start of exponential phase, towards the end of exponential phase and at the stationary phase) but not gram-positive bacteria. These findings were also verified by SEM imaging that revealed a decrease in the aspect ratio of the rod-like gram-negative bacteria [95] .

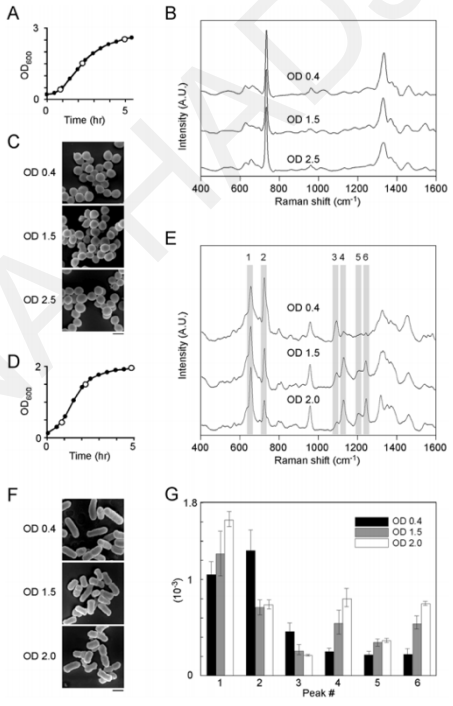


Figure 3.5 SEM images and SERS spectra indicating variations caused from different growth phases

Avci et al., isolated seven different species of bacteria from urine samples received from patients with UTI. Bacterial species were cultured for 24 hours in agar plates to grow and were, subsequently, re-cultured in separate petri-dishes for 1, 2, 4, 6, 8, 10, 12, 18, and 24 h. Raman spectra were acquired at every time slot from the seven species of bacteria and PCA

was performed to differentiate the bacteria. The results after performing PCA showed that all bacteria were discriminated at all time points during their growth. After this experimental study authors concluded that 1 h incubation is sufficient for culture-based SERS studies for the discrimination of bacteria [98].

To overcome the challenge of bacteria immobilization on glass slides Yang et al. created a portable bacteria-grasping chip for SERS identification and classification. The chip was first modified with a positively charged $NH^{+}_{3}$ group so that the glass slide would become positively charged and, therefore, negatively charged bacterial cells could be grasped tightly to the glass through electrostatic adsorption. For this experimental series, bacterial species *Escherichia coli*, *Pseudomonas aeruginosa* and *Proteus mirabilis* were cultured in LB broth culture medium or artificial urine to achieve concentrations of about $1x10^5$ cells/ml. Silver nanoparticles were added and the Raman fingerprints of the pathogens (collected either directly from LB broth or artificial urine or after filtration/centrifugation/washing of the samples) were received. The fingerprints of each bacteria could be clearly observed and recorded. Furthermore, utilizing discriminant analysis, it was feasible to classify and identify the three bacterial species within 1.5 hour [99].

The research team of Tien et al. developed a cylindrical SERS chip for optimum signal enhancement in order to collect data directly from urine samples. Urine samples were collected from 108 UTI patients. A portion of the samples were examined with a BD Phoenix Automated Microbiology System and MALDI-TOF system and the results from the conventional bacterial culture were used as a reference. The rest of the urine samples were centrifuged at 700 rpm for 10 min and the supernatant was loaded onto the cylindrical Raman SERS chip for bacteria identification and antibiotic susceptibility. The cylindrical SERS chip consisted of silver nanoparticles coated on the tip of a 2 mm polymethylmethacrylate rod (AC). The specific SERS substrates showed enough hydrophobicity to restrict aqueous sample to the tip area, preventing the spreading of the solution. The Raman spectra were analyzed resulting in 93 out of 108 samples successfully identified using SERS. Four samples needed further concentration in order to be identified by the SERS system. Antibiotic susceptibility was feasible with SERS in combination with PCA. Finally mixed flora infections could be identified by combining SERS and PCA methods [100].

Mircescu et al. aimed to develop a novel method in order to reproducibly identify strains of *Escherichia coli* and *Proteus mirabilis* bacteria, independently of O-type antigen, strain and growth phase by using immobilization of the bacteria on the glass slide and development of novel SERS substrates. Glass slides were modified by inducing a positive charge to immobilize the negatively charged bacteria on the surface of the slide. For signal

enhancement, the SERS substrates were, first, created in the presence of bacterial species. Silver nitrate was added and let to adhere for 1 hour, and then a hydroxylamine hydrochloride reducing agent was added and let to act for another 1 hour. After several hours, silver islands/dark spots formed as shown in Figure 3.6. The silver islands provided the enhanced Raman spectra. This approach provided reproducible SERS spectra, however, it required a long incubation time and the *in-situ* synthesis that may affect the viability of the bacteria. In order to improve the time efficiency and the viability of the bacterial species, the sample harvested from an overnight culture was applied on the glass surface and left to adsorb for 30 min and then silver NPs (four times concentrated) were added and left for another 30 min. Using this approach, the experimental time was reduced to less than 2 hours. The data were processed utilizing PCA and the results indicate discrimination of *Escherichia coli* and *Proteus mirabilis* with satisfying selectivity.

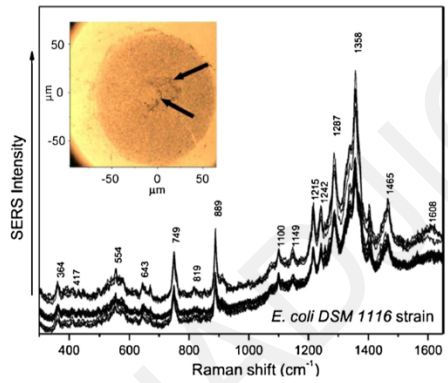


Figure 3.6 SERS spectra were collected after electrostatic immobilization and in situ silver substrate preparation. The arrows indicate silver clusters

A major challenge in bacteria identification from Raman spectra is presented by samples containing more than one bacterial species in the same solution. Yogesha et al., attempted to distinguish bacterial in samples containing two and three species. *Escherichia coli*, *Klebsiella pneumoniae*, *Proteus vulgaris*, *Proteus mirabilis* and *Staphylococcus aureus* were used. For the preparation of mixtures of two or three bacteria, the bacteria were initially incubated individually, overnight at 37 °C, and the pellets of individual bacterial species were resuspended in PBS and mixed. For the two bacterial species solutions, *Escherichia coli* and *Staphylococcus aureus* were used while for the three bacterial species solutions, *Escherichia coli*, *Proteus vulgaris*, and *Staphylococcus aureus* were used. Raman spectra were collected using a micro-Raman setup with an excitation wavelength of 785 nm and processed using the PLS-DA method. An overall accuracy of up to 90% for the two-bacteria mixtures and 93% for the solutions of three bacteria, was demonstrated. The same data were

tested utilizing an SVM model with the overall accuracies increasing to 95% and 96%. These results indicate the bacterial species in a mix flora solution can be accurately identified [101].

Another obstacle that must be overcome is the isolation of bacteria from urine samples. For that purpose, Premasiri et al. used a four-stage gravity filtration system as it is presented in Figure 3.7. Each sequential stage of the filtration system had a decreasing pore size. Initially the sample passed from a 200 mg ball of glass wool, and afterwards the urine passed through 30-, 10-, and 5-μm nylon mesh sheets. Twelve bacterial strains were isolated from clinical urine specimens, overnight cultured in nutrient broth and again grown in freshly collected human urine establishing final concentrations of $1x10^5$cells/ml. Afterwards, SERS spectra were collected, utilizing gold NPs, and the bacterial species were classified with PLS-DA. The sensitivity and specificity, averaged over all twelve classes, were 95.8 and 99.3%, respectively. Furthermore, the classification of an unknown sample grown in non-processed urine was correctly identified as *Escherichia coli*. This growth-free diagnostic was accomplished in less than 1 hour. Another interesting finding in this study was that all observed vibrational features could be attributed to the spectral contributions of six purines: adenine, hypoxanthine, xanthine, guanine, uric acid, and AMP. These molecular species result from the nucleotide and nucleic acid metabolic degradation, due to the relatively rapid bacterial starvation response, and their subsequent secretion into the extracellular regions near the outer cell wall where the NPs are aggregating [102].

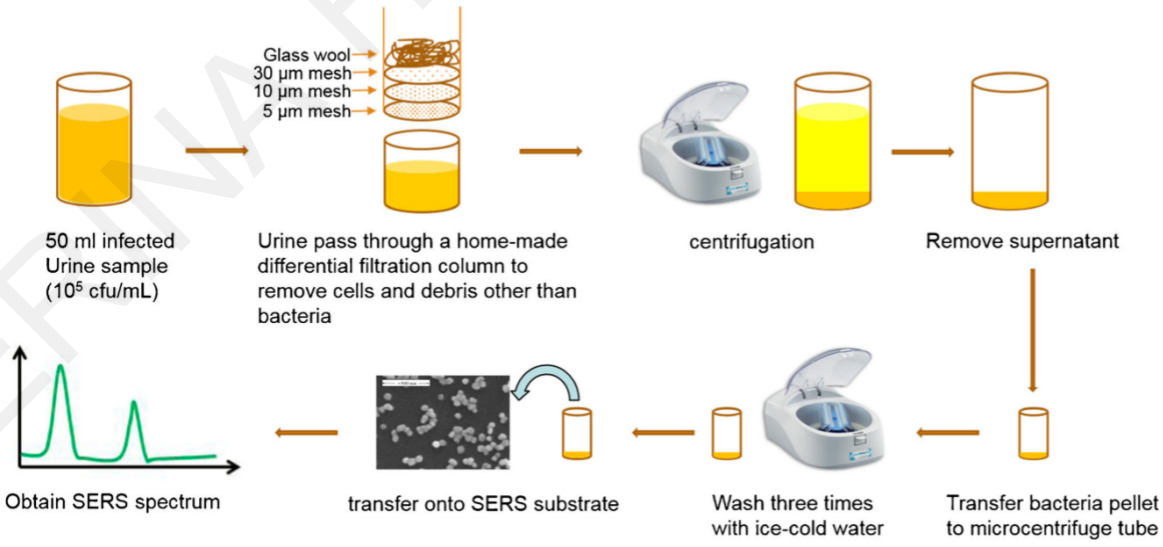


Figure 3.7 An overview of the sample preparation procedure for the acquisition of a SERS spectrum from a human urine sample including a four-stage gravitation filtration system.

For the evaluation of Raman spectroscopy as a reliable tool for identification of bacterial species directly from urine samples, Neugebauer et al. (i) initially created a

reference database of Raman spectra from eleven different bacterial species, including *Escherichia coli*, *Klebsiella spp.*, *Enterococci*, *Staphylococci* and *Pseudomonas aeruginosa*, after overnight culture. All the bacterial species were initially cultured at 37 °C for 24 hours and in total more than 200 spectra were collected from single cells per species resulting in 2952 spectra. The utility of the database for classification was evaluated using (ii) data collected from bacteria that originated from centrifuged urine samples and (iii) data collected from a suspension placed on a dielectrophoresis chip. An SVM model was tested with 514 independently measured Raman spectra from the same eleven bacterial species providing a prediction accuracy of 95%. In order to evaluate the method on samples directly from urine, first, urine samples were centrifuged and the washed bacteria were placed on a Nickel foil and dried. Afterwards, the Raman spectra were recoded and for each single-cell measurement, the correct classification ranged between 66% and 98%. In addition, this study showed that Raman spectroscopic analysis could identify pathogens from urine despite the presence of antibiotics or other growth-inhibitory substances. In a second approach, the Raman spectra were collected directly from urine suspensions. To create the urine suspension, urine samples from different patients with a single pathogen UTIs ($10^5$ cells/ml, *Enterococcus faecalis* or *Escherichia coli*) were filtered utilizing a membrane filter of 5-μm pore diameter (to remove bigger particles such as leukocytes or epithelial cells), and then centrifuged. The pellet was then washed twice with PBS and finally resuspended in PBS. One droplet of the suspension was placed on the dielectrophoresis chip with four gold electrodes (Figure 3.8). An alternating electric field was applied to the gold electrodes so that the bacteria would experience a force pulling them towards the the center. Therefore, bacteria aggregated in a well-defined region from which the Raman spectra were collected. High prediction accuracy was reported for the differentiation of the bacterial species *Escherichia coli* and *Enterococcus faecalis*. The entire procedure required 35 minutes. Additionally, it was proved that the electric field does not influence the viability of the captured bacteria [103].

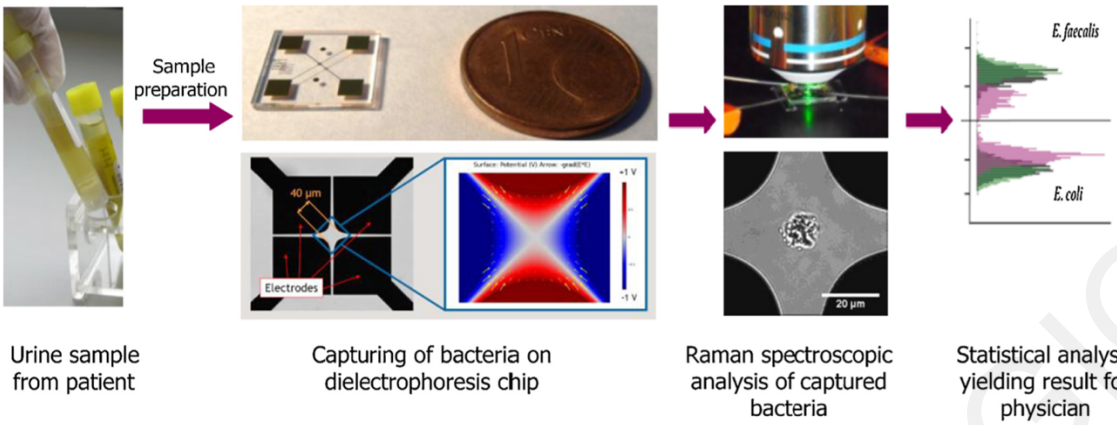


Figure 3.8 An overview of the procedure for bacteria identification utilizing a dielectrophoresis chip

Ting-Ting Liu et al. have worked extensively on the identification of the effects of incubation with antibiotics on the Raman spectra of bacteria. The SERS profiles of bacteria were recorded every five minutes after the addition of the antibiotics (five-fold above the known minimal inhibitory concentrations (MIC)). The results indicated that there were changes in the SERS spectra at about 20 min after the antibiotic exposure while after two hours of antibiotic treatment, the SERS profiles changed significantly indicating cell wall disruption. In addition, the bacterial species *Staphylococcus aureus* were treated with antibiotics that target the cell-wall such as ampicillin, vancomycin and cefotaxime, and with antibiotics which inhibit protein synthesis such gentamicin or tetracycline. The SERS profiles of bacteria exposed to antibiotics that target the cell-wall revealed changes within an hour while SERS profiles of bacteria exposed to antibiotics which inhibit protein synthesis revealed changes after a relatively long treatment of about 9 to 12 hours [95].

The research team of Neugebauer et al. developed a Raman-based method that could distinguish vancomycin-resistant *Enterococci* from vancomycin-sensitive *Enterococci* within 3.5 hours. They demonstrated that changes in the Raman spectra could be observed as early as 30 min from the time that bacteria were mixed with the antibiotic. In addition, the research team utilized a three level PLS-LDA- LDA model to distinguish the sensitive from the resistant strains and the Leave-one-batch-out validation, yielded 86% sensitivity and 93% specificity, with respect to the prediction of vancomycin resistance in *Enterococcus faecalis*, when the model is tested with data of an independent biological replicate. This method provided results in less than 3.5 hours [103].

An interesting approach for defining antibiotic susceptibility directly from clinical urine samples, without the need for urine pre-cultivation, is the combination of single-cell Raman spectroscopy with heavy water labeling (Raman-$D_2O$). It has been observed that, when Raman spectroscopy is combined with stable isotope probing (SIP) such as with C, D, and

N, intracellular assimilation of isotope-labeled substrates can generate characteristic Raman shifts that could be used to quantitatively monitor the microbial activity and alterations due to the exposure to antibiotics. By incorporating a D into the sample, a new C−D bond is generated in a silent spectral region. By comparing the C−D band is feasible to distinguish resistant and susceptible cells due to their different activities in response to antibiotics after a short 30 min incubation. The results of such a study showed that the susceptibility profiles of 14 pathogenic bacterial strains (including 3 in clinical urine samples) in response to antibiotics with different mechanisms of action, were all correctly determined by Raman-$D_2O$ with a 100% categorical agreement in comparison with standard disk diffusion assay. In addition, the total assay time from receiving the urine to S/R readout was shortened to only 2.5 hours. However, 10-fold the MIC antibiotic concentrations were used [104].

Table 3.1 present a brief review of the most recent advancements in the field of UTI diagnosis and antibiogram utilizing SERS.

**Table 3.1 Review of recent advancments in the field**

| **Authors/ Year/ Cite** | **Title** | **ID/ AST/ Time needed/ Direct from urine** | **Bacterial Species/ Antibiotics** | **Application Results/ Algorithms/ Raman System** |
|---|---|---|---|---|
| Kai Yang et al./ 2019/ 9 | Rapid Antibiotic Susceptibility Testing of Pathogenic Bacteria Using Heavy-Water-Labeled Single-Cell Raman Spectroscopy in Clinical Samples | AST/ 2.5h/ Yes | *Escherichia coli*, *Salmonella enterica*, *Shigella flexneri*, *Proteus vulgaris*, *Klebsiella variicola*, *Escherichia fergusonii*, *Providencia rettgeri*, *Klebsiella singaporensis*, *Klebsiella pneumoniae* | AST utilizing heavy water<br>____<br>100% categorical agreement with disk diffusion tests<br>____<br>532nm micro-Raman 100x dry objective<br>____<br>Susceptibility profiles of 14 bacterial strains including 3 in clinical urine samples in response to antibiotics with different mechanisms of action were correctly determined by Raman-$D_2O$ with a 100% categorical agreement regarding standard disk diffusion assay<br>____<br>Performance of AST on a low number of bacteria in clinical samples<br>____<br>10 × CLSI MIC breakpoint |
| Ertug Avci et al./ 2015/ 13 | Discrimination of urinary tract infection pathogens by means of their growth profiles using surface | ID/ 2h/ No | *Escherichia coli*, *Enterococcus faecalis*, *Staphylococcus aureus*, *Staphylococcus* | Analyze spectral variations in different growth phases<br>___<br>Raman microscopy diode laser at 830 nm and 50× objective<br>____ |

| | | | | |
|---|---|---|---|---|
| | enhanced Raman scattering | | *saprophyticus*, and *Klebsiella pneumoniae* | All species were differentiated regardless their growth phase<br>____<br>PCA, Normalization (sum of intensity is 1) |
| Danting Yang et al./ 2018/ 3 | Portable bacteria-capturing chip for direct surface-enhanced Raman scattering identification of urinary tract infection pathogens | ID/ 1.5h/ No/ Yes | *Escherichia coli*, *Pseudomonas aeruginosa* and *Proteus mirabilis* | Identification and classification of bacteria with concentration $1x10^5$ utilizing a positively charged chip<br>____<br>Discriminant analysis (Mahalanobis distance)<br>____<br>Raman microscope using 633 nm laser line |
| Ni Tien et al./ 2018/ 5 | Diagnosis of Bacterial Pathogens in the Urine of Urinary-Tract-Infection Patients Using Surface-Enhanced Raman Spectroscopy | ID/AST/ -/ Yes | *Escherichia coli*, *Pseudomonas*, *Proteus*, *Citrobacter, Staphylococcus aureus, Enterococcus*<br>____<br>Antibiotics: gentamicin, vancomycin, oxacillin, cefazolin, ceftriaxone, ciprofloxacin, gentamicin, ceftazidime | 93 out of 108 samples were successfully identified by SERS technique, four samples needed further concentration in order to be discriminated by the SERS system<br>____<br>Antibiotic susceptibility was feasible by SERS utilizing PCA<br>____<br>Mixed flora infections were identified utilizing PCA<br>____<br>SERS substrates: Cylindrical SERS made up of silver nanoparticles coated on the tip of a 2 mm polymethylmethacrylate rod<br>____<br>Antibiotics with a concentration higher than the minimal inhibitory concentration (MIC) were used.<br>____<br>Raman spectrometer with wavelength of 785 nm |
| Yogesha M et al./ 2019/ 3 | A micro-Raman and chemometric study of urinary tract infection-causing bacterial pathogens in mixed cultures | ID from solutions with mixed bacterial species/-/ No | *Escherichia coli, Klebsiella pneumoniae, Proteus vulgaris, Proteus mirabilis, Staphylococcus aureus* | Correct classification of mixed flora infections:<br>1. x2 bacterial species<br>PLS-DA=90%<br>SVM=95%<br>2. x3 bacterial species<br>PLS-DA=93%<br>SVM=96%<br>____<br>Raman system: 785nm |
| Nicoleta E. Mircescu et al./ 2014/ 34 | Towards a receptor-free immobilization and SERS detection of urinary tract infections causative pathogens | ID/ 2h + overnight culture/ No | *Escherichia coli and Proteus mirabilis* | Discrimination of *Escherichia coli* and *Proteus mirabilis* with satisfying selectivity by utilizing positively charged glass slides for bacteria immobilization and creation of SERS substrates by (i)synthesizing silver islands in the presence of bacteria and (ii) by concentrating AgNPs four times<br>____<br>PCA<br>____ |

| | | | | |
|---|---|---|---|---|
| | | | | Raman microscope with 633-nm line of a HeNe laser |
| Ting-Ting Liu et al./ 2009/ 157 | A High Speed Detection Platform Based on Surface Enhanced Raman Scattering for Monitoring Antibiotic Induced Chemical Changes in Bacteria Cell Wall | ID/ AST/-/ No | *Staphylococcus aureus Escherichia coli, Klebsiella pneumoniae, Mycobacterium species* | There are differences in the SERS spectra of gram-positive and gram-negative bacteria<br>____<br>Variations in the SERS spectra of gram-negative bacteria in different growth phases<br>____<br>Variations in the SERS spectra of bacteria after exposed to antibiotics<br>____<br>Exposure to antibiotics that affect the bacterial cell wall shows spectral changes as early as 20 minutes after antibiotic addition while antibiotics that inhibit protein synthesis reveal changes after 9-12 hours of incubation<br>____<br>Raman microscope equipped with a HeNe laser at 632.8 nm and NA 0.95 100x water-immersion objective lens |
| Premasiri et al./ 2017/ 40 | Rapid urinary tract infection diagnostics by surface-enhanced Raman spectroscopy (SERS): identification and antibiotic susceptibilities | ID/ 50 min +overnight culture/ Yes $1x10^5$ cells/ml diluted in urine from healthy volunteers | *Escherichia coli, Enterococcus faecalis*, *Klebsiella pneumoniae*, *Staphylococcus saprophyticus* | Correct identification of bacteria utilizing PLS-DA classification with >95% sensitivity and >99% specificity<br>____<br>The SERS spectra are due to seven purine components: adenine, hypoxanthine, xanthine, guanine, AMP, uric acid, and guanosine. These molecules result from the starvation response of the bacterial cells in pure water washes following enrichment from nutrient rich environments<br>____<br>Raman microscope employing a 50× objective and 785 nm excitation |
| Ute Neugebauer et al./ 2015/ 28 | Raman spectroscopy towards clinical application: drug monitoring and pathogen identification | ID/ AST/ ID: 35min AST: <3.5h / Yes (pretreated) | *Escherichia coli, Klebsiella spp., Enterococci, Staphylococci and Pseudomonas aeruginosa* | Creation of a reference database for classification (utilizing SVM) that includes 2952 spectra from 11 bacterial species<br>____<br>The database was evaluated with 514 independently measured Raman spectra from the same eleven bacterial species providing a prediction accuracy of 95%<br>____<br>Evaluation of the database utilizing patient's urine samples provided correct classification ranging from 66-98%<br>____<br>High prediction accuracies have been reported for the differentiation of bacterial species *Escherichia coli* and *Enterococcus faecalis* directly |

| | | | | |
|---|---|---|---|---|
| | | | | from urine suspensions utilizing dielectrophoresis in just 35 minutes<br><br>____<br>Successful differentiation of a resistant *Enterococcus faecalis* from a sensitive one in less than 3.5 hours utilizing antibiotic concentrations above 10-fold the MIC<br>Utilization of a three level PLS-LDA- LDA model to distinguish the sensitive from the resistant strain. Leave-one-batch-out validation, yield 86% sensitivity and 93% specificity with respect to the prediction of vancomycin resistance in *Enterococcus faecalis* when the model is tested with data of an independent biological replicate<br><br>____<br>Micro-Raman setup equipped with a 600 lines/mm grating |

# Chapter 4
# Review of Data Analysis Techniques

As it is shown in Figure 4.1 prior to applying any algorithm for classifying the data, data collection and feature extraction must be performed. The methodology for data collection and processing is described extensively in Chapter 5 "Materials, Methodology and Data Analysis". The various procedures applied were the paired t-test, Principal Component Analysis (PCA), Principal Component Transformation, Multivariate Analysis of Variance (MANOVA), Leave One Out Cross Validation (LOOCV) and Linear Discriminant Analysis (LDA) which are described here.

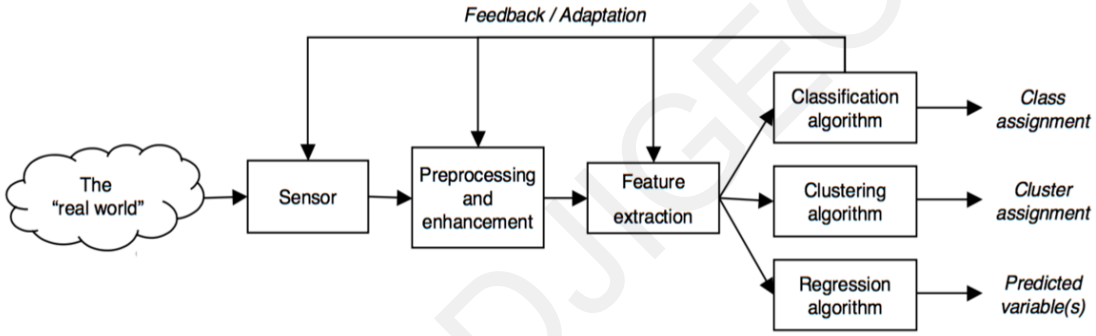


Figure 4.1 Data collection and data analysis process

## 4.1 Classification methods

Classification can be either supervised or unsupervised. Unsupervised classification methods group the data points into clusters without using any information about the class (label) of each data point. On the other hand, supervised classification methods require a set of data points, which are labeled, i.e. their class is known *a priory*. These labeled data points are used to train the algorithm, using the known information about the class (label) of each point and to create a model of the data. Once the supervised model has been trained, it can be used to classify data points, which were not in the training set, by assigning them to one of the classes described in the training set [105].

### 4.1.1 Unsupervised classification methods

Unsupervised classification, or cluster analysis, methods can be distinguished into hierarchical and non-hierarchical [106]. The most commonly applied method in Raman spectroscopy is Hierarchical Cluster Analysis (HCA). HCA does not require a priori labeling of the data points [105]. The first step in hierarchical clustering is to establish a similarity

matrix by calculating the distance between the samples. Euclidian, Manhatten and Minkowski algorithms are appropriate for the calculation of these distances [107]. When the similarity matrix is generated, different linkage methods like single-linkage, complete linkage or average-linkage, are utilized to join the samples into clusters [106]. The resulting clusters are then illustrated as a dendrogram. In this way, HCA can be used to classify a new data point by determining into which cluster this new data point falls. However, this method does not provide good classification performance on data points that are not in the training set. HCA is also a relatively unstable method, because clusters formed in the lower levels of the hierarchy can constrain the clusters formed at the higher levels of the hierarchy, making the analysis unreliable [108].

### 4.1.2 Supervised classification methods

The goal of supervised classification is to assign data points, which were not seen before, into classes determined by a training set assuming that each data point belongs to one of the known classes. For example, Raman spectra that will be obtained from bacteria could be labeled and classified based on the species of the bacterium from which they originated. Each spectrum is a data point, and it belongs to one class. Supervised learning requires that the class of some data points is known (labeled data points). Those points are used as a training set to create a model which can then be used to predict the label of unlabeled data points ("out-of- sample" data points) whose class is not known. Some of the most commonly used supervised learning methods, applicable to the classification of Raman spectra, are listed below including a brief description of their advantages and disadvantages.

***Nearest Neighbor***

The nearest neighbor approach is a very simple method and does not require any learning. The data points in the training set are used to predict future unlabeled data points by detecting the distance between unlabeled and labeled data points in the training set. The unlabeled data point is predicted to belong to the class of the training set to which its data point is closest to. The biggest advantage of this method is that is easy to implement. On the other hand, the prediction could be time consuming because unlabeled data points must be compared to all data points in the training set. Therefore, the prediction speed depends on the size of the training set. The biggest disadvantage of this method is that it is very sensitive in the presence of irrelevant parameters [109].

***Linear Discriminant Analysis***

Linear discriminant analysis (LDA) is a frequently applied classification method due to its simplicity and low computational cost. It is a way to reduce 'dimensionality' while at the same time preserving as much of the class discrimination information as possible. LDA, uses the training information to create new axes and projects the data onto the new axes in such a way as to minimize the variance and maximizes the distance between the means of the two classes [110]. There are three key steps to successfully apply LDA:

1. Calculation of the separability between different classes. This step is also known as between-class variance and is defined as the distance between the mean of different classes.
2. Calculation of the within-class variance. This is the distance between the mean and the sample of every class.
3. Construction of the lower-dimensional space that maximizes the between-class variance and minimizes the within-class variance.

LDA is highly sensitive to outliers since they can greatly affect the shape of the calculated distributions [105]. LDA is very fast because, since it requires little computation, the models produced are concise, therefore easily implemented, and is a good technique for detecting global phenomena. Furthermore, However, LDA is a simple technique that only performs well on data points that are well separated and on features which follow a normal distribution. If one of the independent variables (features) is highly correlated with another, or is a function of another set of features, then the calculations for finding the discriminant function will fail. This case is very common when the number of features (independent variables) is much greater than the number of observations (data points). For this reason, it is better to first transform the features before applying LDA. The two most commonly used methods for transforming the Raman data are Principal Component Analysis (PCA), and Partial Least squares (PLS). This leads to the two classification methods known as PC-DFA (Principal Component Discriminant Function Analysis) and PLS- DA (Partial Least Squares Discriminant Analysis) [105].

***Principle Components Discriminant Function Analysis (PC-DFA)***

PC-DFA uses Principal Component Analysis to first transform the data into a new space, in order to maximize the variance in each dimension, before performing DA. Each dimension is called a principal component. However, in cases where the variance of the features is not a good criterion for class separability, it is better to use another method, such as PLS-DA [111].

***Partial Least Squares Discriminant Analysis (PLS-DA)***

PLS is a data reduction method. The aim of the PLS method is to relate the types of variables in order to find directions, which maximize group separability. PLS-DA is a method, which attempts to increase the separation of groups by representing the data points in a new space. An advantage of PLS-DA is that it can describe complex relationships between features. However, it has been shown that PLS-DA has issues with over-fitting. For this reason, it might produce good results when performing cross validation, but its accuracy on "out-of-sample" data can be low when overfitting the training data occurs [107].

### 4.1.3 Leave One Out Cross Validation

Cross Validation is a tool for assessing the effectiveness of a model and to determine the parameters which will result in the lowest test error. It is a technique for estimating how the results of a statistical analysis model will be generalize to an independent data set. K-fold cross validation is so named because k is the number of groups that the sample is going to be split into for the cross validation. The steps that are followed for this technique are:

1. Mingle the dataset randomly
2. Divide the dataset into k groups
3. For each group:
    a. Take the group as a test data set
    b. Take the remaining groups as a training data set
    c. Fit a model on the training set and evaluate it on the test set
    d. Retain the evaluation score and discard the model
4. Summarize the skill of the model using the average of model evaluation scores

By following this technique every data point gets to be in a validation set once, and gets to be in a training set k-1 times. As a result, this reduces underfitting as most of the data are used for fitting, and also reduces overfitting as most of the data are used in the validation set as well.

Leave one out cross validation is a special case of the k-fold cross validation technique. In this case, k is equal to the number of samples in the dataset. In Leave one out cross validation only one point is selected as the test set and the remaining points are used to build the training model and evaluate the error of the single point held out. A generalization error estimate is obtained by repeating this procedure for each of the training points available, averaging the results. Leave one out cross validation is usually used when there are few data available.

### 4.1.4 Principal Component Analysis (PCA)

Principal Component Analysis (PCA) is used extensively in bacterial classification and characterization. This is due to PCA's ability to reduce the dimensionality of data that must be analyzed prior to bacterial classification. Additionally, PCA improves the accuracy of the classification. To reduce the dimensionality of a data set consisting of a large number of interrelated variables, PCA applies a linear transformation to project the original data into a new coordinate space [112]. These new principal components (PCs) are ordered so that each one successively accounts for less variability of the data set. The first principal component captures the dimension of maximum variance, the second principal component captures the dimension of the second greatest variance and so on [112]. By choosing only the PCs which represent the majority of the variance, one can reduce the dimensionality of the data set [113]. The main question is how many and which PCs should be kept to maintain the maximum information from the original data [113]. Most commonly used are the first PCs although, occasionally, the highest variance may not necessarily translate to maximum sample separability. This can be advantageous in the classification process because the reduced number of features might capture the differences between classes more effectively leading to increased classification accuracy. In addition, the reduced number of variables might decrease the complexity of the classification, lower the computational cost, and improve the speed of the classification procedure [105]. The PCA steps include:

1. Compute the mean for every dimension of the whole dataset.
2. Compute the covariance matrix of the whole dataset.
3. Compute eigenvectors and the corresponding eigenvalues.
4. Sort the eigenvectors by decreasing eigenvalues and choose k eigenvectors with the largest eigenvalues to form a d × k dimensional matrix W.
5. Use this d × k eigenvector matrix to transform the samples onto the new subspace. [110]

### 4.1.5 t-test

A t-test is a type of inferential statistic used to determine if there is a significant difference between the means of two groups, which may be related in certain features. The t-test examines the hypothesis that two independent samples may come from distributions of the same average. The t-test result can be either a 0 or 1. If the result is 0 then is implied that the two independent samples have the same average. Therefore, there is a similarity between the two sample distributions. On the other hand, if the result is 1, it is implied that the two independent distributions do not share the same average. Therefore the two

distributions do not correlate. The distributions have unknown but same variance. The independent distributions might be matrices [110], [114].

### 4.1.6 MANOVA

MANOVA (Multivariate Analysis Of Variance) is a type of multivariate analysis used to analyze data that involves more than one dependent variable at a time. MANOVA tests hypotheses regarding the effect of one or more independent variables on two or more dependent variables. Additionally, MANOVA analysis generates a p-values that are used to determine whether or not the null hypothesis can be rejected [115]. MANOVA is often used to detect differences in the average values of the dependent variables between the different levels of the independent variable. Interestingly, in addition to detecting differences in the average values, a MANOVA test can also detect differences in correlations among the dependent variables between the different levels of the independent variable [115]. MANOVA is also very useful in visualizing otherwise multidimensional data.

## 4.2 Data Analysis and Classification of Raman Spectra

Guicheteau et al., were the first to utilize PCA on SERS spectra exhibiting a clear discrimination between different species and the possible differentiation of strains of Bacillus spores as well as the possibility of gram-positive Bacillus spores to be differentiated from Gram-negative vegetative cells [93]. Beier et al., also used PCA in order to discriminate between samples of *Streptococcus sanguinis* and *Streptococcus mutans* in biofilm form, both in isolation and in pseudo mixed biofilms. For these two validation sets, 97% of 622 spectra were properly identified [116]. Premasiri et al.,who carried out a PCA analysis of five different bacterial types, achieved a clear distinction of SERS spectra between different types of bacteria and between different strains of the same bacteria type [117].

Escoriza et al., utilized PCA-DA in order to study the growth curves of *Escherichia coli* and *Staphylococcus epidermidis*. They showed that *Escherichia coli* and *Staphylococcus epidermidis* exhibit changes of intensity in specific spectral bands over the course of time. These spectral variations correlated with the metabolic changes that cells experience during growth phases [90]. Another study using PCA with DA was by Jarvis and Goodacre, (2005) who achieved a 91.7% variance among three different species of the genus *Bacillus*. Also PCA-DFA was used to group bacteria belonging to the genus *Bacillus* with highly discriminatory results [84]. Similarly, in 2007 Escoriza et al., used PCA-DA multivariate statistical techniques to discriminate viable from non-viable cells. The classification rate obtained considering all the treatments (non-viable cells) and controls (viable cells) at the

same time for each of the species studied was 86%. The classification rate based on species differentiation when all the spectra (viable and non-viable) were used was 87% [94].

Other research groups like Foster et al., and Lopez-Diez et al., for their algorithms used mathematical equation distances like Mahalanobis and Euclidean in combination with PCA. More precisely, Foster et al., by utilizing PCA, regression trees (CART), Mahalanobis distance calculations and internal cross-validation studies successfully classified 100% of the samples into their correct physiological state (sporulated or vegetative) and identified 67% of the samples correctly as to their bacterial strain [78]. Lopez-Diez et al., demonstrated that UV resonance Raman, together with Savitzki-Golay smoothing filter, PCA, DFA and the Euclidean distance between a priori groups centers in DFA space, can be used as a tool for discriminating between very closely related endospore forming bacteria [58]. Cam et al., structured a plot of the Euclidian distance and percent coefficient of variation (CV%) which fell in the range of 4-12%. In that plot, each bacteria species as well as the binary and ternary mixtures fell onto different coordinates, making for a quick assessment of the bacterial sample [53].

Udelhoven et al., carried out PCA and PLS-DA analysis and achieved a high specificity and sensitivity classification of *Lb. kefir* and non-*Lb. kefir* strains [82]. Mello et al., classified 100% of all the types of bacteria in 3 different types of sample tests, unknown, calibration and prediction, by carrying out PCA and PLS-DA analysis [75], [76]. Nikolaou et al., achieved very good quantification of the bacterial levels in both pure and grown in UHT milk samples with kernel PLS (KPLS) [68].

Many research groups, including Gaus et al., Patel et al., Bombalskaa et al., Xie et al., and Jarvis and Goodacre, applied unsupervised methods such as hierarchical cluster analysis (HCA) for classifying the Raman data. More extensively Gaus et al., used HCA and PCA to investigate natural groupings in the data. They demonstrated that by utilizing HCA and PCA, correlation of different strains of bacteria could be achieved. In a second step the spectra were analyzed using several supervised methods like k-nearest neighbor classifier, nearest mean classifier, linear discriminant analysis and support vector machines to perform classification of lactic acid bacteria at a strain level [55], [62], [118], [119]. Patel et al., utilized a combination of PCA, HCA and DFA analysis on four bacterial types. HCA dendrograms illustrated an improved bacterial identification from the barcode spectral data reduction and DFA plots demonstrated a small improvement in bacterial type separation, albeit with more false positive classifications [59]. Bombalskaa et al., used HCA and PCA

to discriminate between bacterial spores, bacteria in vegetative forms and in fungi. Xie et al., were able to discriminate six species of microorganisms either in synchronized cultures or in unsynchronized cultures in the stationary growth phase also utilizing PCA and HCA techniques [62], [118]. Willemse-Erix et al., using the squared Pearson correlation coefficient and an HCA-dentrogram, produced a highly discriminatory technique applied on *Staphylococcus*. Jarvis and Goodacre, in their HCA dendrogram showed clear characterization at the genus level for each of the bacterial groups analyzed and by using PC-DFA or HCA achieved each of the four classes of UTI microorganisms to be correctly resolved into four separate clusters [120].

Harz et al., analyzed the results of their Raman measurements from bulk samples with HCA and SVM techniques. For HCA, they obtained 97% recognition rate for strains and 97.7% for species. For SVM they obtained 94.9% recognition rate for strains and 97%for species. In contrast to the hierarchical cluster analysis, where spectra with spikes were excluded from the clustering, every measured spectrum was used for the classification by means of SVMs. For classification of single bacteria spectra grown under different culturing conditions HCA was not successful in the classification while for the SVMs for strain the average recognition rate is 94.1% and for species average recognition rate was 97.6% [56]. Walter et al., achieved a fast, highly specific and reproducible detection method for reliable bacterial classification by first applying linear SVM to SERS spectra, resulting in an overall accuracy of 90.1%. Then by applying radial basis SVM obtained results with an overall accuracy of 91.0%. Whenever, the CH stretching vibration region was included in the SVM classification, the linear SVM and radial basis SVM results improved with in an overall accuracy of 91.5% and 92.6%. Moreover, Walter et al., demonstrated that using Raman spectroscopy they were able to identify spectral differences between bacterial cultures containing plasmids and those without plasmids. Ampicillin-challenged and non-challenged bacteria of the model strain *Escherichia coli* DH5α were classified and identified with recognition rates of about 92% and 90% by Raman spectroscopy at excitations of 532 and 244 nm, respectively. The SVM loadings also revealed that the pDrive transformed bacterial cultures exhibit a higher DNA content, compared to the untransformed cultures [81]. The group of Rajwa et al., for the analysis of *Salmonella enterica* in the samples used a Bayesian classifier. The Bayesian classifier except from being able, as other methods, to classify biological samples into previously known categories, it can also play a role as autonomous detection system [121].

Also, worth mentioning is the work of Schmid et al., who achieved a high classification performance simultaneously from six different classification approaches. Each tool estimated slightly different classification rates; PLS-DA: 82.5%, LDA: 84.1%, QDA: 80.8%, MDA: 86.6%, 3NN: 83.5% and SVM: 87.3%. External validation results of pairwise MDA and SVM (RBF-Kernel) using 2 loops of 50-fold cross validation exhibited the rates of 86.3% and SVM: 87.0% respectively. These resulted to the successful discrimination of 29 strains of bacteria derived from a variety of species [66].

# Chapter 5
# Materials, Methodology and Data analysis

The aim of this Ph.D. thesis was the development of a fast, accurate diagnosis and antibiogram method for Urinary Tract Infection (UTI) based on Surface Enhanced Raman Spectroscopy (SERS). The project was divided into four tasks:

- Identification of the sample as positive or negative for UTI
- Classification of the causative bacteria
- Determination of bacterial sensitivity to antibiotics (antibiogram) in less than four hours
- Data acquisition directly from urine samples

All four tasks were implemented utilizing an i-Raman Spectrometer B&W Tek with 532nm excitation wavelength. All samples were mixed with metal nanoparticles in order to achieve signal enhancement. The materials required, the experimental procedures and the data analysis methods are presented here.

## 5.1 Materials

### 5.1.1 Bacteria

The bacterial samples that were used for this research have been isolated from patients with UTI. Clinical bacterial isolates were identified by biochemical tests and obtained on LabM blood agar from affiliated clinical laboratories. Frozen stocks were treated in 15% glycerol and stored at -80$^{o}$C.

All bacterial samples were sub-cultured on Mueller Hinton (Oxoid, England) agar petri dishes and cultured in Mueller Hinton Broth. In total 88 bacterial strains from the genera *Citrobacter*, *Proteus*, *Klebsiella* sp., *Escherichia coli* and *Enterobacteur*, were collected for the specific study. The types of bacteria and the number of strains that were used for the project are presented in Table 5.1.

**Table 5.1 Types of bacteria**

| Type of Bacteria | Number of Strains | Strain Number |
|---|---|---|

| | | |
|---|---|---|
| *Citrobacter spp.* | 13 | 1-4, 7-15, 21-24 |
| *Proteus spp.* | 20 | 2-13, 16-23 |
| *Klebsiella spp.* | 24 | 1-22, 25, 28 |
| *Escherichia coli spp.* | 20 | 2-6, 10-15, 20, 28, 30, 31 |
| *Enterobacteu spp.* | 11 | 1, 4-8, 10-14 |

### 5.1.2 Antibiotics

The antibiotics investigated for this project were amoxil, augmentin, cefaclor, cefuroxime, ciprofloxacin, ceftriaxone, cefazolin and amikacin.

Antibiotics for disk diffusion test:

1. Amoxicillin BD BBL AMX-10
2. Cefaclor BD Sensi-Disc CEC-30
3. Cefixime BD BBL CFM-5
4. Cefuroxime BBL CXM-30
5. Amoxicillin/ Clavulanic acid BBL AmC-30
6. Penicillin BD BBL P-10
7. Ciprofloxacin BBL CIP-5

Liquid culture antibiotics

1. Augmentin (Amoxicillin + clavulanate potassium) GlaxoSmithKline 1.2g
2. Zinacef (Cefuroxime sodium) GlaxoSmithKline 1.5g
3. Cefaclor Ceclor MR Phadisco 500mg tablet
4. Noroxin Norfloxacin 400mg Merck Sharp & Dohme B.V. tablet

### 5.1.3 Nanoparticles

SERS enhancement was achieved with silver and gold nanoparticles. The gold nanoparticles were bought pre-fabricated while the silver nanoparticles were synthesized in the lab. Below are the materials required for Ag nanoparticle synthesis:

- Silver nitrate ($AgNO_3$)
- Tri-sodium citrate 2-hydrate ($C_6H_5Na_3O_7.2H_2O$)
- High accuracy weight scale
- Ultrapure $H_2O$
- Conical flask
- Magnet for steering
- Hot plate/Stirrer
- Thermometer that reach 100$^oC$
- Media-lab Pyrex bottle with cap

### 5.1.4 Filters

One important step in bacterial collection directly from urine samples is urine filtration. Urine samples were filtered twice. The first filtering process removed traces of unwanted material, which might have interfered with SERS, and the second filtering process captured bacteria on the filter surface to directly collect spectra from the filter using the Raman spectrometer.

For the first filtering process, Millex PVDF Durapore filters with pore size 5 μm and a diameter of 25mm were used. They are made by hydrophilic PVDF membrane and they are sterilized by ethylene oxide. These filters are suitable for sterile tissue culture media, protein solutions or aqueous solutions. [122]

For the second filtering process, three different filters, with small pore size, were examined. The first filter was Durapore Membrane Filters (GVWP04700) with pore size 0.22μm, diameter 47mm, white, plain. They are produced by Millipore and provide high flow rates, have low extractables and broad chemical compatibility. Additionally, hydrophilic Durapore membrane have very low protein binding to minimize interaction with the sample and maximize recovery. [122]

Another filter used was the Isopore Membrane Filter (GTTP01300). Isopore Membrane Filters are produced by Millipore and are constructed by hydrophilic polycarbonate membrane, have pore size 0.2 μm, 13 mm diameter, are white and plain. The

Isopore™ membrane is a polycarbonate, track-etched screen filter recommended for all analyses in which the sample is viewed on the surface of the membrane. The Isopore™ membrane offers distinct advantages for the analysis of airborne contaminants and other particles using optical or electron microscopy. It is composed of polycarbonate film, which has a smooth, glass-like surface for clearer sample observation. The unique manufacturing process of the membrane ensures a precise pore diameter and a consistent pore size for accurate separation of samples by size. Furthermore, membrane structure retains particles on the surface, simplifying counting and analysis. Isopore™ membranes do not stain, resulting in low background interference, are non-hygroscopic, allowing for rapid drying and reduced sample analysis time and the translucent material does not require clearing for transmitted light microscopy. [122]

The last filter examined for the second stage of filtering was the Silver Membrane Filter. Silver Membrane Filters are produced by Sterlitech. They are fabricated by 99.97% pure metallic silver, are hydrophilic, inorganic membrane filters with pore size 0.2μm and diameter 13mm. [123]

For the 13mm Isopore Membrane Filters and 13mm Silver Membrane Filters a KS 13 Syringe Filter Holder was utilized. The syringe filter holder is stainless steel, is easy to attach with a syringe and filter or clean small volumes of liquids. [123]

### 5.1.5 Nutrient Broth

Nutrient broth was used to support the growth of bacteria in liquid and solid cultures. For liquid cultures, OXOID CM0405 Mueller Hinton Broth (Typical formula: Beef, dehydrated infusion from 300.0; casein hydrolysate 17.5; starch 1.5) was used while for solid cultures, OXOID CM0337 Mueller Hinton Agar (Typical formula: Beef, dehydrated infusion from 300.0; casein hydrolysate 17.5; starch 1.5; agar 17.0) was used instead.

### 5.1.6 Ultrapure Water

All experiments were carried out using Ultrapure water (UPW). UPW is water that has been purified to very strict specifications, containing by definition only $H_2O$, and $H^+$ and $OH^-$ ions in equilibrium. Therefore, ultrapure water conductivity is about 0,055 uS/cm at 25$^oC$, also expressed as resistivity of 18,2 MΩ. [124]

### 5.1.7 Phosphate-buffered saline (PBS)

For the majority of the experiments, bacteria were diluted or washed out with Phosphate-buffered saline (PBS). PBS is a water-based salt solution containing disodium

hydrogen phosphate, sodium chloride and, in some formulations, potassium chloride and potassium dihydrogen phosphate. PBS helps to maintain a constant pH and its osmolarity and ion concentrations match those of the human body.

## 5.2 Equipment

### 5.2.1 Raman Spectrometer

The Raman system that was employed for the experiments in this project was the i-Raman model from BWTEK. The i-Raman is a portable Raman spectrometer. It delivers high resolution combined with field-portability. Furthermore, the excitation wavelength is 532nm with a high resolution ($3.5cm^{-1}$) configuration covering the range from $150cm^{-1}$ to $4000cm^{-1}$. The i-Raman system is equipped with a TE-cooled 2048 pixel CCD detector with maximum effective integration time of 10 minutes, $150cm^{-1}$ off the Rayleigh line and fiber-optic interface for convenient sampling [125].

### 5.2.2 V-650 UV-Vis Spectrophotometer

A V-650 UV-Vis Spectrophotometer was used for the estimation of bacterial concentration from light absorbance. Spectrophotometry measures light absorption of a sample in a gas or liquid state. It can measure the absorption of different substances in the range of 190 nm and 780 nm. A sample's absorption spectrum is a graph of absorbance vs. wavelength. For bacterial solutions the absorbance is measured in Optical Density (OD) units, where 1 OD represents a ten-fold decrease in light intensity and is equivalent to $8x10^{8}$cells/ml.

### 5.2.3 Transmission electron microscopy (TEM)

Transmission electron microscopy (TEM) utilizes an electron microscope to form an image that provides information regarding the topology, morphology and composition of a sample. For the creation of the image an electron beam is generated from an electron source and is accelerated toward the sample by applying a positive electrical potential. The electron beam is then focused onto the sample by using lenses and apertures. The interactions of the electron beam with the material result to various phenomena and give information about the samples morphology and composition. The TEM images for characterization of the silver nanoparticles that were synthesized in the lab were collected by Louiza Potamiti of the Electron Microscopy and Molecular Pathology Department, Cyprus Institute of Neurology and Genetics[126].

## 5.3 Methodology

### 5.3.1 Bacterial Preparation

Prior to each experiment, it was necessary to prepare a new batch of bacteria. The process began with a solid culture of bacteria from the frozen stock, converting the solid culture into a liquid culture of bacteria and preparing the bacteria for Raman spectroscopy.

***Preparation of a solid culture of bacteria***

The steps for preparing a solid culture of bacteria from frozen stocks were the following:

1. Prepare the Mueller Hinton Agar. 38 grams of OXOID CM0337 Mueller Hinton Agar are suspended in 1 liter of distilled water. The solution is sterilized by autoclaving at 121$^{o}$C for 15 minutes.
2. Pour enough proportion of the liquid agar into petri dishes in order to create a gel of 4mm thickness.
3. Pick up a small portion of bacteria from frozen glycerol stock (-80$^{o}$C) using a sterile loop. Small portions are needed in order for distinct colonies to be formed.
4. Streak the bacteria using proper streaking technique
5. Place the petri dishes in an incubator at a temperature of 37$^{o}$C. The bacteria are incubated for 15 hours in order to grow.

The main process steps are graphically illustrated in Figure 5.1.

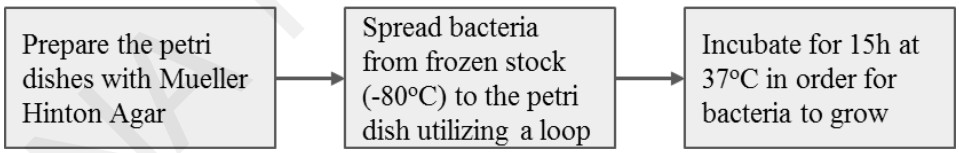


Figure 5.1 Process for preparation of a solid culture of bacteria

***Conversion of the solid culture of bacteria into a liquid culture***

The steps for the conversion of a solid bacterial culture into a liquid one were the following:

1. Prepare Mueller Hinton Broth. 21grams of OXOID CM0405 Mueller Hinton Broth are added into 1 liter of distilled water and mixed in order to dissolve. Afterwards, the solution is sterilized by autoclaving at 121$^{o}$C for 15 minutes.
2. Transfer 5 ml of Mueller Hinton broth into a 10 ml tube. Use proper aseptic technique, by flaming the bottle opening, the cap, and the pipets briefly, to avoid contamination."
3. Collect one colony of bacteria from the solid culture using an inoculating loop and dissolve within the broth.

4. Finally, place the 10ml tubes with the liquid culture in an incubator/shaker at 37°C, for fifteen hours in order for the bacteria to grow.

The main process steps are graphically illustrated in Figure 5.2.

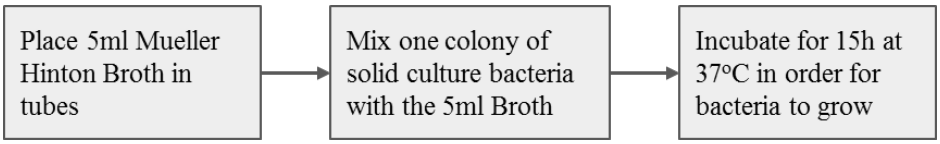


Figure 5.2 Conversion of solid culture bacteria into a liquid culture

***Preparation of bacteria for Raman spectroscopy***

Broadly, nutrient mediums contain carbon sources such as glucose, salts and amino acids (beef broth, yeast extract). These materials exhibit SERS signal that overlaps with bacterial signal [Mosier-Boss, Pamela A. "Review on SERS of Bacteria." Biosensors 7, no. 4 (2017): 51]. In order to avoid these interruptions and obtain valid results from the Raman spectroscopy, the Mueller Hinton broth was removed from the liquid culture. The steps that followed are outlined below:

1. Separate the mixture of bacteria and broth equally into 1.5ml tubes. This is because the available centrifuge in the laboratory can take 1.5 ml tubes.
2. Centrifuge the sample for 5 minutes in order to allow separation of bacteria from broth. Bacteria remain at the bottom of tube whereas broth will flow above.
3. Remove the Mueller Hinton broth, the supernatant in this case, carefully with a pipette leaving the bacteria in the bottom of the tube.
4. Pour 1,5ml 1xPBS in the 1,5ml tube with the remained bacteria and mix the solution in order for bacteria to be dissolved with the 1xPBS. The 1.5ml mixture is then centrifuged for three minutes and the supernatant is removed again leaving only the bacteria in the bottom of the tube.
5. Proceed with "washing of bacteria". Repeat twice in order to assure complete removal of the broth from bacteria.
6. After washing, bacterial pellets, which originated from the same culture, are combined in a single tube. In this way, all samples have the same concentration.

The main process steps are graphically illustrated in Figure 5.3.

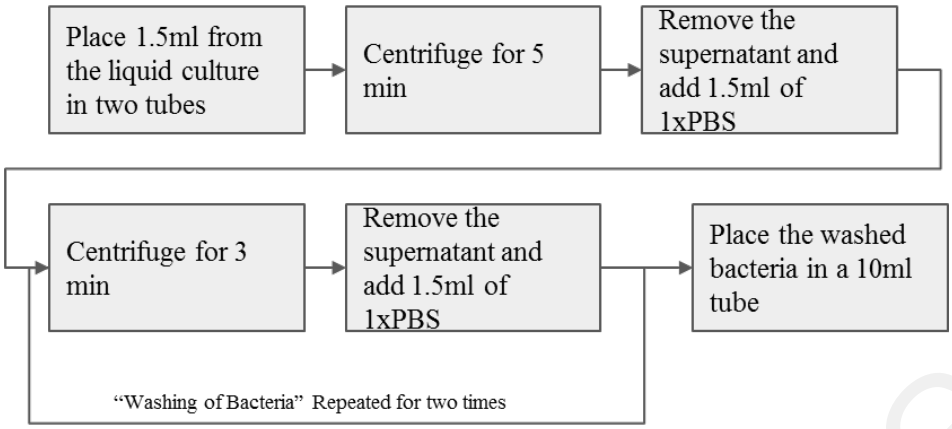


Figure 5.3 Preparation of bacteria for Raman Spectroscopy

### 5.3.2 Synthesis of Silver Nanoparticles (Ag np)

For the synthesis of 10-100nm radius silver nanoparticles, the experimental procedure described by Lee et al. [127], was followed. The steps of the procedure were:

1. Weigh:
    a. 45mg of silver nitrate ($AgNO_3$)
    b. 0.05g of tri-sodium citrate 2-hydrate ($C_6H_5Na_3O_7.2H_2O$)
2. Dissolve the 0.05g of sodium citrate in 5ml of ultrapure $H_2O$. In this way, the solution retain concentration of 1% sodium citrate.
3. Dissolve 45 mg of AgNO3 in 250 ml of ultrapure H2O, by mixing them in a conical flask
4. Put the conical flask with the $H_2O$-$AgNO_3$ solution on a hot plate. As a hot plate, the ARE Heating Magnetic Stirrer is utilized and is set in 300$^o$C with the stirrer set in 3. Additionally, small magnet is placed in the conical flask to allow the solution to stir.
5. Wait until the solution reaches the temperature of 100$^o$C.
6. Add 5ml of 1% sodium citrate solution.
7. Allow the AgNO3- sodium citrate solution to boil for 1 hour.
8. Watch the color of the solution. The solution from transparent becomes yellow to green. After 1 hour the solution becomes a dark greenish-grey color.
9. Put the solution in a media-lab Pyrex bottle with cap.
10. Place the solution at 4$^o$C.

The main process steps are graphically illustrated in Figure 5.4.

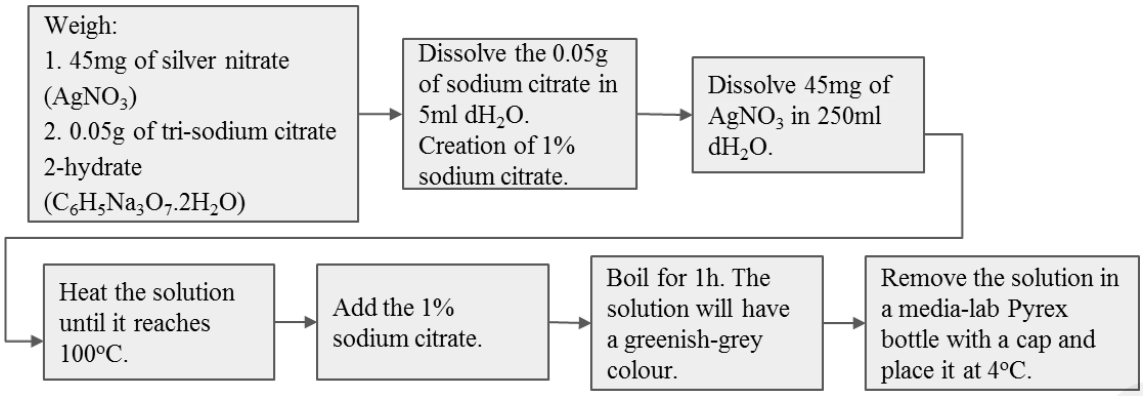


Figure 5.4 Preparation of silver nanoparticles

### 5.3.3 Identification of the sample as positive or negative for UTI

One of the main goals of this project was to determine whether a sample was positive or negative for a UTI. According to the current standard, a urine culture is considered infected when the concentration of the bacteria is $\geq 1x10^5$ cells/ml. For the specific experimental process, bacteria were serially diluted to various concentrations. The protocol for this experimental process was as follows:

1. Prepare bacteria for Raman Spectroscopy as it is indicated in the protocol for preparation of bacteria for Raman Spectroscopy (Figure 5.3).
2. Dilute bacteria in the following concentrations $1x10^3$, $1x10^4$, $1x10^5$, $1x10^6$, $1x10^7$, $1x10^8$cells/ml. Assume that concentrations of $10^3$-$10^4$ cells/ml are a "negative" for a UTI and $10^5$-$10^8$ cells/ml are a "positive" for a UTI.
3. Mix 20μl of bacteria with 20μl silver nanoparticles (AgNP). Take 20μl of the bacteria/nanoparticle solution to spot on a glass slide. Repeat this step for all bacteria concentrations.
4. Place the slide in an incubator at 37°C and wait until the spot has dried.
5. Collect the Raman spectra utilizing the 532nm i-Raman spectrophotometer. Collect three spectra from each spot.
6. Additionally, collect three control spectra from a spot that is created by blending 20μl 1xPBS with 20μl silver nanoparticles in a tube and spotting 20μl of the solution on the slide.

Figures 5.5 and 5.6 represent the procedures followed to create various concentrations of bacteria and to collect the Raman spectra for identifying if a sample was negative or positive to UTI.

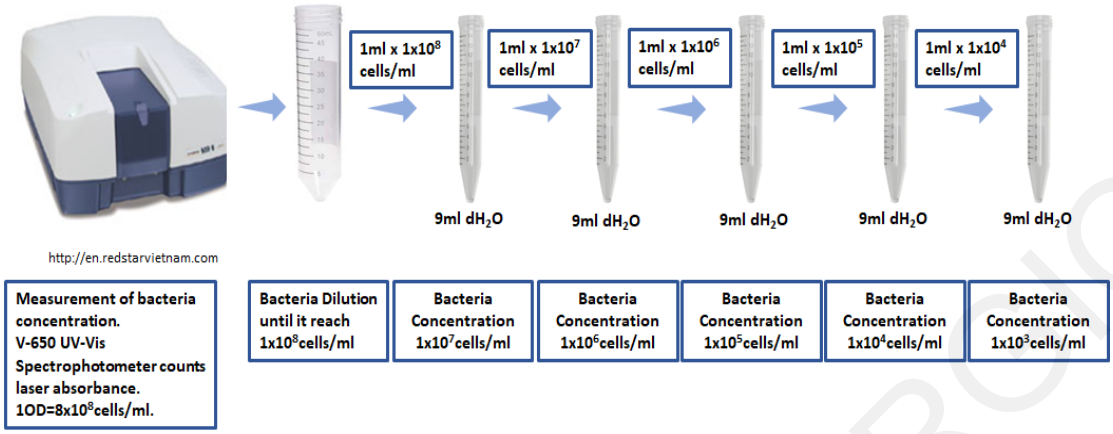


Figure 5.5 Dilutions of bacteria from $1x10^3$, $1x10^4$, $1x10^5$, $1x10^6$, $1x10^7$ to$1x10^8$cells/ml

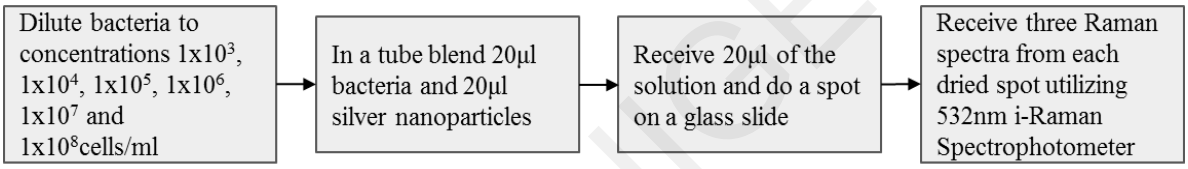


Figure 5.6 Procedure to collect Raman spectra for identifying if a sample was negative or positive for a UTI

### 5.3.4 Classification of the causative bacteria

An important step in this research project was to develop a method that could correctly classify the bacteria according to their species. For this experimental process, bacteria of species *Proteus*, *Klebsiella* sp. and *Escherichia coli* were investigated, at a concentration $1x10^5$ cell/ml, which is also the clinical limit for urinary tract infections. The steps were as follows:

1. Prepare bacteria for Raman Spectroscopy as it is indicated in the protocol for Preparation of bacteria for Raman Spectroscopy (Figure 5.3).
2. Dilute the bacteria to a concentration of $1x10^5$ cell/ml (Figure 5.5).
3. Mix 20μl bacteria with 20μl silver nanoparticles in a tube and spot 20μl on a glass slide.
4. Place the slide in an incubator at 37°C and wait until the spot has dried
5. Collect the Raman spectra utilizing the 532nm i-Raman spectrophotometer. Collect three spectra from each spot.
6. Additionally, collect three control spectra from a spot that is created by blending 20μl 1xPBS with 20μl silver nanoparticles in a tube and spotting 20μl of the solution on the slide.

7. Repeat the above procedure with gold nanoparticles (Au NPs) instead of silver nanoparticles.

Figure 5.7 presents the procedure that was followed in order to collect Raman spectra for the classification of causative bacteria.

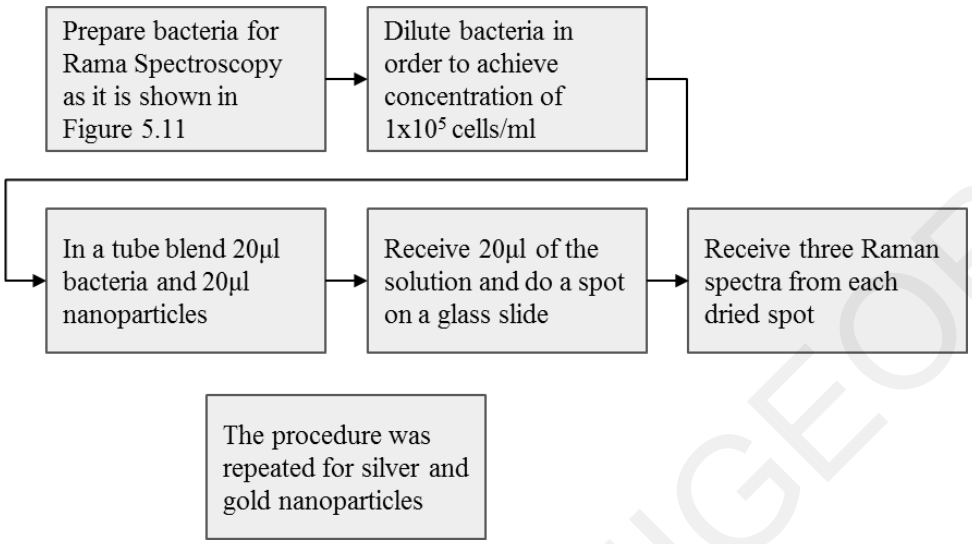


Figure 5.7 Procedure in order to collect Raman spectra for classification of causative bacteria

### 5.3.5 Determination of bacterial sensitivity to antibiotics

The main steps to acquire the data for determining the bacterial sensitivity to antibiotics via Raman Spectroscopy was as follows:

1. Prepare a solid culture antibiogram to determine susceptibility to antibiotics of each bacterium, using the current standard method described below which requires 24 hours to provide accurate results.
2. Prepare liquid culture antibiograms to verify the concentration of antibiotic that prevents the growth of each bacterium. The current standard method is described below and requires 48 hours to provide accurate results.
3. Use the above data as the reference points for comparison with the data collected from Raman Spectroscopy.
4. Expose bacteria to antibiotics for 0, 2 and 4 hours.
5. For each time point, each bacterium and each antibiotic, collect the Raman spectra utilizing the 532nm i-Raman spectrophotometer (see below for details).

***Solid culture Antibiogram***

For the determination of the bacterial antibiotic sensitivity or resistance, an antibiogram was required. For this experimental process susceptibility-test disks, enriched with an antibiotic were used. The main steps of the procedure are described below:

1. Spread a large number of bacteria, with a cotton swab, in a petri dish with Mueller-Hinton agar.
2. Spread the bacteria vertically, horizontally, and diagonally throughout the petri dish in order to create a lawn.
3. Dip the tip of a pair of tweezers in ethanol and flame it to sterilize it.
4. Grab a susceptibility-test disk with the sterilized pair of tweezers.
5. Place the susceptibility-test disk in the petri dish with the bacteria (the pair of tweezers should strictly only come in contact with the disk and not with the bacteria). Use susceptibility-test disks with the following antibiotics:
    a. Amoxycillin
    b. Ciprofloxacin
    c. Cefuroxime
    d. Tricef Bial
6. Place the petri dishes in the incubator at 37$^{o}$C for 24 hours. In order to obtain clear results, susceptibility-test disks should be allowed to react with bacteria for at least 24 hours.
7. After 24 hours, observe whether the area around the disk is clear/transparent. If the area is clear/transparent, it is an indication that the bacteria could not grow in the periphery of the disk and, thus, the bacteria are sensitive to the specific antibiotic. On the other hand, if bacteria could grow around the periphery of the disk, it is an indication that the bacteria are resistant to the specific antibiotic.
8. Determine bacterial resistance or susceptibility to specific antibiotics considering the zone diameters for various antibiotics in solid culture antibiograms presented in Table 2.1.

Figure 5.8 illustrates the procedure followed in order to prepare solid antibiograms.

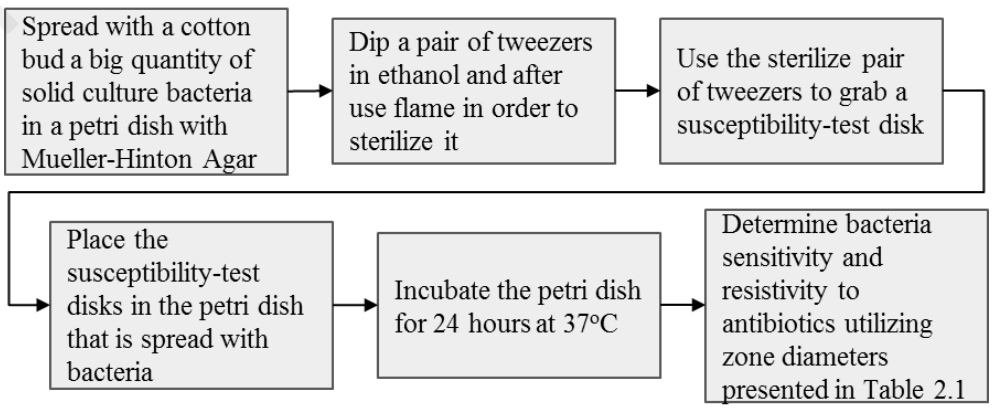


Figure 5.8 Solid culture antibiogram procedure

***Liquid Culture Antibiogram***

To expose the bacteria to appropriate concentrations of antibiotic, it was necessary to know the Minimal Inhibitory Concentration (MIC) for every antibiotic to each one of the bacteria tested. MIC is the lowest concentration of a drug, which prevents visible growth of a bacterium. To get the MIC a liquid antibiogram was used. By default, the MIC of the antibiotics is measured for bacteria with concentration of $1x10^6$ cells/ml. The following steps are implemented in order to provide liquid antibiogram results.

8. Measure the concentration of bacteria, grown in a liquid culture, utilizing UV-VIS spectrometer

9. Dilute bacteria in Mueller Hinton Broth until the concentration is $2x10^6$ cells/ml. Figure 5.9 presents the steps that have to be followed.

10. Dilute bacteria in Mueller Hinton broth until the solution has double the concentration of the indicated one (MIC).

11. Mix bacteria double in concentration with double in concentration antibiotics. The final solution reach the appropriate concentrations.

12. Incubate at 37°C for 48 hours.

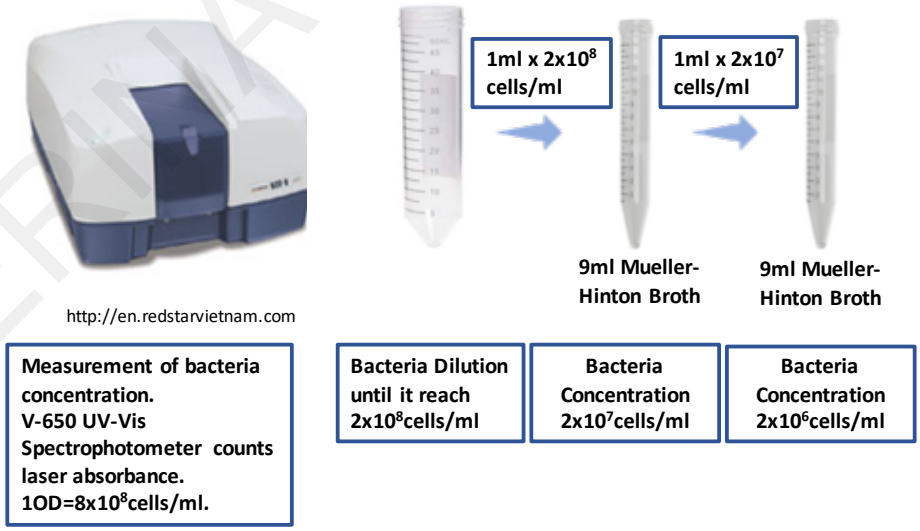


Figure 5.9 Dilution of liquid culture bacteria until the sample reach concentration of $1x10^6$cells/ml

The aim of this research task was to study how *Citrobacter spp*, *Proteus*, *Klebsiella* sp., *Escherichia coli* and *Enterobacter*bacteria react to the following eight antibiotics:

1. Amoxil
2. Augmentin
3. Cefaclor
4. Cefuroxime
5. Ciprofloxacin
6. Ceftriaxone
7. Cefazolin
8. Amikacin

Table 2.2 presents the concentration of various antibiotics, at which bacteria show susceptibility, intermediate susceptibility, or resistance, according to the literature. The term susceptible implies that the solution of bacteria and an antibiotic, with concentration similar to the referenced MIC (μg/ml), results in a transparent solution after 48 hours exposure at 37$^{o}$C, implying that bacterial activity was terminated by the antibiotic. On the other hand, the term resistant implies that the solution of bacteria and an antibiotic, with concentration higher than the referenced MIC (μg/ml), results in a turbid solution after 48 hours exposure at 37$^{o}$C.

For the liquid antibiograms, the antibiotics were diluted into four different concentrations that cover the susceptibility/resistance range and were tested on every bacterial strain. Table 5.2 presents the antibiotic concentrations that have been tested while Figure 5.10 describes the process of serial dilutions of the antibiotic to concentrations 2, 1, 0.5 and 0.25μg/ml in soluble Mueller Hinton Broth. The same procedure was repeated for all antibiotics for all indicated concentrations as are presented in Table 5.2.

**Table 5.2 Tested antibiotic concentrations**

| Antibiotic | Concentrations (μg/ml) |
|---|---|
| **Amoxil** | 32, 16, 8, 4 |
| **Augmentin** | 36, 18, 9, 4.5 |
| **Cefaclor** | 64, 32, 16, 8, 4 |
| **Cefuroxime** | 32, 16, 8, 4 |
| **Ciprofloxacin** | 2, 1, 0.5, 0.25 |
| **Ceftriaxone** | 64, 32, 16, 8, 4 |
| **Cefazolin** | 64, 32, 16, 8, 4 |
| **Amikacin** | 32, 16, 8, 4 |

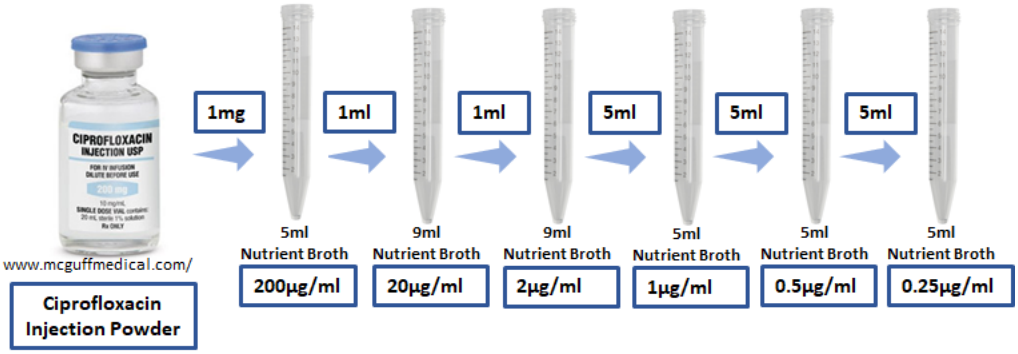


Figure 5.10 Serial dilutions of the antibiotic ciprofloxacin to concentrations 2, 1, 0.5 and 0.25µg/ml in Mueller Hinton Broth

The next step was to mix 1ml of antibiotic with 1ml bacteria. That solution was incubated at 37°C for 48 hours to allow for interaction between bacteria and antibiotics. It is important to note that the initial concentration of all bacterial and antibiotic solutions were doubled in order to achieve final bacterial concentration of $1x10^6$ cells/ml and appropriate antibiotic concentrations after mixing the two parts.

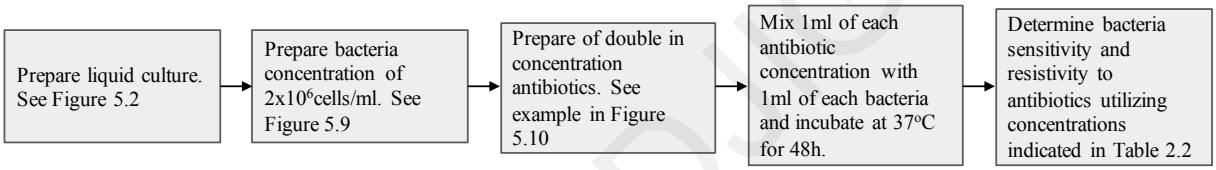


Figure 5.11 Liquid culture antibiogram process

### *Data Collection for Antibiogram utilising SERS*

The last step in the task to determine bacterial sensitivity to antibiotics was to acquire Raman spectra. Prior to the collection of the spectra the following steps were performed:

1. Prepare bacteria for Raman Spectroscopy as it is described in the protocol for Preparation of bacteria for Raman Spectroscopy (Figure 5.3).
2. Prepare bacterial dilutions with concentration $2x10^5$ cells/ml as described before (Figure 5.9). Bacterial solutions are prepared with double the required concentration.
3. Prepare antibiotic solutions of amoxil, augmentin, cefaclor, cefuroxime, ciprofloxacin, ceftriaxone, cefazolin and amikacin. Dilute antibiotics to the appropriate concentrations with 1xPBS. The most appropriate concentration are determined experimentally from the liquid antibiograms (Figure 5.11). Again, these solutions must be at double the required concentration.
4. Mix 1ml of bacteria with concentration $2x10^5$ cells/ml and 1 ml antibiotic with the double concentration in a tube. The result will be a solution of bacteria with $1x10^5$ cells/ml concentration and the appropriate antibiotic concentration.

5. Mix 20μl silver nanoparticles in a tube with 20μl of the antibiotic/bacteria solution. Spot 20μl of nanoparticle/antibiotic/bacteria solution on a glass slide. Place the glass slide at 37$^{o}$C in the incubator until it dries.
6. Collect Raman spectra after zero hours of exposing the bacteria to the antibiotics utilising the 532nm Raman spectrometer. Collect three spectra per spot.
7. After mixing bacteria with antibiotics leave the solution for two hours at 37$^{o}$C in order for bacteria to interact with the antibiotics.
8. Again, after two hours, mix 20μl of the solution with 20μl silver nanoparticles, create a spot and collect Raman spectra of bacteria that have been exposed to antibiotics for two hours.
9. Leave the antibiotic/bacteria solution in the incubator at 37$^{o}$C for another two hours in order for bacteria to interact with antibiotics for a total of four hours. Again, mix the solution with nanoparticles, create a spot and collect data for bacteria that have been exposed to antibiotics for four hours.
10. Finally, create a spot only with the antibiotics and nanoparticles and collect control Raman spectra.
11. Additionally, collect control Raman Spectra created of just silver nanoparticles and 1xPBS.

The above process was repeated for all antibiotics for each bacterium tested.

It is important to note that when the spots of nanoparticle/antibiotic/bacteria dried, the glass slide was placed in the refrigerator (4$^{o}$C) to avoid any further interaction between bacteria and antibiotic or bacteria and silver nanoparticle.

The above procedure was repeated for all bacteria in order to get enough information to compare with the conventional antibiograms. The steps are graphically illustrated in Figure 5.12.

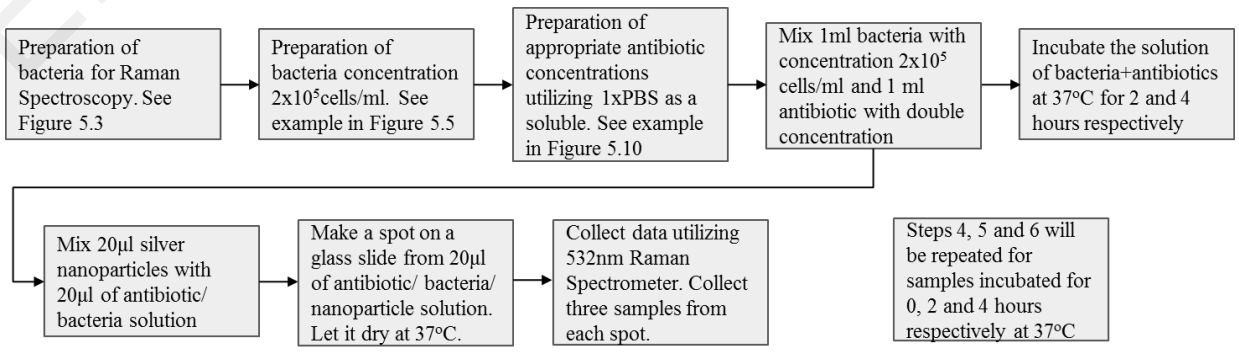


Figure 5.12 Proposed SERS antibiogram procedure

### 5.3.6 Direct data collection from urine samples

The final part of the project was to repeat the tasks of identification of the sample as positive or negative for UTI and of classification of the causative bacteria directly from urine. The samples used consisted of urine from healthy volunteers with known concentrations of bacteria diluted in it. The experimental procedure was as follows:

1. Prepare bacteria for Raman Spectroscopy as it is indicated in the protocol for Preparation of bacteria for Raman Spectroscopy (Figure 5.3).
2. Filter 50ml urine received from healthy volunteers utilizing PVDF Durapore filters with pore size 5 μm.
3. Dilute bacteria in the urine sample to prepare solutions with concentrations of $10^3$, $10^4$, $10^5$, $10^6$, $10^7$, $10^8$ bacteria/ml.
4. Filter 5ml of solutions of different concentrations with isopore filters with pore size 0.2μm and diameter 13mm.
5. Add 50μl of Ag NPs on top of the filter.
6. Collect Raman spectra directly from the filter with bacteria and nanoparticles. Collect three spectra per filter.
7. Repeat step 4-6 using silver membrane filters with pore size 0.2μm and diameter 13mm.

Figure 5.13 describes the procedure that was followed for data collection directly from urine samples.

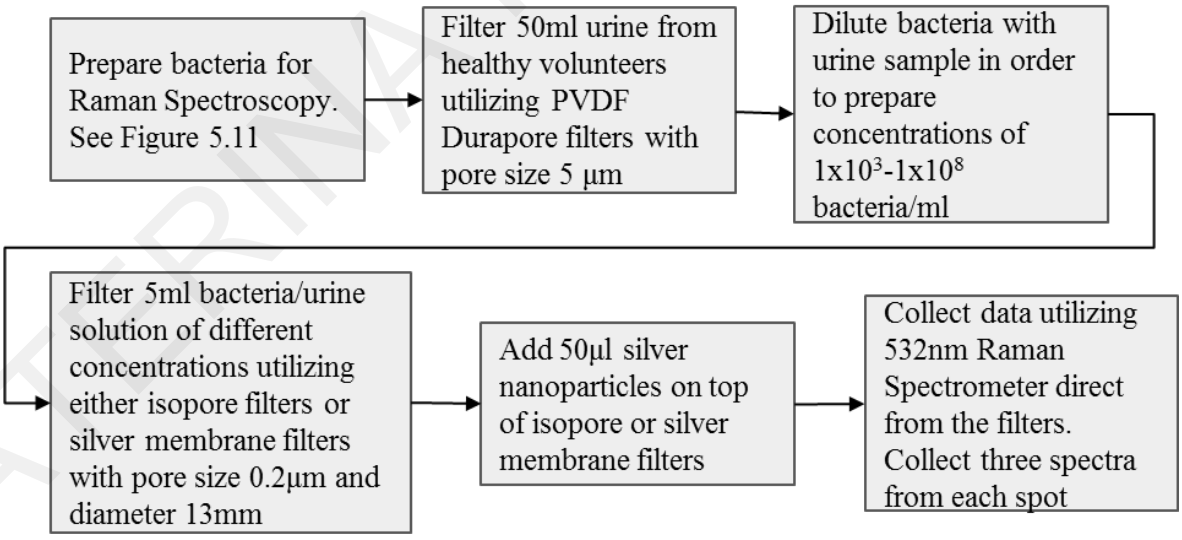


Figure 5.13 Proposed procedure for direct data collection from urine samples

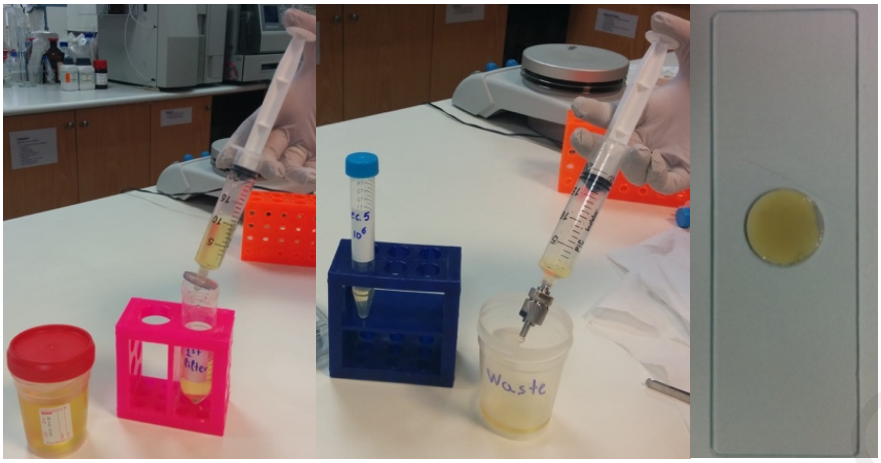


Figure 5.14 Fist and second filtration to filter and isolate bacteria on the top surface of filter

## 5.4 Data Analysis

This section describes the algorithms that have been developed in order to process the SERS data collected. These algorithms include pre-processing, identification of samples as positive or negative for UTI based on bacterial load, classification of bacterial species in positive sample as well as determination of bacteria susceptibility to various antibiotics. The required steps are graphically illustrated in Figure 5.15 and explained in Sections 5.4.1-5.4.4.

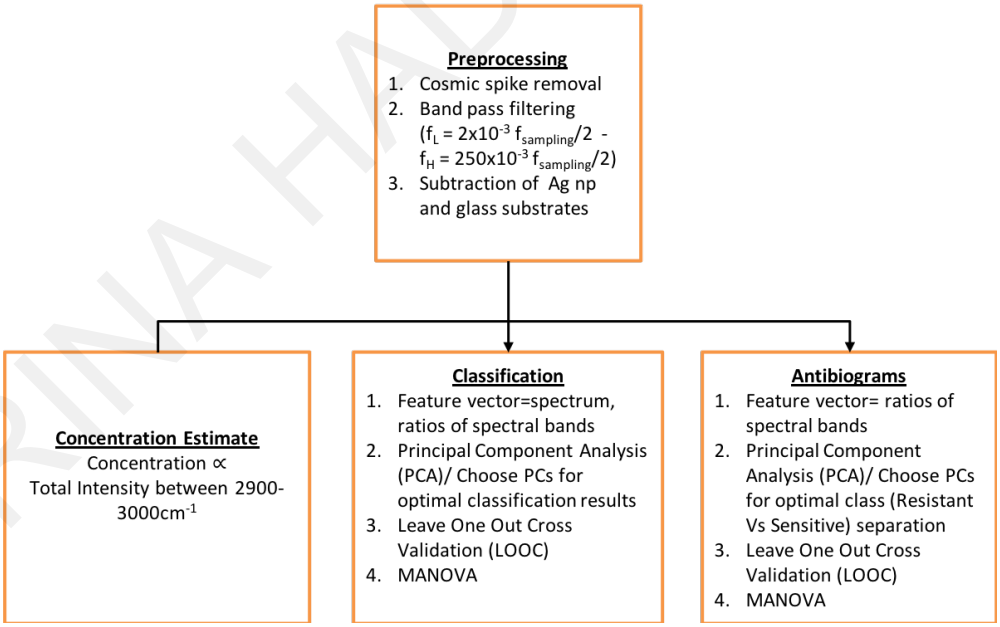


Figure 5.15 Procedure implemented for data processing

### 5.4.1 Preprocessing

All SERS spectra were acquired with the i-Raman Spectrometer and included data ranging from 300 $cm^{-1}$ to 3000 $cm^{-1}$ inclusive. Figure 5.16 shows unprocessed raw spectra of bacterial species *Escherichia coli* diluted at various concentrations.

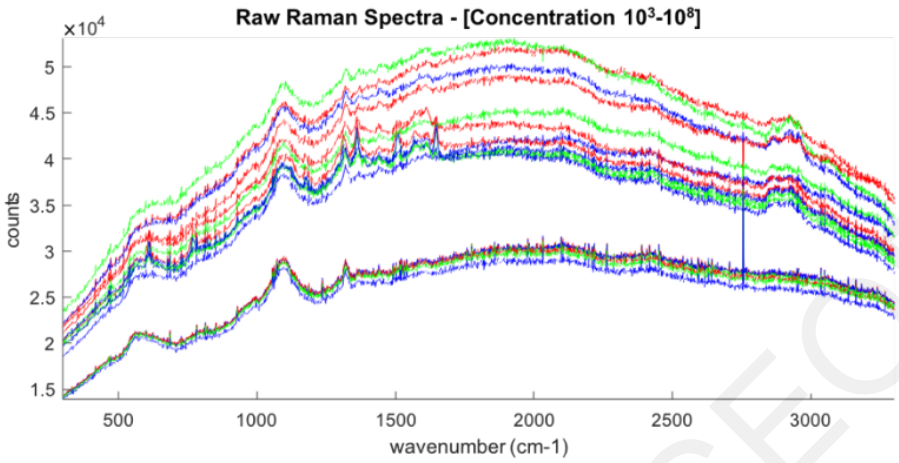


Figure 5.16 Unprocessed raw spectra of *Escherichia coli* at concentrations $1x10^3$-$1x10^8$ cells/ml

The raw spectra have three main sources of noise which are (i) high frequency noise from the electronics, (ii) low frequency fluorescence background, and (iii) "cosmic" spikes. High frequency noise comes from the acquisition electronics and other sources. A median or low-pass filtering can be used to remove this type of noise. Low frequency background arises from ambient light entering the spectrograph and fluorescence emission from the sample which, in the case of biological samples, can significantly reduce the dynamic range of the measurement. High-pass filtering was used to remove the low frequency background and to improve the accuracy of the classification. The third source of noise are so-called "cosmic" spikes, which have the form of very narrow spikes. They are called cosmic spikes because they resemble the spikes due to cosmic radiation in astronomy but in reality they are an artifact of the detection electronics. Cosmic spikes were removed by interpolating the values between the beginning and end of each spike from all spectra. Cosmic spikes appeared in the acquired data at the following wavenumbers: 611, 771, 1121, 1181, 1309, 1322, 1361, 1403, 1508, 1524, 1571, 1646, 2033, 2264, 2454 and 2773. The spectra after the removal of cosmic spikes are illustrated at Figure 5.17.

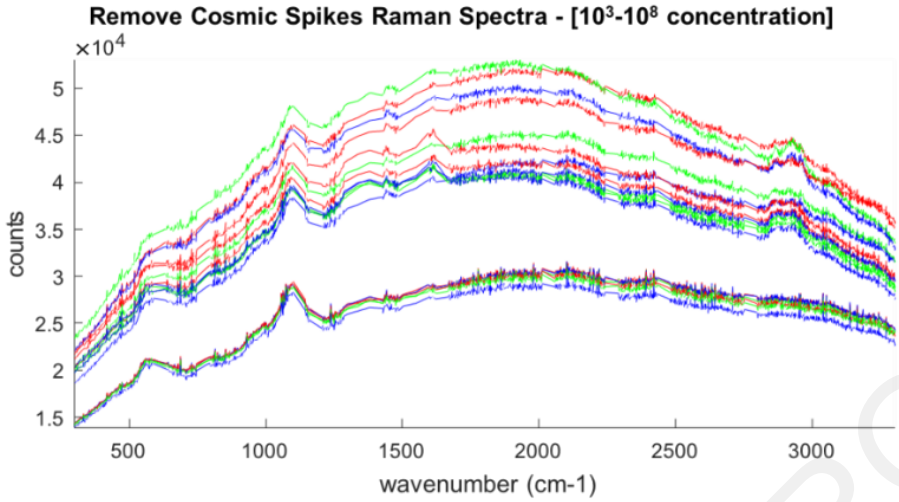


Figure 5.17 Cosmic Spikes Removal

To eliminate the high and low frequency noise, a band pass filter ($f_L$ = 0.002 $f_{sampling}/2$, $f_H = 0.250 f_{sampling}/2$) was used. The results of noise removal are displayed in Figure 5.18.

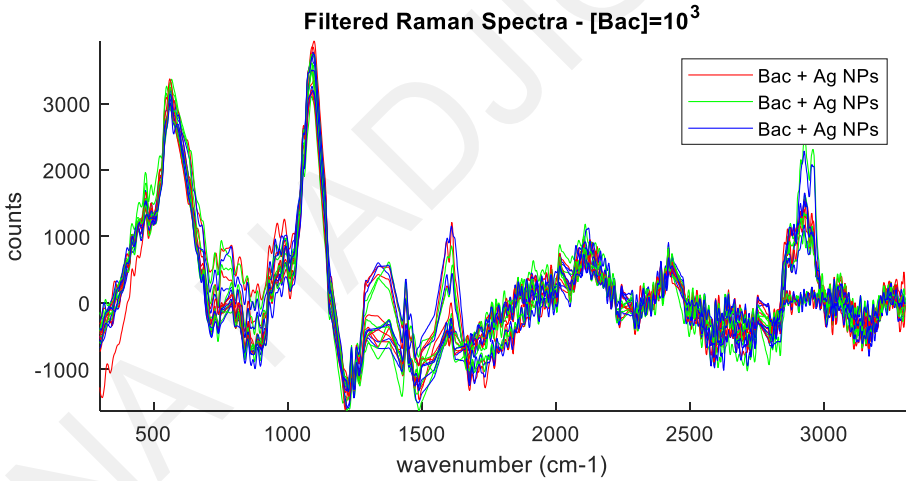


Figure 5.18 Application of band pass filter for background noise removal

The SERS spectra acquired from bacterial samples include the spectra of silver NPs and the glass slide. In order to isolate the spectra of the bacteria alone, it was necessary to subtract the NP and glass spectra. This was performed via vector projection of the total spectrum to that of the background. Figure 5.19 illustrates the average Raman spectrum collected from three spots composed by 20μl silver NPs and 20μl of 1xPBS (green) as well as the spectra collected directly from the glass slide (green). Figure 5.20 displays the spectra of Figure 5.18 after subtraction of the NP and glass spectra.

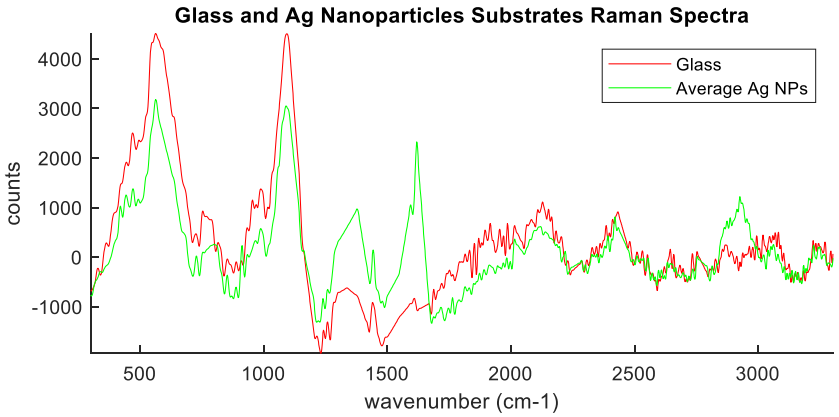


Figure 5.19 Raman spectra of glass slide and silver NPs substrates

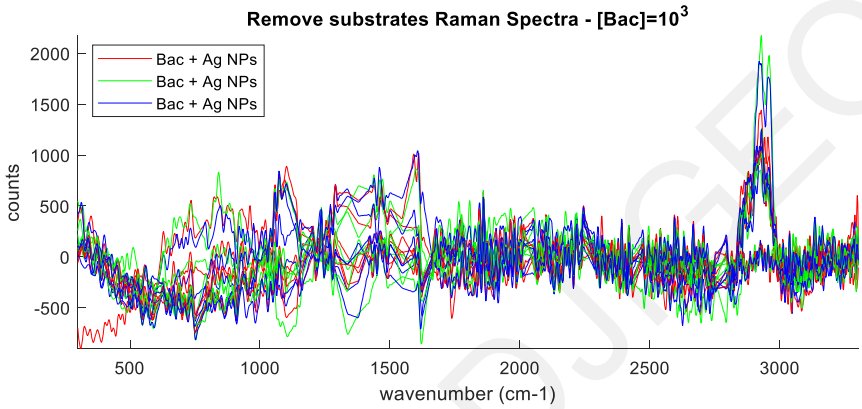


Figure 5.20 Raman spectra from bacteria after substrate removal

The last step in the pre-processing was data normalization. As it was explained in Section 5.3, three spectra were collected from every sample. These spectra usually exhibit different spectral intensity. Such variations between the spectra can affect the success of the classification of the data. Normalization to the highest peak, i.e. all the spectra modified so that they have the same minimum and maximum values, was used to eliminate this effect.

### 5.4.2 Classification of a sample as positive or negative for a UTI based on the bacterial load

The first task of this PhD research was the identification of a sample as positive or negative for a UTI. As already mentioned in Chapter 1, a sample can be considered positive for UTI when the concentration of bacteria in the sample is over $10^5$ cfu/ml, while a concentration of less than $10^4$ cfu/ml is considered a negative.

Wavenumbers around 2800-3100cm$^{-1}$ contain information about carbohydrates, lipids and proteins. These compounds are present in lipopolysaccharides which can be found

in the outer membrane of gram-negative bacteria, according to the literature. Therefore, the high-wave region of the spectrum (2500 to 3500 $cm^{-1}$) is proportional to the bacterial walls in the solution. Hence, the total intensity of the main peak (2900 to 3000 $cm^{-1}$) is proportional to the bacterial load and can be used to estimate the concentration of the bacteria in the sample. Figures 5.21 and 5.22 highlight the difference of Raman intensity in the high-wave region from sample containing $1x10^8$cells/ml and $1x10^4$cells/ml respectively.

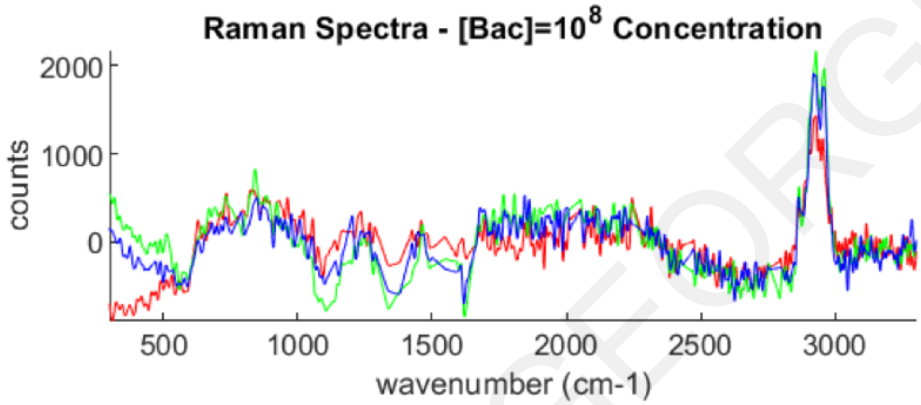


Figure 5.21 Raman spectra of bacterial samples with concentration of $1x10^8$cells/ml

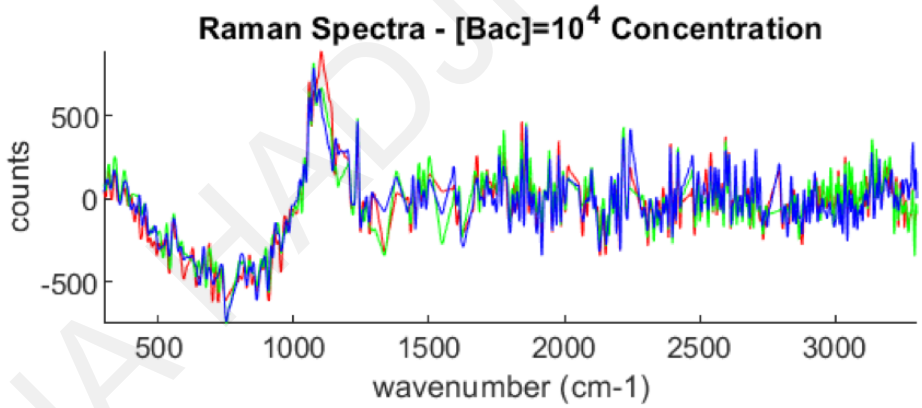


Figure 5.22 Raman spectra of bacterial samples with concentration of $1x10^4$cells/ml

### 5.4.3 Classification of bacterial species

After determining whether a sample was positive for a UTI, the next task was the classification of the bacterial species using the procedure below:

1. Spectra were pre-processed as described in section 5.4.1.
2. Bacteria were assigned to classes (E: *Escherichia coli*, K: *Klebsiella* sp. and P: *Proteus*)

3. Creation of an appropriate set of features which effectively describes variations in the spectra. For this study, a novel feature set was used, based on the ratios between different segments of the Raman spectrum, which resulted in much improved classification while keeping the analysis algorithm simple[128]. To get the spectral band ratios, each spectrum was divided into 300cm$^{-1}$ segments and the mean intensity for each segment was calculated. The ratios of each segment's mean intensity to each other segment's mean intensity were calculated. A total of 41 non-redundant ratios were produced and therefore each bacterial sample had a feature vector consisting of 41 features. These ratios provided a comparison between the relative intensities of different Raman bands and constituted an effective method for reducing noise, self-calibrating intensity differences and, more importantly, enhancing the subtle differences in the Raman spectra of different bacterial species. Figure 5.23 shows an example of the ratios used as contour plots. In addition to ratios, feature vectors using the pre-processed Raman spectra as well as their first and second derivatives were tested but were not found beneficial.

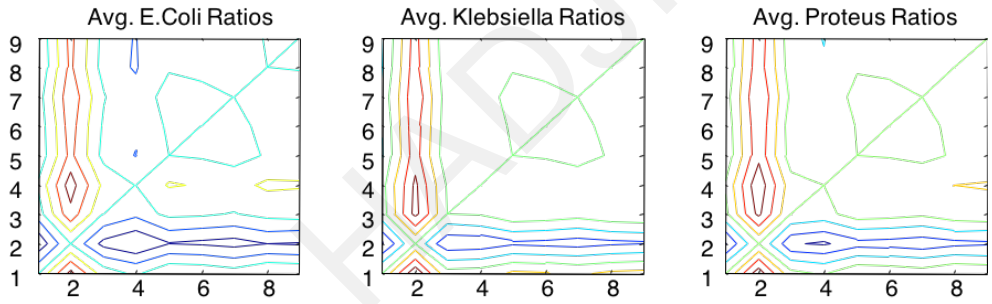


Figure 5.23 Contour plots of average ratios of the mean intensity of the segments of the Raman spectrum of *Escherichia coli*, *Klebsiella* sp. and *Proteus*. The axes correspond to the Raman spectrum segments, numbered from 1 to 9 starting from 300cm$^{-1}$ to 3000cm$^{-1}$ in 300cm$^{-1}$ step

4. A principal components transformation was utilized in order to reduce the dimensionality of the feature vectors. This was important in order to improve the accuracy of the classification results. It was also necessary for creating a positive definite feature matrix required for the Discriminant Analysis algorithm. Only principal components describing the highest variance of the original data were retained, and the rest were discarded.

5. Classification of the data using Linear Discriminant Analysis (LDA) followed. Leave-One Out Cross Validation was used to evaluate the performance of the classifier.

6. Finally, MANOVA was performed for display purposes. Scatter plots were created to visually illustrate the class clustering resulting from the classification procedure.

The same procedure was followed for the classification of data that are retrieved after filtering urine samples. A flow chart showing the procedure that was followed for bacteria classification based on their species is presented in Figure 5.24.

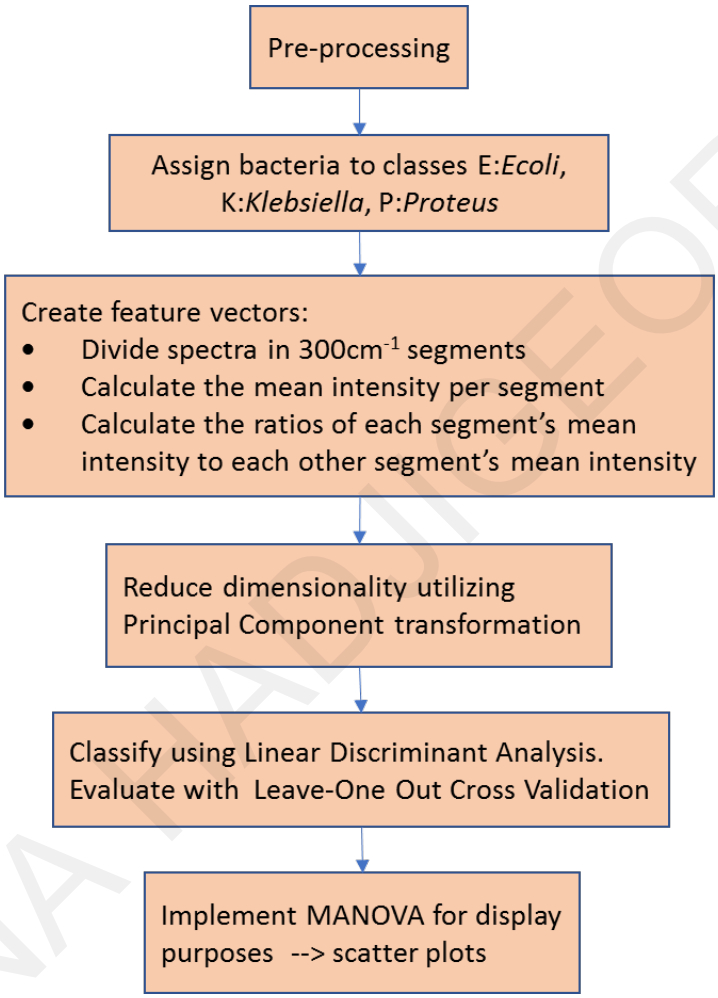


Figure 5.24 Flow chart of the procedure that was followed for bacteria classification based on their species

### 5.4.4 Classification of bacteria as resistant or sensitive to an antibiotic

In the study of antibiotic sensitivity, for the classification of bacteria as sensitive or resistant to antibiotics, SERS spectra were collected from 16 bacterial strains after 0, 2 and 4 hours of exposure to seven antibiotics or PBS (control). The procedure for their classification as sensitive or resistance is shown below:

1. Spectra were pre-processed as described in section 5.4.1.

2. Bacteria were assigned to classes (S: Sensitive, R: Resistant)

3. Subtraction of the control spectrum collected at 0 hours from the spectra collected after 2 and 4 hours exposure to antibiotics was performed. This step removed any background from the bacteria and/or the antibiotics. By embeding this step in the data analysis, only contributions associated with changes due to the antibiotic activity were taken into account.

4. An appropriate set of features which effectively describe variations in the spectra was created. The spectral ratios were used here as well. For this classification, various filter ranges (High Frequency Cutoff: 0.15, 0.25 or 0.50 of $f_s/2$) and window sizes (600, 400, 200, 100 or 50 $cm^{-1}$) were tested in order to find the optimal settings for best classification results for each case.

5. A principal components transformation in order to reduce the dimensionality of the feature vectors was utilized.

6. The bacteria were classified as sensitive or resistant using Linear Discriminant Analysis (LDA) at 2 hours of exposure or, separately, at 4 hours of exposure. The performance of the classifier was evaluated utilizing a Leave-One Out Cross Validation.

7. Finally, MANOVA was performed for display purposes. Scatter plots were created to visually illustrate the class clustering resulting from the classification procedure.

A flow chart of the above procedure for determining susceptibility of bacteria to antibiotics is illustrated in Figure 5.25.

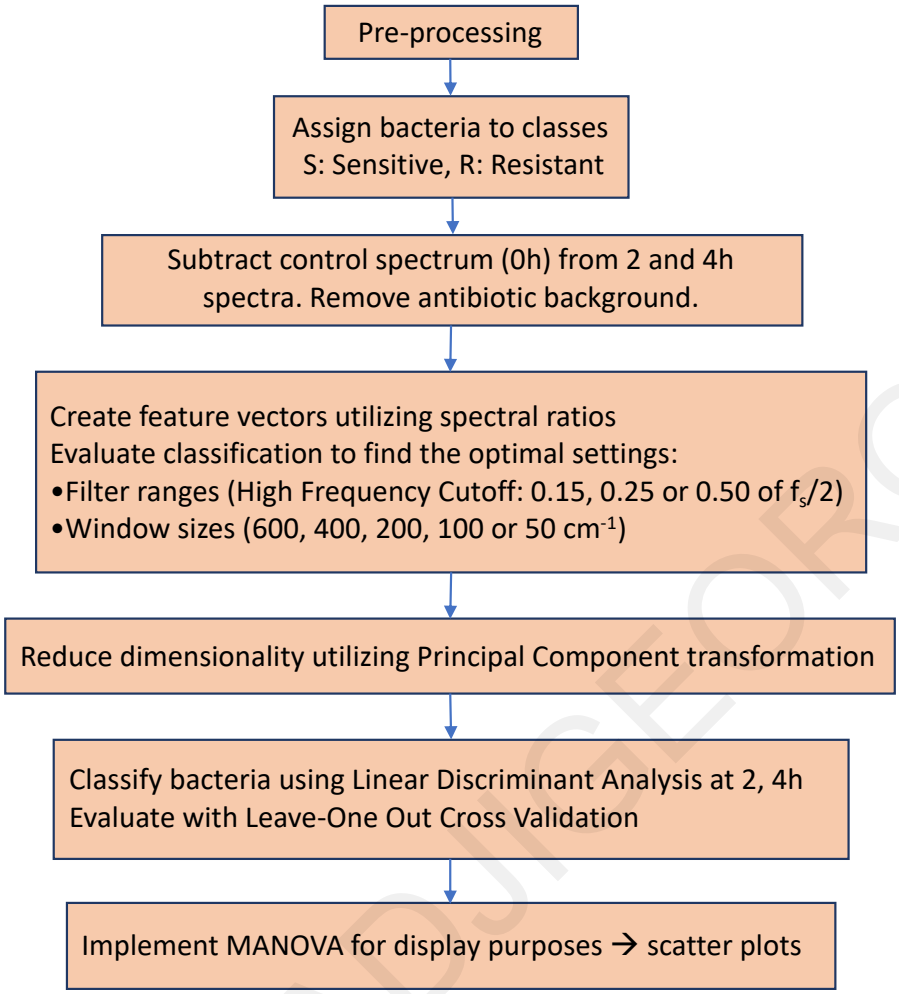


Figure 5.25 Flow chart of the procedure followed to determine susceptibility of bacteria to antibiotics

# Chapter 6
# RESULTS

## 6.1 Silver Nanoparticles

Experimental procedures were performed using synthesized silver nanoparticles (Ag NPs) according to the protocol of Lee et.al that is described analytically in Chapter 5 section 5.3.2. This protocol produces silver nanoparticles of 10-100nm radius. In order to characterize the shape, size and morphology of the produced Ag NPs, UV-Vis spectroscopy and Transmission Electron Microscopy (TEM) were used.

The characteristic optical absorption spectrum acquired with the UV-Vis spectrophotometer is shown in Figure 6.1. The graph reveals that:

1. There is a single major peak indicating that the solution is composed mainly by spherical NPs.
2. The absorbance peak occurs at 415nm indicating that the majority of the particles in the solution have a diameter around 40-50nm and are not aggregated.

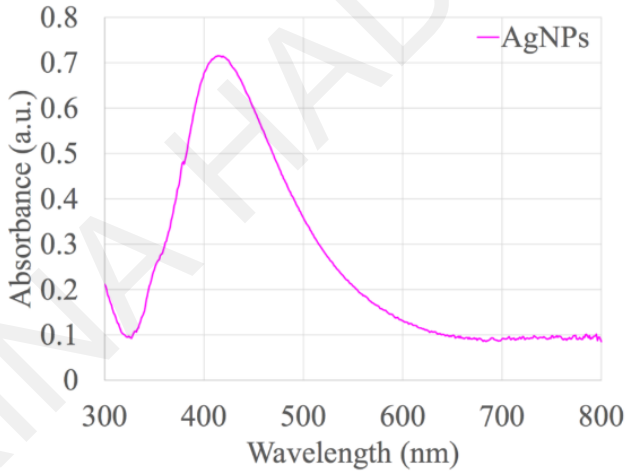


Figure 6.1 UV-Vis spectra of tested Ag NPs

Figure 6.2 is a TEM image showing the morphology of NPs. It is obvious from the image that the solution is composed of NPs with various diameters and shapes. The majority of NPs have a diameter around 50-100nm but there are also nanorods with transverse width around 50nm.

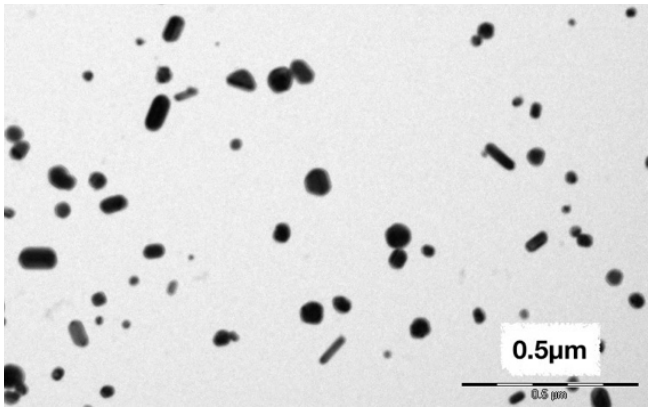


Figure 6.2 TEM images of Ag nanoparticles

## 6.2 Liquid Antibiogram Results

For the SERS antibiotic test, a "golden standard" antibiogram data set from liquid antibiograms was created. The measurements were obtained from the incubation of the bacteria to the relevant antibiotics for 48hours at 37$^{o}$C. Each bacterium was identified as Resistant, Sensitive or Intermediate Resistant for each of the antibiotics. As illustrated in Table 6.1 and Table 6.2, five types of bacteria were incubated with eight antibiotics. The column R indicates the resistant bacteria while S indicates the bacteria which are sensitive and IR denotes intermediate resistance. The results of the liquid antibiogram using various concentrations of antibiotics for all bacteria is included in Appendix A.

**Table 6.1 Numbers of samples which were resistant, intermediate resistant or sensitive to antibiotics Amoxil, Augmentin, Cefaclor and Ceftriaxone**

| | **Amoxil** | | **Augmentin** | | **Cefaclor** | | | **Ceftriaxone** | |
|---|---|---|---|---|---|---|---|---|---|
| Susceptibility / Bacteria | R | S | R | S | R | S | IR | R | S |
| ***Citrobacteur*** | 17 | 0 | 6 | 11 | 1 | 0 | 4 | 1 | 15 |
| ***Proteus*** | 13 | 7 | 7 | 13 | 2 | 1 | 2 | 0 | 20 |
| ***Klebsiella* sp.** | 7 | 0 | 1 | 6 | 5 | 0 | 0 | 1 | 4 |
| ***Escherichia coli*** | 11 | 5 | 3 | 13 | 5 | 1 | 1 | 0 | 16 |
| ***Enterobacteur*** | 11 | 0 | 11 | 1 | - | - | - | 5 | 7 |
| Total | 59 | 12 | 28 | 44 | 13 | 2 | 7 | 7 | 62 |

**Table 6.2 Numbers of samples which were resistant, intermediate resistant or sensitive to antibiotics Amikacin, Cefazolin, Ciprofloxacin and Cefuroxime**

| | **Amikacin** | | **Cefazolin** | | **Ciprofloxacin** | | **Cefuroxime** | |
|---|---|---|---|---|---|---|---|---|
| Susceptibility / Bacteria | R | S | R | S | R | S | R | S |
| ***Citrobacteur*** | 3 | 9 | 1 | 4 | 6 | 14 | 9 | 8 |
| ***Proteus*** | 16 | 2 | 2 | 3 | 5 | 8 | 5 | 15 |
| ***Klebsiella* sp.** | 0 | 2 | 2 | 3 | 7 | 10 | 5 | 2 |
| ***Escherichia coli*** | 6 | 2 | 0 | 7 | 1 | 14 | 5 | 11 |
| ***Enterobacteur*** | 4 | 8 | - | - | 2 | 9 | 11 | 1 |
| Total | 29 | 23 | 5 | 17 | 21 | 55 | 35 | 37 |

## 6.3 Classification of Samples as Positive or Negative.

In order to identify whether a sample was negative or positive for a UTI, eighteen SERS spectra were collected from serial dilutions of *Escherichia coli* bacteria. Then data was analyzed as described in section 5.4.2. Figure 6.3 shows the SERS spectra of samples with concentrations of $1x10^8$, $1x10^7$, $1x10^6$, $1x10^5$, $1x10^4$ and $1x10^3$ cells/ml. The characteristic peak in the high-wave region is clearly present for concentrations $1x10^8$-$1x10^5$ cells/ml while for concentrations $1x10^4$ and $1x10^3$ the peak cannot be seen. From the literature is known that the Raman bands at wavenumbers 2800-3100$cm^{-1}$ contain information regarding carbohydrates, lipids and proteins [18,19]. These molecules are found in the lipopolysaccharides [17] that are placed in the bacterial cell wall.

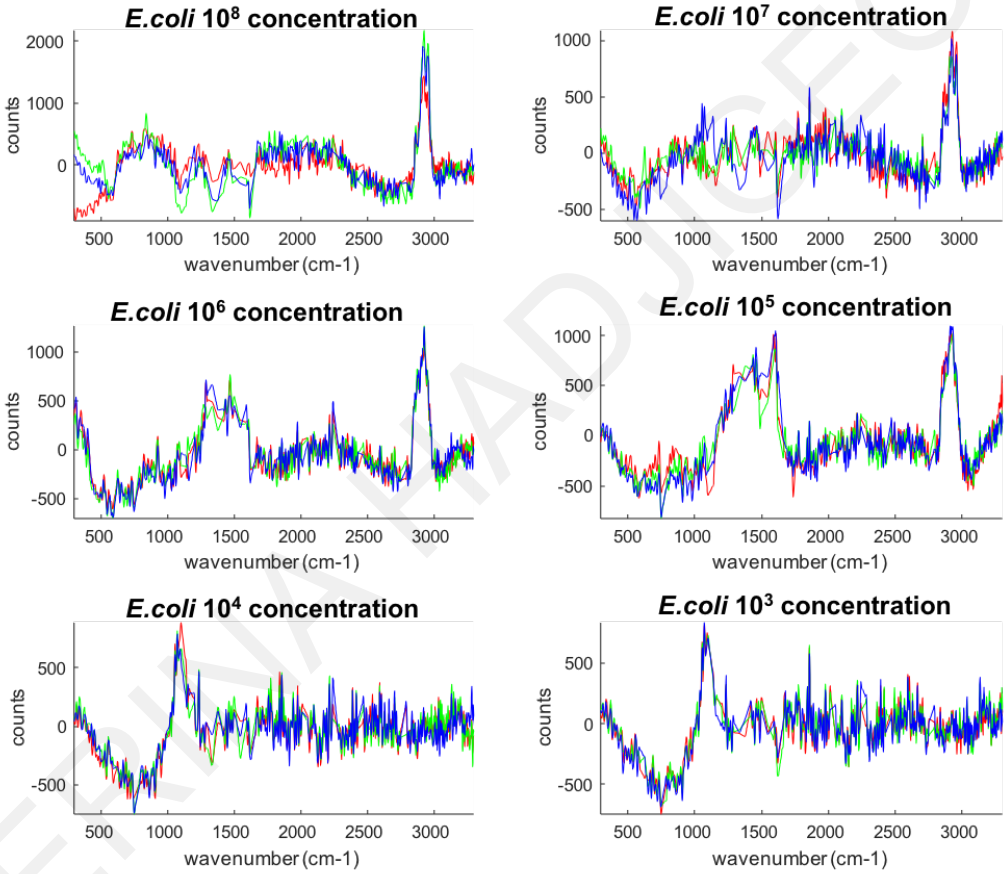


Figure 6.3 SERS spectra from *Escherichia coli* samples at concentrations varying from $10^3$-$10^8$ cells/ml

As shown in Figure 6.3, the total intensity of the high-wave region is increasing for concentrations from $1x10^3$ cells/ml until $1x10^8$ cells/ml. So, the research question at this point is whether the intensity of the peak in the high-wave region is proportional to bacterial concentration. For this reason, we sum the intensities of wavenumbers in the region 2800-3100$cm^{-1}$ in order to calculate the total intensity of the high-wave region for every concentration. We used the results of the total intensities and in order to create Figure 6.4

that shows that the total intensity is positively correlated with bacteria concentration and that there is a high degree of correlation between the actual concentration and the concentration estimated based on the intensity of the high wave region. These results prove that the SERS spectra could be used not only for determining whether a sample contains bacteria or not but also to estimate the concentration of bacteria in the sample. The dashed line in Figure 6.4 indicates the threshold (concentration between $10^4$ and $10^5$ bacteria/ml) above which a sample would be considered as positive for a UTI, illustrating a clear division of the positive and negative categories.

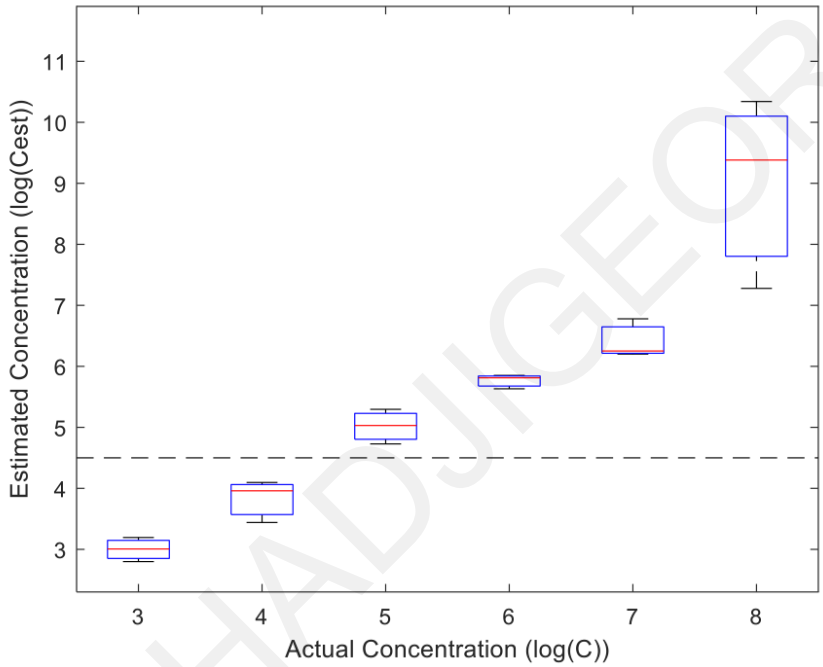


Figure 6.4 Actual concentration Vs. concentration estimated from the intensity of the high wave region of the SERS spectra.

## 6.4 Classification of bacterial species using SERS

In order to identify the pathogen that causes the UTI and classify it according to its species, the methodology described in section 5.3.4 and data analysis techniques of section 5.4.3 were applied. To create the appropriate feature vectors, the spectral band ratios between different segments of the Raman spectrum as well as the normalized and pre-processed Raman spectra were utilized. In Figure 6.5, are the contour plots of the average ratios of *Escherichia coli*, *Klebsiella* sp. and *Proteus*. The axes correspond to the Raman spectrum segments, numbered from 1 to 9 starting, from 300 $cm^{-1}$ to 3000 $cm^{-1}$ in 300 $cm^{-1}$ steps (segment size). In addition, principal components 1, 2, 4, and 6 were retained for maximal class separation.

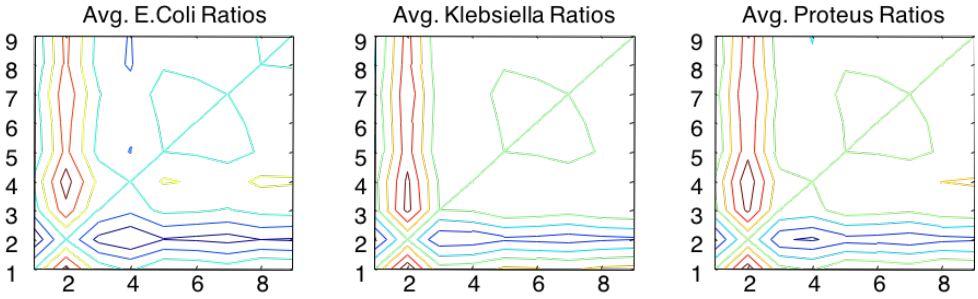


Figure 6.5 Feature vectors for classification due to bacteria species

The results of the classification of bacteria that belonged to three different classes (*Escherichia coli*, *Klebsiella* sp. and *Proteus*) using SERS was very accurate, providing correct classification rate of 93.75%. As shown in Table 6.3, only one bacterium out of 16 was wrongly classified (a *Klebsiella* sp. was misclassified as *Proteus*). Figure 6.6, a scatter plot of the MANOVA scores, illustrates how the bacteria are clearly separated into three classes: (+) *Escherichia coli* (+) *Proteus* and (+) *Klebsiella* sp.. In addition, Figure 6.6 shows how an unknown *Escherichia coli* correctly classified. In conclusion, the results of the classification suggest that unknown bacteria can be effectively identified and classified with high accuracy using SERS.

**Table 6.3 Bacterial species classification results**

| Bacterial Species | |
|---|---|
| **Class** | **Predicted** |
| *Proteus* | *Proteus* |
| *Proteus* | *Proteus* |
| *Proteus* | *Proteus* |
| *Proteus* | *Proteus* |
| *Proteus* | *Proteus* |
| *Klebsiella* sp. | *Klebsiella* sp. |
| *Klebsiella* sp. | *Proteus* |
| *Klebsiella* sp. | *Klebsiella* sp. |
| *Klebsiella* sp. | *Klebsiella* sp. |
| *Escherichia coli* | *Escherichia coli* |
| *Escherichia coli* | *Escherichia coli* |
| *Escherichia coli* | *Escherichia coli* |
| *Escherichia coli* | *Escherichia coli* |
| *Escherichia coli* | *Escherichia coli* |
| *Escherichia coli* | *Escherichia coli* |
| *Escherichia coli* | *Escherichia coli* |

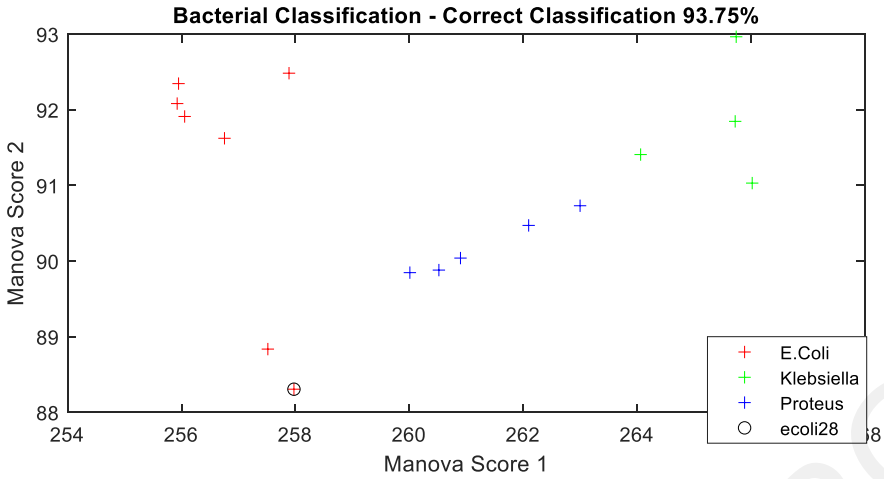


Figure 6.6 Correct Classification of an unknown *Escherichia coli* sample

## 6.5 Antibiotic susceptibility testing of bacteria using SERS

For the experimental determination of bacterial susceptibility to antibiotics, sixteen bacterial strains (seven *Escherichia coli*, four *Klebsiella* sp. and five *Proteus spp*.) were exposed to the antibiotic's amoxicillin, amoxicillin/clavulanic acid, cefaclor, cefazolin, ceftriaxone, cefuroxime and ciprofloxacin, according to the protocols described in section 5.3.5. Figure 6.7 shows the Raman spectra received only by the seven antibiotics. Furthermore, SERS spectra of the solutions were collected after two and four hours of exposure.

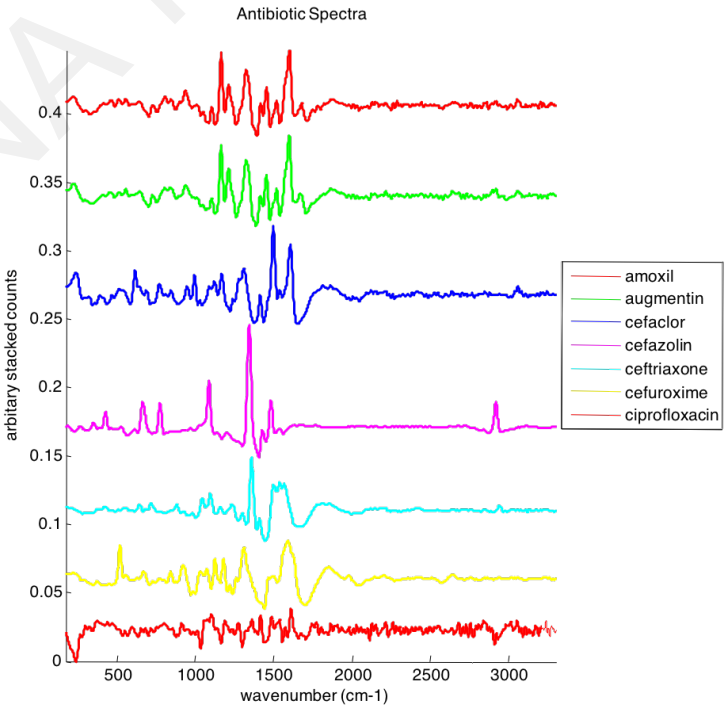


Figure 6.7 Raman spectra of antbiotics after pre-processing

The algorithm to determine antibiotic susceptibility, described in section 5.4.4, was applied with various high pass filters, ratio segment sizes and number of principle components. Tables 6.2 and 6.3 summarize the correct classification rate of antibiotic susceptibility or resistance after two and four hours of exposure respectively. The tables also include the filter cutoff, ratio segment size and number of principal components that were used to provide the best results. The correct classification rates ranged from 81.25-93.75% after two hours of exposure to the antibiotics while higher correct classification was achieved after four hours exposure, reaching in as high as 100% correct classification for the antibiotic cefuroxime. Figures 6.8 and 6.9 are the MANOVA score scatter plots for 4 hours of exposure to the antibiotics, showing a sensitive *Escherichia coli* and a resistant *Klebsiella* sp. correctly classified. These results suggest that SERS could be used to determine the antibiotic susceptibility of bacteria as early as two to four hours after incubation with the antibiotics.

**Table 6.4 Antibiotic classification results after a 2-hour exposure**

| Antibiotic | %Correct | $f_s/2$ | PCs | W ($cm^{-1}$) |
|---|---|---|---|---|
| Amoxil | 81,25 | 0.25 | 1, 2, 3, 4 | 200 |
| Augmentin | 93,75 | 0.15 | 1,2 | 200 |
| Cefaclor | 81,25 | 0.15 | 1,2 | 100 |
| Cefazolin | 81,25 | 0.5 | 1,2,2 | 100 |
| Ceftriaxone | 93,75 | 0.15 | 1,2 | 100 |
| Cefuroxime | 87,5 | 0.5 | 2,3,4,5,6 | 50 |
| Ciprofloxacin | 93,75 | 0.15 | 1,2,3,4,5,6,7,8,9 | 400 |
| **Mean** | **87,5** | | | |

**Table 6.5 Antibiotic classification results after a 4-hour exposure**

| Antibiotic | %Correct | $f_s/2$ | PCs | W ($cm^{-1}$) |
|---|---|---|---|---|
| Amoxil | 87.50 | 0.25 | 1, 2 | 600 |
| Augmentin | 93.75 | 0.15 | 1,2 | 100 |
| Cefaclor | 81.25 | 0.5 | 1,2,3,4 | 400 |
| Cefazolin | 81.25 | 0.15 | 2,3,4,5, | 100 |
| Ceftriaxone | 93.75 | 0.5 | 1,2,3 | 50 |
| Cefuroxime | 100.00 | 0.15 | 3,4,5,6,7,8,9,10,11,12,13 | 600 |
| Ciprofloxacin | 87.50 | 0.15 | 4,5 | 200 |
| **Mean** | **89,29** | | | |

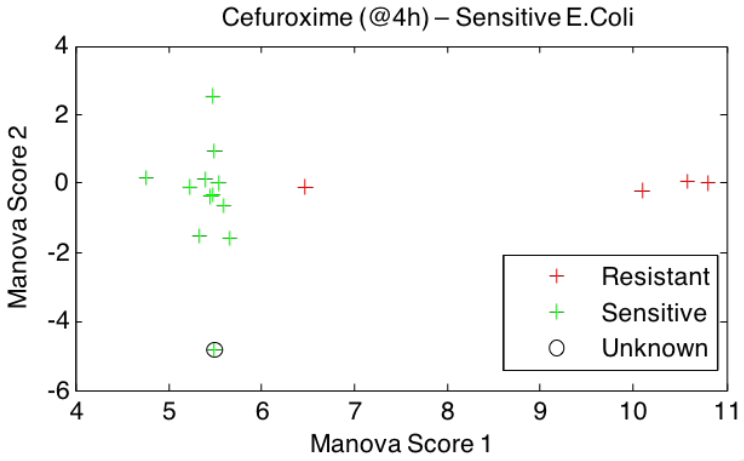


Figure 6.8 Correct classification of an *Escherichia coli* as sensitive to cefuroxime

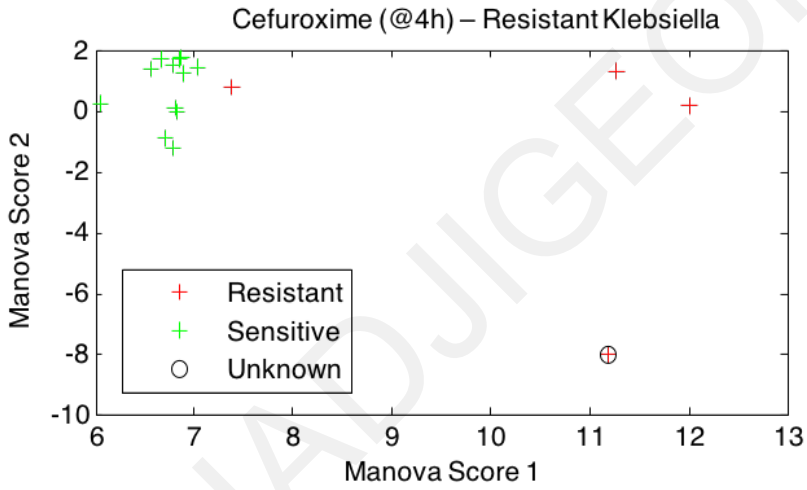


Figure 6.9 Correct classification of a *Klebsiella* sp. as resistant to cefuroxime

## 6.6 Spectral contributors to the antibiotic sensitivity testing

It is interesting to note that the SERS method proposed here provides successful antibiotic susceptibility results not only for antibiotics such as augmentin or cefuroxime that act on the bacterial cell wall but also for ciprofloxacin that acts on the bacterial DNA. This is somewhat of a paradox since (1) the enhancement effect is caused by NPs which accumulate on the outer wall of the bacteria whereas the ciprofloxacin site of action is intracellular and (2) the effect of ciprofloxacin could not become evident in as little as two to four hours since it interferes with gene expression which requires longer to become evident. These observations triggered further investigation of the classification process.

After taking the spectral ratios and performing PCA, one can work backwards and assign to each wavenumber in the spectrum a weight proportional to its significance in the

classification process. Figure 6.10 shows these classification weights for ciprofloxacin with the most significant peaks, positive or negative, annotated.

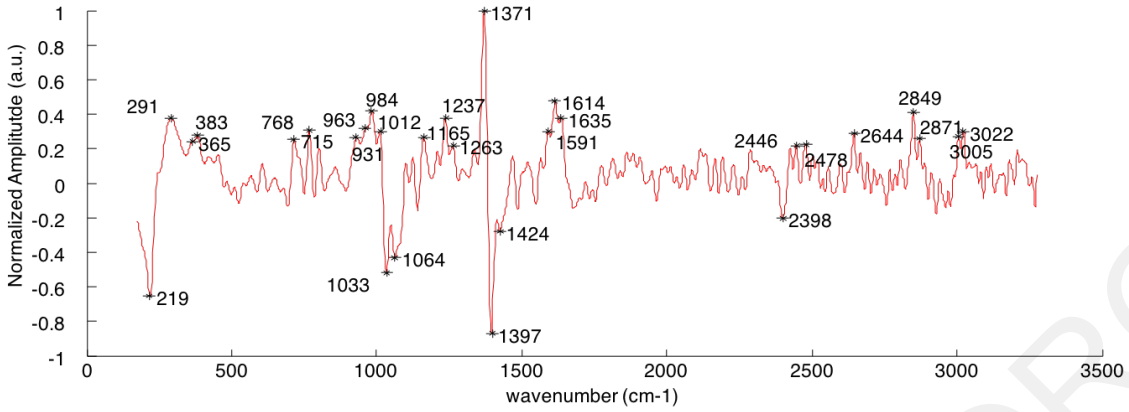


Figure 6.10 Average weights of principal components used for antibiotic sensitivity classification. The peaks with the largest amplitudes are those contributing the most to the classification of the bacteria

Based on these classification weights, two theories have emerged that could explain this paradox:

1. The most significant classification weights have peaks that correspond or are very similar to DNA Raman peaks. In the literature, adenine was shown to have a major peak at 1420 $cm^{-1}$, guanine at 375 $cm^{-1}$, 1336 $cm^{-1}$ and 1369 $cm^{-1}$, and cytosine at 1613 $cm^{-1}$[18,19]. Also, in the literature, it is mentioned that ciprofloxacin affects the bacterial DNA and that it causes the extracellular release of adenine, guanine and cytosine. If these molecules are hence adjacent to the NPs used for enhancement, our SERS method could be detecting their corresponding Raman spectra and thus correctly classifying such bacteria as susceptible to ciprofloxacin.

2. The most significant classification weights also have peaks that correspond or are very similar to those of the antibiotic, ciprofloxacin. An overlay of the classification weights over the Raman spectrum of ciprofloxacin, in Figure 6.11, shows significant overlap between the two. A common mechanism of antibiotic resistance to ciprofloxacin, as well as other fluoroquinolones, is to actively export the antibiotic agents via antibiotic efflux pumps to the environment [129]. These pumps actively remove the antibiotic from the bacterial cytoplasm, preventing the antibiotic from ever reaching its target site. It is, therefore, possible that the SERS spectra of resistant bacteria contain the spectrum of ciprofloxacin, which is now close to the NPs.

Of course, none of these theories can be proven without further investigation.

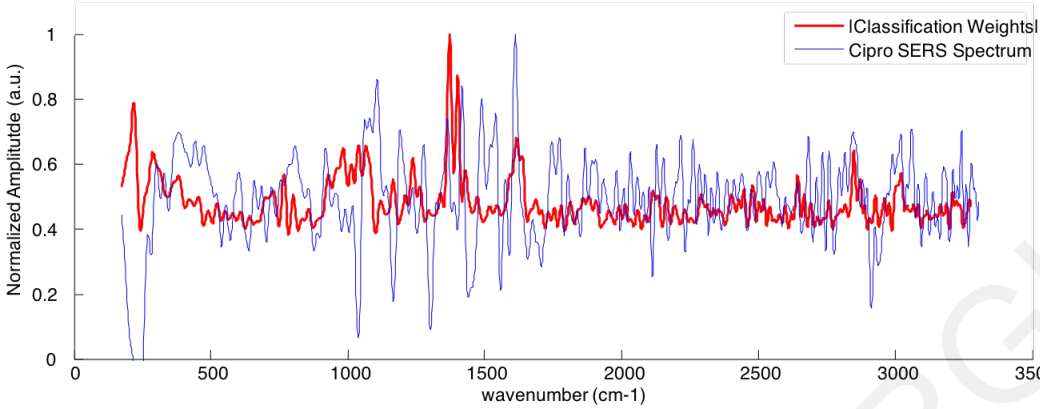


Figure 6.11 Absolute values of average weights of principal components (red) overlaid on the Raman spectrum of ciprofloxacin (blue)

## 6.7 Classification of bacteria species from urine

The next step in the evaluation SERS as a tool for UTI diagnosis was to isolate bacteria from urine. For this reason, bacteria were diluted in urine, collected from healthy volunteers and filtered twice as described in section 5.3.6. The first filtering was implemented utilizing PVDF Durapore filters with pore size 5 μm in order to remove epithelial or white blood cells, which could be present in the sample, while the second filtering was achieve by using with isopore filters with pore size 0.2μm and diameter 13mm. By utilizing these filters, the bacteria contained in the sample were concentrated on the top surface of the filter and Raman spectra were collected directly from the top surface of the filter. The second filtering was also tested for silver membrane filters instead of isopore filters. The data collected though, utilizing the silver membrane filters, were saturated so we did not continue collecting spectra from silver membrane filters. For these experiments, the following bacteria were included: 5 strains of *Escherichia coli*, 5 strains of *Klebsiella* sp. and 4 strains of *Proteus*. All bacteria were diluted to a concentration of $1x10^6$cells/ml.

For the classification of the bacteria, the algorithm described in section 5.4.3 was applied. The feature vector consisted of the spectral band ratios, with a window size of 300 $cm^{-1}$, and principal components 1 and 2. Figure 6.12 illustrates contour plots of the average ratios for *Escherichia coli*, *Klebsiella* sp. and *Proteus*. Figure 6.13 shows the average Raman spectra of different bacteria after pre-processing. Unfortunately, the spectra collected appear to have very low SNR.

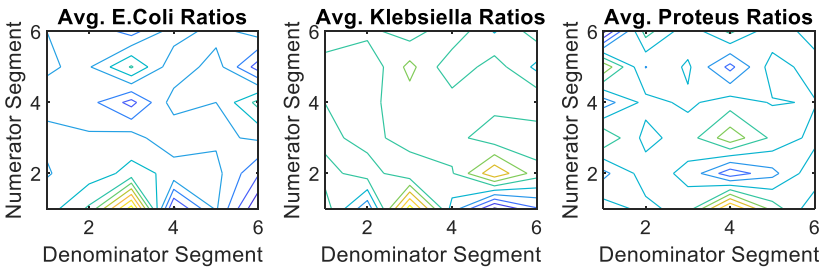


Figure 6.12 Average spectral band ratios for the bacterial species used in this study.

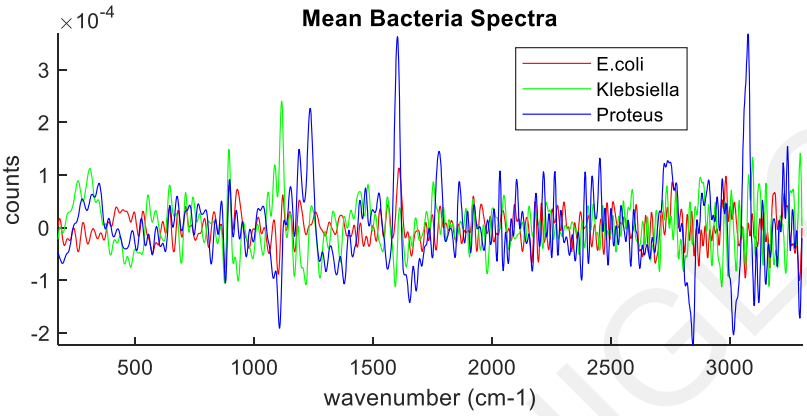


Figure 6.13 Raman spectra of bacteria after filtration and pre-processing.

Three samples were misclassified resulting in overall classification of 78.6%. In Table 6.6 the classification of each sample is shown. Figure 6.14 is a scatter plot of the MANOVA scores of the bacterial species with an unknown *Escherichia coli* correctly classified. These results indicate that the technique of utilizing filters to collect and concentrate bacteria from urine samples, before collecting their SERS spectra, requires further refinement.

**Table 6.6 Correct classification rate per bacterial species**

| Bacterial species | Classification |
|---|---|
| *Escherichia coli* | *Escherichia coli* |
| *Escherichia coli* | *Escherichia coli* |
| *Escherichia coli* | *Klebsiella* sp. |
| *Escherichia coli* | *Escherichia coli* |
| *Escherichia coli* | *Escherichia coli* |
| *Klebsiella* sp. | *Klebsiella* sp. |
| *Klebsiella* sp. | *Klebsiella* sp. |
| *Klebsiella* sp. | *Escherichia coli* |
| *Klebsiella* sp. | *Klebsiella* sp. |
| *Klebsiella* sp. | *Klebsiella* sp. |
| *Proteus* | *Proteus* |
| *Proteus* | *Proteus* |
| *Proteus* | *Klebsiella* sp. |
| *Proteus* | *Proteus* |

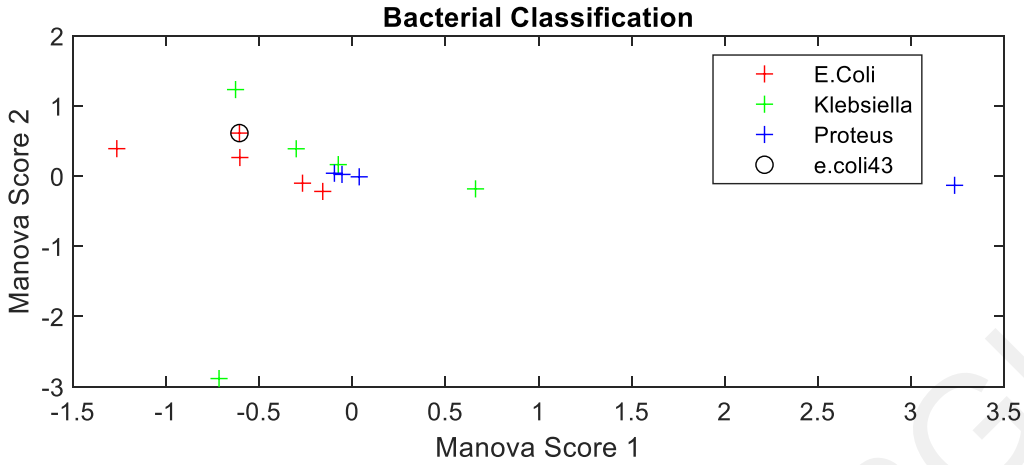


Figure 6.14 Classification of bacteria samples collected directly from filters. An unknown *Escherichia coli* sample was correctly classified.

# Chapter 7
# Conclusions and Future Work

## 7.1 Conclusions

This PhD thesis focused on the development of a SERS-based method that in a short period of time could detect if a patient is suffering from UTI, identify the bacterial species causing it and determine the most effective antibiotic to treat the infection. This work addresses a significant diagnostic challenge since UTIs affect more than 30% of the population worldwide, posing a severe strain on the patients and the health care system, and since the current diagnostic methods require about 48 hours for a definitive diagnosis and antibiogram. As a result of that, physicians prescribe broad-spectrum antibiotics that may cause recurrent infections and bacterial resistance to the antibiotics.

SERS provides spectra containing biochemical information regarding the molecular structure of the surface of the bacteria sampled. The usually low intensity of the Raman spectra was enhanced using silver nanoparticles (SERS). These spectra were analyzed, producing novel feature vectors of spectral band rations, and classified with PCA and LDA. The results of this work indicate that:

1. It is possible to both identify if a sample is infected by a UTI as well as estimate the concentration of bacteria in the sample using SERS. This is achieved by calculating the total intensity of the high-wave region of the spectra coming from "positive" or "negative" UTI samples. A "positive" sample corresponds to a concentration of more than $10^5$ bacteria/ml while a "negative" sample corresponds to a concentration of less than $10^4$ bacteria/ml. Data analysis proved that there is almost a linear relationship between the high-wave region total intensity and concentrations between $1x10^3$ to $1x10^8$ cells/ml.

2. It is feasible to classify bacterial species using SERS. Data analysis of spectra from samples of *Escherichia coli*, *Klebsiella* sp. and *Proteus* bacteria, at a concentration of $1x10^5$cells/ml, has shown that the bacteria can classified in three distinct classes with accuracy of 93.75%.

3. It is possible to distinguish bacteria that are sensitive to an antibiotic from the bacteria that are resistant to an antibiotic after just 2 to 4 hours exposure, using SERS. The

preliminary results of sixteen bacteria strains exposed to seven antibiotics resulted to 81.25-100% correct classification.

4. The classification of bacteria as resistant or sensitive was successful for different categories of antibiotics that either affect the bacterial cell wall or interfere with the synthesis of bacterial DNA. SERS can identify changes in the structure of the bacterial cell wall in a few hours. The mechanism of the classification of bacteria as sensitive or resistant to antibiotics affecting the synthesis of DNA is still under investigation but may be because of the efflux of purines, pyrimidines or the antibiotic itself to the external environment.

5. The experiments for classification of bacterial strains directly from urine samples utilizing filters did not provide as impressive results. For this experimental procedure, urine samples containing bacteria were filtered in order to isolate and concentrate the bacteria. Raman spectra were collected directly from the filters. The results of this procedure were 78.6% correct classification among fourteen bacterial strains belonging to three different bacterial species. The techniques for the isolation of bacteria from urine samples must be furthered refined.

The research in this PhD is still preliminary and must be significantly expanded utilizing more bacterial strains, more antibiotics and testing new methods for bacteria isolation from urine. However, the results presented in this Thesis compare favorably and in many cases exceed the current state-of-the-art. They were all obtained using clinically realistic conditions, while at the same time the techniques used are very straight-forward and inexpensive. These results provides sufficient indications that SERS could be used for the development of an innovative tool that could provide same day results regarding the presence of a UTI and the most effective antibiotic for treatment. Such a technology could have significant benefits for patients and for the public health care system by reducing disease recurrence, the cost of diagnosis, the unnecessary use of antibiotics and finally, the long-term bacterial resistance to antibiotics.

## 7.2 Discussion

As it has been described in detail in section 2.3 “Current and emerging diagnostics methods for UTIs” the state-of-the-art and the emerging methodologies, which are widely used in hospitals and clinical labs or aim to penetrate the market for UTI diagnosis and antibiogram, belong to three main categories: (i) phenotypic methods (culture based), (ii)

molecular techniques and (iii) spectroscopic techniques. Each technique has specific advantages and limitations.

The definitive diagnostic technique for UTI diagnosis, identification of the causative bacteria and AST is the bacterial culture. It delivers high accuracy with relatively low cost but requires 24-72 hours to provide results, since bacterial cultures must grow at least overnight. In order to improve the culture-based approaches, automatic lab instrumentation, such as the BD Phoenix and the Vitek bioMérieux, have been developed. They have automated and standardized the process to easily manage high workloads but still require a pure pathogen culture that must be incubated overnight. Other limitations of these instruments include the fact that they cannot process samples directly from urine and, additionally, cannot identify all the possible bacterial species and antibiotics, since the systems rely on specific, pre-existing, libraries.

Techniques that require substantially less time to provide results are the molecular PCR-based methods. Currently, these approaches provide identification and AST in less than 6 hours, with high accuracy, directly from urine samples. However, the drawbacks of this technique are that it requires (i) a DNA extraction step from isolated strains, (ii) a high number of cells to obtain adequate DNA, (iii) previous knowledge on the sequences to amplify and (iv) significant training and expertise. Hence, these technologies are not suitable for daily use in clinical microbiology. Other techniques, that include the spectrometry approaches like MALDI-TOF MS and PCR/ESI-MS, can detect concentrations as low as $10^4$ and 128 CFU/ml respectively and provide results in a matter of a few minutes. However, they are very expensive and do not provide AST.

Emerging methods for UTI diagnosis are focusing on imaging technologies and lab-on-a-chip devices. By utilizing these novel technologies, the time required to obtain results has dropped to less than 5 hours, high accuracies of around 95% are achieved and diagnosis directly from urine samples is possible. However, these platforms require further improvements in order to be established in the market as definitive diagnosis and antibiogram tools.

As described in detail in section 3.5 “Relevant applications of Raman spectroscopy”, there are multiple groups studying the SERS profiles of bacterial species in order to classify them based on their species. However, only few research groups worldwide have attempted to detect bacterial species directly from urine or develop an antibiogram susceptibility test. Some of these groups tried to filter, centrifuge or apply dielectrophoresis in order to isolate the bacteria from the urine samples, demonstrating relevant high accuracy ranging from 66-

98%. Other research groups aimed to characterize samples containing up to three different bacterial strains, obtaining high accuracies with advanced classification algorithms.

Only four groups, worldwide, have studied the effects of antibiotic treatment to the SERS profiles of bacteria. Neugebauer et al. utilized a three level PLS-LDA-LDA model to distinguish the sensitive from the resistant strain of *Enterococcus faecalis* achieving 86% sensitivity and 93% specificity, with respect to the prediction of vancomycin resistance in *Enterococcus faecalis*, when the model is tested with data of an independent biological replicate. In addition, Ting-Ting Liu et al. where able to study the effect of antibiotics to the bacterial cell wall, demonstrating spectral changes as early as 20 minutes after antibiotics addition. Furthermore, Ni Tien et al. showed that antibiotic susceptibility was feasible from samples received directly from urine samples utilizing PCA, while Kai Yang et al. recently demonstrated that the susceptibility profiles of fourteen bacterial strains including three in clinical urine samples can be correctly classified utilizing Raman-$D_2O$ with a 100% categorical agreement regarding standard disk diffusion tests. However, all of these studies used antibiotics with a concentration higher than the indicated minimal inhibitory concentration (MIC).

## 7.3 Future Work

As it has been discussed in the previous chapters, Surface Enhanced Raman Spectroscopy (SERS) is a very promising method that could be utilized in the future as a powerful diagnostic tool for UTI diagnosis and antibiogram. However, there are some challenges that must be overcome towards the development of a final product that would provide same day results for UTIs.

The first challenge that must be addressed is the development of a method to isolate and concentrate bacteria from urine and acquire their SERS spectra. Through in this work, filters were utilized to isolate bacteria, the results were not very encouraging. Other approaches have to be explored and the optimal technology has to be implemented.

Furthermore, it has been shown that there is significant variation in the SERS spectra collected from the same spot of the glass slide. This is due to the fact that SERS, in general, suffers from low reproducibility due to an inhomogeneous and a rather uncontrollable aggregation of the nanoparticles. The fluctuations of spectral characteristics are getting even worse when different colloid batches are used. An approach to make SERS more reproducible and standardized is needed.

Both of the above challenges could be addressed by the use of microfluidics. Microfluidics provide a well-defined detection environment that can lead to constant aggregation of nanoparticles and additionally can be used for manipulation, filtration and separation of the sample. Furthermore, through microfluidics the whole procedure of filtration and isolation can be carried out in nanoliter volumes, in an automatic and reproducible manner eliminating the interaction with the human factor.

In order for this technique to truly become a Point-Of-Care diagnostic test, the cost and portability must be further addressed. The validation of the methods using a commercial, portable and inexpensive Raman system will reduce dramatically the price of the final product. In addition, the fabrication of the nanoparticles used for SERS must be better controlled and optimized. The nanoparticles produced for this research were not uniform and their peak absorption at 415 nm was not optimal for the 532 nm excitation of the Raman system used. Thus, new recipes for nanoparticle synthesis must be tested for creating higher quality nanoparticles with more appropriate spectra.

Furthermore, all the experimental procedures for classification of bacterial species and antibiotic sensitivity must be extended with a broader spectrum of antibiotics and a wider range of bacteria. The use of a more antibiotics and bacteria will prove that the methodology is statistically valid and will provide accurate and reliable results.

The introduction of microfluidic filtration and isolation, the utilization of low-cost Raman systems, the extension of the experiments to include a wider range of bacteria, antibiotics and improved nanoparticles could lead to a more robust technique that could provide reproducible, accurate and reliable diagnosis of UTI in a matter of a few hours.

# REFERENCES


[1] P. Tenke, B. Kovacs, T. E. Bjerklund, T. Matsumoto, P. A. Tambyah, and K. G. Naber, "European and Asian guidelines on management and prevention of catheter-associated urinary tract infections," *Int. J. Antimicrob. Agents*, vol. 31, no. 1, pp. 68–78, 2008.

[2] G. Schmiemann, E. Kniehl, K. Gebhardt, M. M. Matejczyk, and E. Hummers-pradier, "The Diagnosis of Urinary Tract Infection," *Dtsch. Arztebl. Int.*, vol. 107, no. 21, pp. 361–368, 2010.

[3] J. E. Simmering, F. Tang, J. E. Cavanaugh, L. A. Polgreen, and P. M. Polgreen, "The increase in hospitalizations for urinary tract infections and the associated costs in the United States, 1998-2011," *Open Forum Infect. Dis.*, vol. 4, no. 1, pp. 1–7, 2017.

[4] "Urinary tract infection (UTI) - Symptoms and causes - Mayo Clinic." [Online]. Available: https://www.mayoclinic.org/diseases-conditions/urinary-tract-infection/symptoms-causes/syc-20353447. [Accessed: 10-Dec-2019].

[5] "Tests Index | Lab Tests Online." [Online]. Available: https://labtestsonline.org/tests-index. [Accessed: 10-Dec-2019].

[6] C. W. Tan and M. P. Chlebicki, "Urinary tract infections in adults," *Singapore Med*, vol. 57, no. 9, pp. 485–490, 2016.

[7] "Surveillance Atlas of Infectious Diseases." [Online]. Available: https://atlas.ecdc.europa.eu/public/index.aspx?Dataset=27&HealthTopic=4. [Accessed: 10-Dec-2019].

[8] S. Dason, J. T. Dason, and A. Kapoor, "Guidelines for the diagnosis and management of recurrent urinary tract infection in women," *Can. Urol. Assoc. Journa*, vol. 5, no. 5, pp. 316–322, 2011.

[9] M. Grabe *et al.*, "Guidelines on urological infections," *Eur. Assoc. Urol.*, vol. 182, no. March, pp. 237–257, 2015.

[10] D. Inverarity, "Oxford handbook of infectious diseases and microbiology," *J. Hosp.*

*Infect.*, vol. 75, no. 2, p. 148, 2010.

[11] H. C. Neu, "Effect of 3-Lactamase Location in Escherichia coli on Penicillin Synergy," *Appl. Environ. Microbiol.*, vol. 17, no. 6, pp. 783–786, 1969.

[12] J. M. Blondeau, "Fluoroquinolones : Mechanism of Action , Classification ," *Surv. Ophthalmol.*, vol. 49, no. March, pp. 1–6, 2004.

[13] European Center for Disease Prevention and Control, "Annual Epidemiological Report. Antimicrobial resistance and healthcare-associated infections. 2014. Available http://ecdc.europa.eu/en/publications/Publications/antimicrobial-resistance-annual-epidemiological-report.pdf. Accessed: 10/10/2015.," 2014.

[14] "Urinalysis (Urine) Test: Types, Drugs, Alcohol, Results and Interpretation." [Online]. Available: https://www.medicinenet.com/urinalysis/article.htm. [Accessed: 28-May-2020].

[15] "(PDF) Infection control and patient discomfort with an alternative plastic barrier in intraoral digital radiography." [Online]. Available: https://www.researchgate.net/publication/312222937_Infection_control_and_patient_discomfort_with_an_alternative_plastic_barrier_in_intraoral_digital_radiography. [Accessed: 28-May-2020].

[16] "Disk Diffusion - an overview | ScienceDirect Topics." [Online]. Available: https://www.sciencedirect.com/topics/immunology-and-microbiology/disk-diffusion. [Accessed: 28-May-2020].

[17] "Testing the Effectiveness of Antimicrobials | Microbiology." [Online]. Available: https://courses.lumenlearning.com/microbiology/chapter/testing-the-effectiveness-of-antimicrobials/. [Accessed: 28-May-2020].

[18] G. Maugeri, I. Lychko, R. Sobral, and A. C. A. Roque, "Identification and Antibiotic-Susceptibility Profiling of Infectious Bacterial Agents: A Review of Current and Future Trends," *Biotechnol. J.*, vol. 14, no. 1, p. 1700750, 2019.

[19] "ETEST® Ceftolozane/Tazobactam (C/T) - clinical diagnostics products | bioMérieux Clinical Diagnostics." [Online]. Available: https://www.biomerieux-diagnostics.com/etest-ceftolozane-tazobactam. [Accessed: 28-May-2020].

[20] "New ETEST® Ceftolozane/Tazobactam (C/T 256): MIC determination helps optimize therapy for serious infections - BIOMÉRIEUX iNEWS." [Online]. Available: https://www.biomerieux-microbio.com/solutions/new-etest-ceftolozane-tazobactam-c-t-256-mic-determination-helps-optimize-therapy-for-serious-infections/. [Accessed: 28-May-2020].

[21] B. W. Buchan, N. W. Anderson, and N. A. Ledeboer, "Comparison of BD Phoenix and bioMérieux Vitek 2 automated systems for the detection of macrolide-lincosamide-streptogramin B resistance among clinical isolates of Staphylococcus," *Diagn. Microbiol. Infect. Dis.*, vol. 72, no. 3, pp. 291–294, 2012.

[22] "Home - BioSense Solutions." [Online]. Available: https://biosensesolutions.dk/. [Accessed: 28-May-2020].

[23] "Accelerate Pheno™ system." [Online]. Available: http://acceleratediagnostics.com/products/accelerate-pheno-system/#features. [Accessed: 28-May-2020].

[24] D. T. Quach, G. Sakoulas, V. Nizet, J. Pogliano, and K. Pogliano, "Bacterial Cytological Profiling (BCP) as a Rapid and Accurate Antimicrobial Susceptibility Testing Method for Staphylococcus aureus," *EBioMedicine*, vol. 4, pp. 95–103, 2016.

[25] A. L. Roberts, U. Joneja, T. Villatoro, E. Andris, J. A. Boyle, and J. Bondi, "Evaluation of the BacterioScan 216Dx for standalone preculture screen of preserved urine specimens in a clinical setting," *Lab Med.*, vol. 49, no. 1, pp. 35–40, 2018.

[26] L. C. O'Keefe *et al.*, "Innovations in Worksite Diagnosis of Urinary Tract Infections and the Occupational Health Nurse," *Work. Heal. Saf.*, vol. 67, no. 6, pp. 268–274, 2019.

[27] "GeneCapture scientists preview new technology for rapid antimicrobial susceptibility testing." [Online]. Available: https://www.uah.edu/news/research/genecapture-scientists-preview-new-technology-for-rapid-antimicrobial-susceptibility-testing. [Accessed: 28-May-2020].

[28] M. Fredborg, F. S. Rosenvinge, E. Spillum, S. Kroghsbo, M. Wang, and T. E.

Sondergaard, “Rapid antimicrobial susceptibility testing of clinical isolates by digital time-lapse microscopy,” *Eur. J. Clin. Microbiol. Infect. Dis.*, vol. 34, no. 12, pp. 2385–2394, 2015.

[29] A. Charnot-Katsikas *et al.*, “Use of the accelerate pheno system for identification and antimicrobial susceptibility testing of pathogens in positive blood cultures and impact on time to results and workflow,” *J. Clin. Microbiol.*, vol. 56, no. 1, pp. 1–13, 2018.

[30] “DrugBank.” [Online]. Available: https://www.drugbank.ca/. [Accessed: 12-Dec-2019].

[31] FDA, “Augmentin,” *AGPL17 Prescr. Inf.*, pp. 3–18, 2006.

[32] “Alphaviruses (Togaviridae) and Flaviviruses (Flaviviridae) - PubMed.” [Online]. Available: https://pubmed.ncbi.nlm.nih.gov/21413253/. [Accessed: 28-May-2020].

[33] “Gram-negative bacteria - Wikipedia.” [Online]. Available: https://en.wikipedia.org/wiki/Gram-negative_bacteria. [Accessed: 28-May-2020].

[34] A. Kulkarni *et al.*, “A novel nanometric DNA thin film as a sensor for alpha radiation,” *Sci. Rep.*, vol. 3, p. 2062, 2013.

[35] M. Chisanga, H. Muhamadali, D. I. Ellis, and R. Goodacre, “Surface-Enhanced Raman Scattering (SERS) in Microbiology: Illumination and Enhancement of the Microbial World,” *Appl. Spectrosc.*, vol. 72, no. 7, pp. 987–1000, 2018.

[36] M. Culha, D. Stokes, L. R. Allain, and T. Vo-Dinh, “Surface-Enhanced Raman Scattering Substrate Based on a Self-Assembled Monolayer for Use in Gene Diagnostics,” *Anal. Chem.*, vol. 75, no. 22, pp. 6196–6201, 2003.

[37] A. Pal, N. R. Isola, J. P. Alarie, D. L. Stokes, and T. Vo-Dinh, “Synthesis and characterization of SERS gene probe for BRCA-1 (breast cancer),” *Faraday Discuss.*, vol. 132, pp. 293–301, 2006.

[38] P. R. G. D. J. Graves and D. Gardiner, *Practical Raman Spectroscopy*. Springer Berlin Heidelberg, 1989.

[39] “HORIBA.” [Online]. Available: https://www.horiba.com/en_en/. [Accessed: 10-Dec-2019].

[40] "Princeton Instruments." [Online]. Available: https://www.princetoninstruments.com/. [Accessed: 10-Dec-2019].

[41] "Remote Sensing Using Lasers." [Online]. Available: https://seos-project.eu/laser-rs/laser-rs-c07-s03-p04.html. [Accessed: 28-May-2020].

[42] "Advanced Physics Laboratory." [Online]. Available: https://www.physics.utoronto.ca/~phy326/. [Accessed: 10-Dec-2019].

[43] "The Raman Spectrophotometer." [Online]. Available: https://www.sas.upenn.edu/~crulli/TheRamanSpectrophotometer.html. [Accessed: 22-Apr-2020].

[44] R. Petry, M. Schmitt, and J. Popp, "Raman Spectroscopy – A Prospective Tool in the Life Sciences," *ChemPhysChem*, vol. 4, no. 1, pp. 14–30, 2003.

[45] I. R. Lewis and H. G. M. Edwards, *Handbook of Raman Spectroscopy*. CRC Press, 2001.

[46] "Raman spectroscopy." [Online]. Available: https://iopscience.iop.org/chapter/978-1-6817-4071-3/bk978-1-6817-4071-3ch3.pdf. [Accessed: 10-Dec-2019].

[47] R. M. Jarvis and R. Goodacre, "Characterisation and identification of bacteria using SERS," *Chem. Soc. Rev.*, vol. 37, no. 5, 2008.

[48] M. Angelidou, "Biomedical Imaging and Applied Optics Laboratory Design of Nanosurfaces With Optimized Optical Properties Using the DDA Algorithm," no. May, 2007.

[49] P. J. Vikesland, "Surface-Enhanced Raman Spectroscopy ( SERS ) for Environmental Analyses," pp. 7749–7755, 2010.

[50] R. Pilot, C. Durante, L. Orian, M. Bhamidipati, and L. Fabris, "A Review on Surface-Enhanced Raman Scattering," *Biosensors*, vol. 9, no. 2, p. 57, 2019.

[51] "Gold Nanorods - an overview | ScienceDirect Topics." [Online]. Available: https://www.sciencedirect.com/topics/physics-and-astronomy/gold-nanorods. [Accessed: 22-Apr-2020].

[52] "Silver Nanoparticles: Optical Properties – nanoComposix." [Online]. Available:

https://nanocomposix.com/pages/silver-nanoparticles-optical-properties#target. [Accessed: 23-Apr-2020].

[53] D. Cam, K. Keseroglu, M. Kahraman, F. Sahin, and M. Culha, "Multiplex identification of bacteria in bacterial mixtures with surface-enhanced Raman scattering," *J. Raman Spectrosc. An Int. J. Orig. Work all Asp. Raman Spectrosc. Incl. High. Order Process. also Brillouin Rayleigh Scatt.*, vol. 41, no. 5, pp. 484–489, 2010.

[54] S. Efrima and L. Zeiri, "Understanding SERS of bacteria," *J. Raman Spectrosc. An Int. J. Orig. Work all Asp. Raman Spectrosc. Incl. High. Order Process. also Brillouin Rayleigh Scatt.*, vol. 40, no. 3, pp. 277–288, 2009.

[55] K. Gaus *et al.*, "Classification of Lactic Acid Bacteria with UV-Resonance Raman Spectroscopy," *Biopolym. Orig. Res. Biomol.*, vol. 82, no. 4, pp. 286–290, 2006.

[56] M. Harz, P. Ro, K. Peschke, O. Ronneberger, H. Burkhardt, and J. Popp, "Micro-Raman spectroscopic identification of bacterial cells of the genus Staphylococcus and dependence on their cultivation conditions," *Analyst*, vol. 130, no. 11, pp. 1543–1550, 2005.

[57] H. Kudo, T. Itoh, T. Kashiwagi, M. Ishikawa, H. Takeuchi, and H. Ukeda, "Chemistry Surface enhanced Raman scattering spectroscopy of Ag nanoparticle aggregates directly photo-reduced on pathogenic bacterium ( Helicobacter pylori )," *J. Photochem. Photobiol. A Chem.*, vol. 221, no. 2–3, pp. 181–186, 2011.

[58] López-Díez, E. Consuelo, and R. Goodacre, "Characterization of Microorganisms Using UV Resonance Raman Spectroscopy and Chemometrics," *Anal. Chem.*, vol. 76, no. 3, pp. 585–591, 2004.

[59] I. S. Patel, W. R. Premasiri, D. T. Moir, and L. D. Ziegler, "Barcoding bacterial cells : a SERS-based methodology for pathogen identification," *J. Raman Spectrosc. An Int. J. Orig. Work all Asp. Raman Spectrosc. Incl. High. Order Process. also Brillouin Rayleigh Scatt.*, vol. 39, no. 11, pp. 1660–1672, 2008.

[60] W. R. Premasiri, N. Krieger, and W. R. Associates, "Characterization of the Surface Enhanced Raman Scattering ( SERS ) of Bacteria," *J. Phys. Chem. B*, vol. 109, no. 1, pp. 312–320, 2005.

[61] A. Sengupta, M. L. Laucks, N. Dildine, E. Drapala, and E. J. Davis, "Bioaerosol characterization by surface-enhanced Raman spectroscopy (SERS)," *J. Aerosol Sci.*, vol. 36, no. 5–6, pp. 651–664, 2005.

[62] C. Xie, D. Chen, and Y. Li, "Raman sorting and identification of single living micro-organisms with optical tweezers," *Opt. Lett.*, vol. 30, no. 14, pp. 1800–1802, 2005.

[63] J. B. Forrester, N. B. Valentine, Y. Su, and T. J. Johnson, "Analytica Chimica Acta Chemometric analysis of multiple species of Bacillus bacterial endospores using infrared spectroscopy : Discrimination to the strain level," *Anal. Chim. Acta*, vol. 651, no. 1, pp. 24–30, 2009.

[64] K. Maquelin *et al.*, "Raman Spectroscopic Method for Identification of Clinically Relevant Microorganisms Growing on Solid Culture Medium," *Anal. Chem.*, vol. 72, no. 1, pp. 12–19, 2000.

[65] L. Zeiri and S. Efrima, "Surface-enhanced Raman spectroscopy of bacteria : the effect of excitation wavelength and chemical modification of the colloidal milieu," *J. Raman Spectrosc. An Int. J. Orig. Work all Asp. Raman Spectrosc. Incl. High. Order Process. also Brillouin Rayleigh Scatt.*, vol. 36, no. 6–7, pp. 667–675, 2005.

[66] U. Schmid, P. Rösch, M. Krause, M. Harz, J. Popp, and K. Baumann, "Chemometrics and Intelligent Laboratory Systems Gaussian mixture discriminant analysis for the single-cell differentiation of bacteria using micro-Raman spectroscopy," *Chemom. Intell. Lab. Syst.*, vol. 96, no. 2, pp. 159–171, 2009.

[67] J. Guicheteau, S. Christesen, and A. Tripathi, "Bacterial mixture identification using Raman and surface-enhanced Raman chemical imaging," *J. Raman Spectrosc.*, vol. 41, no. 12, pp. 1632–1637, 2010.

[68] N. Nicolaou, Y. Xu, and R. Goodacre, "Fourier Transform Infrared and Raman Spectroscopies for the Rapid Detection, Enumeration, and Growth Interaction of the Bacteria Staphylococcus aureus and Lactococcus lactis ssp. cremoris in Milk," *Anal. Chem.*, vol. 83, no. 14, pp. 5681–5687, 2011.

[69] A. J. Berger and Q. Zhu, "Identification of oral bacteria by raman microspectroscopy," *J. Mod. Opt.*, vol. 50, no. 15–17, pp. 2375–2380, 2003.

[70] S. Nie and S. R. Emory, "Probing Single Molecules and Single Nanoparticles by Surface-Enhanced Raman Scattering," *Science (80-. ).*, vol. 275, no. 5303, pp. 1102–1106, 1997.

[71] K. Kneipp *et al.*, "Single Molecule Detection Using Surface-Enhanced Raman Scattering ( SERS )," *Phys. Rev. Lett.*, vol. 78, no. 9, pp. 1667–1670, 1997.

[72] C. Fan, Z. Hu, L. K. Riley, G. A. Purdy, A. Mustapha, and M. Lin, "Detecting Food- and Waterborne Viruses by Surface-Enhanced Raman Spectroscopy," *J. Food Sci.*, vol. 75, no. 5, pp. 302–307, 2010.

[73] H. Cheng, S. Huan, H. Wu, G. Shen, and R. Yu, "Surface-Enhanced Raman Spectroscopic Detection of a Bacteria Biomarker Using Gold Nanoparticle," *Anal. Chem.*, vol. 81, no. 24, pp. 9902–9912, 2009.

[74] D. Hutsebaut, K. Maquelin, P. De Vos, P. Vandenabeele, L. Moens, and G. J. Puppels, "Effect of Culture Conditions on the Achievable Taxonomic Resolution of Raman Spectroscopy Disclosed by Three Bacillus Species," *Anal. Chem.*, vol. 76, no. 21, pp. 6274–6281, 2004.

[75] C. Mello, D. Ribeiro, and F. Novaes, "Rapid differentiation among bacteria that cause gastroenteritis by use of low-resolution Raman spectroscopy and PLS discriminant analysis," *Anal. Bioanal. Chem.*, vol. 383, no. 4, pp. 701–706, 2005.

[76] C. Mello, E. Ricci, L. Coelho, and R. J. Poppi, "Fast Differentiation of Bacteria causing Pharyngitis by Low Resolution Raman Spectroscopy and PLS-Discriminant Analysis," *J. Braz. Chem. Soc.*, vol. 19, no. 1, pp. 29–34, 2008.

[77] O. Preisner, J. A. Lopes, and J. C. Menezes, "Uncertainty assessment in FT-IR spectroscopy based bacteria classi fi cation models," *Chemom. Intell. Lab. Syst.*, vol. 94, no. 1, pp. 33–42, 2008.

[78] N. S. Foster, S. E. Thompson, N. B. Valentine, J. E. Amonette, and T. J. Johnson, "Identification of Sporulated and Vegetative Bacteria Using Statistical Analysis of Fourier Transform Mid-infrared Transmission Data," *Appl. Spectrosc.*, vol. 58, no. 2, pp. 203–211, 2004.

[79] P. C. A. M. Buijtels *et al.*, "Rapid Identification of Mycobacteria by Raman Spectroscopy," *J. Clin. Microbiol.*, vol. 46, no. 3, pp. 961–965, 2008.

[80] G. C. Green *et al.*, "Identification of Listeria Species Using a Low-Cost Surface-Enhanced Raman Scattering System With Wavelet-Based Signal Processing," *IEEE Trans. Instrum. Meas.*, vol. 58, no. 10, pp. 3713–3722, 2009.

[81] A. Walter *et al.*, "Raman spectroscopic detection of physiology changes in plasmid-bearing Escherichia coli with and without antibiotic treatment," *Anal. Bioanal. Chem.*, vol. 400, no. 9, pp. 2763–2773, 2011.

[82] T. Udelhoven *et al.*, "Development of a method based on chemometric analysis of Raman spectra for the discrimination of heterofermentative lactobacilli," vol. 54, no. 10, pp. 1660–1672, 2010.

[83] R. M. Jarvis, A. Brooker, and R. Goodacre, "Surface-Enhanced Raman Spectroscopy for Bacterial Discrimination Utilizing a Scanning Electron Microscope with a Raman Spectroscopy Interface," *Anal. Bioanal. Chem.*, vol. 76, no. 17, pp. 5198–5202, 2004.

[84] R. M. Jarvis and R. Goodacre, "Surface-enhanced Raman scattering for the rapid discrimination of bacteria," *Faraday Discuss.*, vol. 132, pp. 281–292, 2006.

[85] M. C. Demirel *et al.*, "Bio-organism sensing via surface enhanced Raman spectroscopy on controlled metal / polymer nanostructured substrates," *Biointerphases*, vol. 4, no. 2, pp. 35–41, 2009.

[86] A. E. Grow, L. L. Wood, J. L. Claycomb, and P. A. Thompson, "New biochip technology for label-free detection of pathogens and their toxins," *J. Microbiol. Methods*, vol. 53, no. 2, pp. 221–233, 2003.

[87] M. Knauer, N. P. Ivleva, X. Liu, R. Niessner, and C. Haisch, "Surface-enhanced Raman scattering-based label-free microarray readout for the detection of microorganisms," *Anal. Chem.*, vol. 82, no. 7, pp. 2766–2772, 2010.

[88] K. C. Schuster, I. Reese, E. Urlaub, J. R. Gapes, and B. Lendl, "Multidimensional Information on the Chemical Composition of Single Bacterial Cells by Confocal Raman Microspectroscopy," *Anal. Chem.*, vol. 72, no. 22, pp. 5529–5534, 2000.

[89] S. M. Ede, L. M. Hafner, and P. M. Fredericks, "Structural Changes in the Cells of Some Bacteria During Population Growth : A Fourier Transform Infrared – Attenuated Total Re ectance Study," *Appl. Spectrosc.*, vol. 58, no. 3, pp. 317–322,

2004.

[90] M. F. Escoriza, J. M. Vanbriesen, S. Stewart, and J. Maier, “Studying Bacterial Metabolic States Using Raman Spectroscopy,” *Appl. Spectrosc.*, vol. 60, no. 9, pp. 971–976, 2006.

[91] J. De Gelder, K. De Gussem, P. Vandenabeele, P. De Vos, and L. Moens, “Methods for extracting biochemical information from bacterial Raman spectra : An explorative study on Cupriavidus metallidurans,” *Anal. Chim. Acta*, vol. 585, no. 2, pp. 234–240, 2007.

[92] L. Baek, P. Christensen, H. Vlassara, and L. S. A. Nielsen, “Endotoxin-Stimulated Human Monocyte Secretion of Interleukin 1 , Tumour Necrosis Factor Alpha , and Prostaglandin E2 Shows Stable Interindividual Differences,” *Scand. J. Immunol.*, vol. 27, no. 6, pp. 705–716, 1988.

[93] J. Guicheteau, L. Argue, D. Emge, A. Hyre, M. Jacobson, and S. Christesen, “Bacillus Spore Classification via Surface-Enhanced Raman Spectroscopy and Principal Component Analysis,” *Appl. Spectrosc.*, vol. 62, no. 3, pp. 267–272, 2008.

[94] M. F. Escoriza, J. M. V. A. N. Briesen, S. Stewart, and J. Maier, “Raman Spectroscopic Discrimination of Cell Response to Chemical and Physical Inactivation,” *Appl. Spectrosc.*, vol. 61, no. 8, pp. 812–823, 2007.

[95] T. Liu *et al.*, “A High Speed Detection Platform Based on Surface- Enhanced Raman Scattering for Monitoring Antibiotic- Induced Chemical Changes in Bacteria Cell Wall,” *PLoS One*, vol. 4, no. 5, 2009.

[96] C. Mustafa, M. Kahraman, and K. Keserog, “On Sample Preparation for Surface-Enhanced Raman Scattering ( SERS ) of Bacteria and the Source of Spectral Features of the Spectra,” *Appl. Spectrosc.*, vol. 65, no. 5, pp. 500–506, 2011.

[97] López-Díez, E. Consuelo, C. L. Winder, L. Ashton, F. Currie, and R. Goodacre, “Monitoring the Mode of Action of Antibiotics Using Raman Spectroscopy : Investigating Subinhibitory Effects of Amikacin on Pseudomonas aeruginosa,” *Anal. Chem.*, vol. 77, no. 9, pp. 2901–2906, 2005.

[98] E. Avci, N. S. Kaya, G. Ucankus, and M. Culha, “Discrimination of urinary tract infection pathogens by means of their growth profiles using surface enhanced

Raman scattering," *Anal. Bioanal. Chem.*, vol. 407, no. 27, pp. 8233–8241, 2015.

[99] D. Yang, H. Zhou, N. E. Dina, and C. Haisch, "Portable bacteria-capturing chip for direct surfaceenhanced Raman scattering identification of urinary tract infection pathogens," *R. Soc. Open Sci.*, vol. 5, no. 9, 2018.

[100] N. Tien *et al.*, "Diagnosis of bacterial pathogens in the urine of urinary-tract-infection patients using surface-enhanced Raman spectroscopy," *Molecules*, vol. 23, no. 12, pp. 1–14, 2018.

[101] M. Yogesha, K. Chawla, A. Bankapur, M. Acharya, J. S. D'Souza, and S. Chidangil, "A micro-Raman and chemometric study of urinary tract infection-causing bacterial pathogens in mixed cultures," *Anal. Bioanal. Chem.*, vol. 411, no. 14, pp. 3165–3177, 2019.

[102] W. R. Premasiri, Y. Chen, P. M. Williamson, D. C. Bandarage, C. Pyles, and L. D. Ziegler, "Rapid urinary tract infection diagnostics by surface-enhanced Raman spectroscopy (SERS): identification and antibiotic susceptibilities," *Anal. Bioanal. Chem.*, vol. 409, no. 11, pp. 3043–3054, 2017.

[103] U. Neugebauer, P. Rösch, and J. Popp, "Raman spectroscopy towards clinical application: Drug monitoring and pathogen identification," *Int. J. Antimicrob. Agents*, vol. 46, pp. S35–S39, 2015.

[104] K. Yang *et al.*, "Rapid Antibiotic Susceptibility Testing of Pathogenic Bacteria Using Heavy-Water-Labeled Single-Cell Raman Spectroscopy in Clinical Samples," *Anal. Chem.*, vol. 91, no. 9, pp. 6296–6303, 2019.

[105] A. Subasi and M. I. Gursoy, "EEG signal classification using PCA, ICA, LDA and support vector machines," *Expert Syst. Appl.*, vol. 37, no. 12, pp. 8659–8666, 2010.

[106] A. J. Izenman, "Introduction to Random-Matrix Theory," pp. 1–25, 2008.

[107] M. Sattlecker, N. Stone, and C. Bessant, "Assessment of robustness and transferability of classification models built for cancer diagnostics using Raman spectroscopy," *J. Raman Spectrosc.*, vol. 42, no. 5, pp. 897–903, 2011.

[108] "RPubs - Unsupervised Learning with HCA." [Online]. Available: https://rpubs.com/mpfoley73/489493. [Accessed: 23-Apr-2020].

[109] "KNN Classification." [Online]. Available: https://www.saedsayad.com/k_nearest_neighbors.htm. [Accessed: 23-Apr-2020].

[110] "The Mathematics Behind Principal Component Analysis." [Online]. Available: https://towardsdatascience.com/the-mathematics-behind-principal-component-analysis-fff2d7f4b643. [Accessed: 12-Dec-2019].

[111] "Chapter 4 PLS - Discriminant Analysis (PLS-DA) | mixOmics vignette." [Online]. Available: https://mixomicsteam.github.io/Bookdown/plsda.html. [Accessed: 23-Apr-2020].

[112] I. T. Olliffe and J. Cadima, "Principal Component Analysis, Second Edition," *Philos. Trans. R. Soc. A Math. Phys. Eng. Sci.*, vol. 374, no. 2065, p. 20150202, 2016.

[113] L. Petersen, P. Minkkinen, and K. H. Esbensen, "Representative sampling for reliable data analysis : Theory of Sampling," vol. 77, pp. 261–277, 2005.

[114] "Leave-one-out cross-validation – EFavDB." [Online]. Available: http://efavdb.com/leave-one-out-cross-validation/. [Accessed: 12-Dec-2019].

[115] "MANOVA - Statistics Solutions." [Online]. Available: https://www.statisticssolutions.com/directory-of-statistical-analyses-manova-analysis/. [Accessed: 12-Dec-2019].

[116] B. D. Beier, R. G. Quivey, and A. J. Berger, "Identification of different bacterial species in biofilms using confocal Raman microscopy," *J. Biomed. Opt.*, vol. 15, no. 6, p. 066001, 2010.

[117] W. R. Premasiri, Y. Gebregziabher, and L. D. Ziegler, "On the Difference Between Surface-Enhanced Raman Scattering ( SERS ) Spectra of Cell Growth Media and Whole Bacterial Cells," *Appl. Spectrosc.*, vol. 65, no. 5, pp. 493–499, 2011.

[118] A. Bombalska *et al.*, "Classification of the biological material with use of FTIR spectroscopy and statistical analysis," *Spectrochim. Acta - Part A Mol. Biomol. Spectrosc.*, vol. 78, no. 4, pp. 1221–1226, 2011.

[119] R. M. Jarvis, R. Goodacre, P. O. Box, S. Street, and M. Manchester, "Discrimination of Bacteria Using Surface-Enhanced Raman Spectroscopy," *Anal.*

*Chem.*, vol. 76, no. 1, pp. 40–47, 2004.

[120] R. M. Jarvis and R. Goodacre, "Ultra-violet resonance Raman spectroscopy for the rapid discrimination of urinary tract infection bacteria," *FEMS Microbiol. Lett.*, vol. 232, no. 2, pp. 127–132, 2004.

[121] B. Rajwa *et al.*, "Discovering the Unknown : Detection of Emerging Pathogens Using a Label-Free Light-Scattering System," *Cytom. Part A*, vol. 77, no. 12, pp. 1103–1112, 2010.

[122] "Merck | Life Science | Industrial & Lab Chemicals | eShop." [Online]. Available: http://www.merckmillipore.com/INTL/en. [Accessed: 12-Dec-2019].

[123] "Laboratory Filtration Solutions and Equipment | Sterlitech." [Online]. Available: https://www.sterlitech.com/. [Accessed: 12-Dec-2019].

[124] "Ultrapure water." [Online]. Available: https://www.lenntech.com/industries/ultrapure-water.htm. [Accessed: 12-Dec-2019].

[125] "Spectroscopy | Instrumentation | Solutions | Spectrometer Manufacturer." [Online]. Available: https://bwtek.com/. [Accessed: 12-Dec-2019].

[126] "Transmission Electron Microscopy (TEM)." [Online]. Available: https://warwick.ac.uk/fac/sci/physics/current/postgraduate/regs/mpagswarwick/ex5/techniques/structural/tem/. [Accessed: 28-May-2020].

[127] P. C. Lee and D. Melsel, "Adsorption and Surface-Enhanced Raman of Dyes on Silver and Gold Sols1," *J. Phys. Chem.*, vol. 86, no. 17, pp. 3391–3395, 1982.

[128] A. Kyriakides, E. Kastanos, K. Hadjigeorgiou, and C. Pitris, "Classification of Raman spectra using the correlation kernel," *J. Raman Spectrosc.*, vol. 42, no. 5, pp. 904–909, 2011.

[129] A. Y. Coban, B. Ekinci, and B. Durupinar, "A multidrug efflux pump inhibitor reduces Fluoroquinolone resistance in Pseudomonas aeruginosa isolates," *Chemotherapy*, vol. 50, no. 1, pp. 22–26, 2004.

# APPENDIX A

**Liquid Antibiograms**

**A. Amoxil**

| MIC (μg/ml) | Interpretation |
|---|---|
| ≤ 8 | Susceptible = S |
| > 8 | Resistant = R |

| Amoxil (μg/ml) / Bacteria | 32 | 16 | 8 | 4 | Final resistance or susceptibility of bacteria |
|---|---|---|---|---|---|
| **Citrobacter 1** | R | R | R | R | R |
| **Citrobacter 2** | R | R | R | R | R |
| **Citrobacter 3** | R | R | R | R | R |
| **Citrobacter4** | R | R | R | R | R |
| **Citrobacter 7** | R | R | R | R | R |
| **Citrobacter8** | R | R | R | R | R |
| **Citrobacter 9** | R | R | R | R | R |
| **Citrobacter 10** | R | R | R | R | R |
| **Citrobacter 11** | R | R | R | R | R |
| **Citrobacter 12** | R | R | R | R | R |
| **Citrobacter 13** | R | R | R | R | R |
| **Citrobacter 14** | R | R | R | R | R |
| **Citrobacter 15** | R | R | R | R | R |
| **Citrobacter 21** | R | R | R | R | R |
| **Citrobacter 22** | R | R | R | R | R |
| **Citrobacter 23** | R | R | R | R | R |
| **Citrobacter 24** | R | R | R | R | R |
| | | | | | |
| **Proteus 2** | R | R | R | R | R |
| **Proteus 3** | R | R | R | R | R |
| **Proteus 4** | S | S | S | S | S |
| **Proteus 5** | S | S | S | S | S |
| **Proteus 6** | S | S | R | R | R |
| **Proteus 7** | R | R | R | R | R |
| **Proteus 8** | R | R | R | R | R |
| **Proteus 9** | R | R | R | R | R |
| **Proteus 10** | R | R | R | R | R |
| **Proteus 11** | R | R | R | R | R |
| **Proteus 12** | R | R | R | R | R |
| **Proteus 13** | R | R | R | R | R |
| **Proteus 16** | S | S | S | S | S |
| **Proteus 17** | S | S | S | S | S |

| | | | | | |
|---|---|---|---|---|---|
| **Proteus 18** | S | S | S | R | S |
| **Proteus 19** | S | S | S | S | S |
| **Proteus 20** | R | R | R | R | R |
| **Proteus 21** | R | R | R | R | R |
| **Proteus 22** | S | S | S | S | S |
| **Proteus 23** | R | R | R | R | R |
| | | | | | |
| **Klebsiella 1** | R | R | R | R | R |
| **Klebsiella 2** | R | R | R | R | R |
| **Klebsiella 3** | R | R | R | R | R |
| **Klebsiella 4** | R | R | R | R | R |
| **Klebsiella 22** | R | R | R | R | R |
| **Klebsiella 25** | R | R | R | R | R |
| **Klebsiella 28** | R | R | R | R | R |
| | | | | | |
| **E.coli 2** | S | S | S | S | S |
| **E.coli 3** | S | S | S | S | S |
| **E.coli 4** | R | R | R | R | R |
| **E.coli 5** | S | S | S | R | S |
| **E.coli 6** | R | R | R | R | R |
| **Ecoli 10** | S | S | S | S | S |
| **E.coli 11** | R | R | R | R | R |
| **E.coli 12** | R | R | R | R | R |
| **E.coli 13** | R | R | R | R | R |
| **E.coli 14** | R | R | R | R | R |
| **E.coli 15** | R | R | R | R | R |
| **E.coli 20** | R | R | R | R | R |
| **E.coli 28** | S | R | R | R | R |
| **E.coli 30** | S | R | R | R | R |
| **E.coli 31** | S | S | R | R | R |
| **E.coli 34** | S | S | S | S | S |
| | | | | | |
| **Enterobacter1** | R | R | R | R | R |
| **Enterobacter4** | R | R | R | R | R |
| **Enterobacter5** | R | R | R | R | R |
| **Enterobacter6** | R | R | R | R | R |
| **Enterobacter7** | R | R | R | R | R |
| **Enterobacter8** | R | R | R | R | R |
| **Enterobacter10** | R | R | R | R | R |
| **Enterobacter11** | R | R | R | R | R |
| **Enterobacter12** | R | R | R | R | R |
| **Enterobacter13** | R | R | R | R | R |
| **Enterobacter14** | R | R | R | R | R |

| **Bacteria** | **Resistant** | **Sensitive** |
|---|---|---|
| **Citrobacter** | **17** | **0** |

| | | |
|---|---|---|
| **Proteus** | **13** | **7** |
| **Klebsiella** | **7** | **0** |
| **E.coli** | **11** | **5** |
| **Enterobacteur** | **11** | **0** |
| **Total** | **59** | **12** |

**→ The antibiograms with SERS have been implemented with concentration 8μg/ml.**

**B. Augmentin**

| MIC (μg/ml) | Interpretation |
|---|---|
| ≤ 18 | Susceptible = S |
| > 18 | Resistant = R |

| **Augmentin (μg/ml)** **Bacteria** | **36** | **18** | **9** | **4.5** | **Final resistance or susceptibility of bacteria** |
|---|---|---|---|---|---|
| **Citrobacter 1** | S | S | S | R | S |
| **Citrobacter 2** | S | S | R | R | S |
| **Citrobacter 3** | S | S | R | R | S |
| **Citrobacter 4** | S | S | S | R | S |
| **Citrobacter 7** | S | S | S | S | S |
| **Citrobacter 8** | S | R | R | R | R |
| **Citrobacter 9** | S | R | R | R | R |
| **Citrobacter 10** | S | S | S | S | S |
| **Citrobacter 11** | R | R | R | R | R |
| **Citrobacter 12** | S | R | R | R | R |
| **Citrobacter 13** | S | S | R | R | S |
| **Citrobacter 14** | R | R | R | R | R |
| **Citrobacter 15** | S | S | R | R | S |
| **Citrobacter 21** | S | S | S | S | S |
| **Citrobacter 22** | S | S | S | R | S |
| **Citrobacter 23** | S | S | S | S | S |
| **Citrobacter 24** | S | R | R | R | R |
| | | | | | |
| **Proteus 2** | S | S | R | R | S |
| **Proteus 3** | R | R | R | R | R |
| **Proteus 4** | S | S | S | S | S |
| **Proteus 5** | S | S | S | S | S |
| **Proteus 6** | S | S | R | R | S |
| **Proteus 7** | R | R | R | R | R |
| **Proteus 8** | R | R | R | R | R |
| **Proteus 9** | R | R | R | R | R |
| **Proteus 10** | R | R | R | R | R |
| **Proteus 11** | S | S | R | R | S |

| | | | | | |
|---|---|---|---|---|---|
| **Proteus 12** | R | R | R | R | R |
| **Proteus 13** | S | S | R | R | S |
| **Proteus 16** | S | S | S | S | S |
| **Proteus 17** | S | S | S | S | S |
| **Proteus 18** | S | S | S | S | S |
| **Proteus 19** | S | S | S | S | S |
| **Proteus 20** | S | S | S | S | S |
| **Proteus 21** | S | R | R | R | R |
| **Proteus 22** | S | S | S | S | S |
| **Proteus 23** | S | S | S | R | S |
| | | | | | |
| **Klebsiella 1** | R | R | R | R | R |
| **Klebsiella 2** | S | S | S | S | S |
| **Klebsiella 3** | S | S | S | R | S |
| **Klebsiella 4** | S | S | S | R | S |
| **Klebsiella 22** | S | S | S | S | S |
| **Klebsiella 25** | S | S | S | S | S |
| **Klebsiella 28** | S | S | S | S | S |
| | | | | | |
| **E.coli 2** | S | S | S | S | S |
| **E.coli 3** | S | S | S | S | S |
| **E.coli 4** | R | R | R | R | R |
| **E.coli 5** | S | S | S | S | S |
| **E.coli 6** | S | S | S | S | S |
| **E.coli 10** | S | S | S | S | S |
| **E.coli 11** | S | R | R | R | R |
| **E.coli 12** | S | S | R | R | S |
| **E.coli 13** | S | S | R | R | S |
| **E.coli 14** | S | S | R | R | S |
| **E.coli 15** | S | S | S | R | S |
| **E.coli 20** | S | R | R | R | R |
| **E.coli 28** | S | S | S | R | S |
| **E.coli 30** | S | S | S | S | S |
| **E.coli 31** | S | S | S | S | S |
| **E.coli 34** | S | S | S | R | S |
| | | | | | |
| **Enterobacter1** | R | R | R | R | R |
| **Enterobacter4** | R | R | R | R | R |
| **Enterobacter5** | R | R | R | R | R |
| **Enterobacter6** | R | R | R | R | R |
| **Enterobacter7** | R | R | R | R | R |
| **Enterobacter8** | R | R | R | R | R |
| **Enterobacter9** | R | R | R | R | R |
| **Enterobacter10** | R | R | R | R | R |
| **Enterobacter11** | R | R | R | R | R |
| **Enterobacter12** | S | S | S | S | S |

| | | | | | |
|---|---|---|---|---|---|
| **Enterobacter13** | R | R | R | R | R |
| **Enterobacter14** | R | R | R | R | R |

| Bacteria | Resistant | Sensitive |
|---|---|---|
| **Citrobacter** | **6** | **11** |
| **Proteus** | **7** | **13** |
| **Klebsiella** | **1** | **6** |
| **E.coli** | **3** | **13** |
| **Enterobacteur** | **11** | **1** |
| **Total** | **28** | **44** |

**→ The antibiograms with SERS have been implemented with concentration Augmentin 18µg/ml.**

**C. Cefaclor**

| MIC (µg/ml) | Interpretation |
|---|---|
| ≤ 8 | Susceptible = S |
| 16 | Intermediate = I |
| > 32 | Resistant = R |

| Cefaclor (µg/ml) / Bacteria | 64 | 32 | 16 | 8 | 4 | Final resistance or susceptibility of bacteria |
|---|---|---|---|---|---|---|
| **Citrobacter 7** | S | S | S | R | R | I |
| **Citrobacter 10** | S | S | S | R | R | I |
| **Citrobacter 21** | S | S | S | R | R | I |
| **Citrobacter 22** | S | S | R | R | R | R |
| **Citrobacter 23** | S | S | S | R | R | I |
| | | | | | | |
| **Proteus 4** | S | S | S | R | R | I |
| **Proteus 5** | S | S | S | S | R | S |
| **Proteus 11** | R | R | R | R | R | R |
| **Proteus 12** | R | R | R | R | R | R |
| **Proteus 22** | S | S | S | R | R | I |
| | | | | | | |
| **Klebsiella 1** | R | R | R | R | R | R |
| **Klebsiella 2** | R | R | R | R | R | R |
| **Klebsiella 22** | R | R | R | R | R | R |
| **Klebsiella 25** | S | R | R | R | R | R |
| **Klebsiella 28** | S | S | R | R | R | R |
| | | | | | | |
| **E.coli 2** | S | S | R | R | R | R |

| | | | | | | |
|---|---|---|---|---|---|---|
| **E.coli 3** | S | S | R | R | R | R |
| **Ecoli 10** | S | S | S | R | R | I |
| **E.coli 28** | R | R | R | R | R | R |
| **E.coli 30** | S | S | S | S | S | S |
| **E.coli 31** | S | S | R | R | R | R |
| **E.coli 34** | R | R | R | R | R | R |

**→ The antibiograms with SERS have been implemented with concentration cefaclor 8μg/ml.**

**D. Cefuroxime**

| MIC (μg/ml) | Interpretation |
|---|---|
| ≤ 8 | Susceptible = S |
| > 8 | Resistant = R |

| **Cefuroxime (μg/ml)** **Bacteria** | **32** | **16** | **8** | **4** | **Final resistance or susceptibility of bacteria** |
|---|---|---|---|---|---|
| **Citrobacter 1** | **S** | **R** | **R** | **R** | **R** |
| **Citrobacter 2** | **S** | **S** | **S** | **R** | **S** |
| **Citrobacter 3** | **S** | **S** | **S** | **R** | **S** |
| **Citrobacter 4** | **S** | **S** | **S** | **S** | **S** |
| **Citrobacter 7** | **S** | **S** | **S** | **R** | **S** |
| **Citrobacter 8** | **S** | **S** | **R** | **R** | **R** |
| **Citrobacter 9** | **S** | **R** | **R** | **R** | **R** |
| **Citrobacter 10** | **S** | **S** | **S** | **R** | **S** |
| **Citrobacter 11** | **S** | **R** | **R** | **R** | **R** |
| **Citrobacter 12** | **S** | **S** | **S** | **S** | **S** |
| **Citrobacter 13** | **S** | **S** | **S** | **R** | **S** |
| **Citrobacter 14** | **S** | **R** | **R** | **R** | **R** |
| **Citrobacter 15** | **S** | **R** | **R** | **R** | **R** |
| **Citrobacter 21** | **S** | **S** | **R** | **R** | **R** |
| **Citrobacter 22** | **S** | **R** | **R** | **R** | **R** |
| **Citrobacter 23** | **S** | **S** | **S** | **R** | **S** |
| **Citrobacter 24** | **S** | **R** | **R** | **R** | **R** |
| | | | | | |
| **Proteus 2** | **S** | **S** | **S** | **R** | **S** |
| **Proteus 3** | **S** | **R** | **R** | **R** | **R** |
| **Proteus 4** | **S** | **S** | **S** | **S** | **S** |
| **Proteus 5** | **S** | **S** | **S** | **S** | **S** |
| **Proteus 6** | **S** | **S** | **S** | **R** | **S** |
| **Proteus 7** | **R** | **R** | **R** | **R** | **R** |
| **Proteus 8** | **S** | **S** | **S** | **R** | **S** |
| **Proteus 9** | **S** | **R** | **R** | **R** | **R** |

| | | | | | |
|---|---|---|---|---|---|
| Proteus 10 | S | S | S | S | S |
| Proteus 11 | S | S | S | S | S |
| Proteus 12 | S | S | R | R | R |
| Proteus 13 | S | S | S | S | S |
| Proteus 16 | S | S | S | S | S |
| Proteus 17 | S | S | S | S | S |
| Proteus 18 | R | R | R | R | R |
| Proteus 19 | S | S | S | S | S |
| Proteus 20 | S | S | S | R | S |
| Proteus 21 | S | S | S | S | S |
| Proteus 22 | S | S | S | S | S |
| Proteus 23 | S | S | S | S | S |
| | | | | | |
| Klebsiella 1 | R | R | R | R | R |
| Klebsiella 2 | R | R | R | R | R |
| Klebsiella 3 | S | S | R | R | R |
| Klebsiella 4 | S | S | R | R | R |
| Klebsiella 22 | S | S | S | R | S |
| Klebsiella 25 | S | S | S | R | S |
| Klebsiella 28 | S | S | R | R | R |
| | | | | | |
| E.coli 2 | S | S | S | R | S |
| E.coli 3 | S | S | S | R | S |
| E.coli 4 | S | R | R | R | R |
| E.coli 5 | S | S | S | R | S |
| E.coli 6 | S | S | R | R | R |
| E.coli 10 | S | S | S | S | S |
| E.coli 11 | S | S | R | R | R |
| E.coli 12 | S | S | R | R | R |
| E.coli 13 | R | R | R | R | R |
| E.coli 14 | S | S | S | R | S |
| E.coli 15 | S | S | S | R | S |
| E.coli 20 | S | S | S | R | S |
| E.coli 28 | S | S | S | R | S |
| E.coli 30 | S | S | S | S | S |
| E.coli 31 | S | S | S | R | S |
| E.coli 34 | S | S | S | R | S |
| | | | | | |
| Enterobacter 1 | R | R | R | R | R |
| Enterobacter4 | S | S | R | R | R |
| Enterobacter5 | R | R | R | R | R |
| Enterobacter6 | S | R | R | R | R |
| Enterobacter7 | R | R | R | R | R |
| Enterobacter8 | S | R | R | R | R |
| Enterobacter9 | R | R | R | R | R |
| Enterobacter10 | S | R | R | R | R |

| | | | | | |
|---|---|---|---|---|---|
| Enterobacter11 | S | S | R | R | R |
| Enterobacter12 | S | S | S | R | S |
| Enterobacter13 | R | R | R | R | R |
| Enterobacter14 | S | R | R | R | R |

| Bacteria | Resistant | Sensitive |
|---|---|---|
| Citrobacter | 9 | 8 |
| Proteus | 5 | 15 |
| Klebsiella | 5 | 2 |
| E.coli | 5 | 11 |
| Enterobacteur | 11 | 1 |
| Total | 35 | 37 |

**→ The antibiograms with SERS have been implemented with concentration cefuroxime 8µg/ml.**

**E. Ciprofloxacin**

| MIC (µg/ml) | Interpretation |
|---|---|
| ≤ 0.5 | Susceptible = S |
| > 1 | Resistant = R |

| Cipro (µg/ml) / Bacteria | 2 | 1 | 0.5 | 0.25 | Final resistance or susceptibility of bacteria |
|---|---|---|---|---|---|
| Citrobacter 7 | S | S | S | S | S |
| Citrobacter 10 | S | S | S | S | S |
| Citrobacter 21 | S | S | S | S | S |
| Citrobacter 22 | S | S | S | S | S |
| Citrobacter 23 | S | S | S | S | S |
| | | | | | |
| Proteus 4 | S | S | S | S | S |
| Proteus 5 | S | S | S | S | S |
| Proteus 11 | R | R | R | R | R |
| Proteus 12 | S | S | S | S | S |
| Proteus 22 | S | S | S | S | S |
| | | | | | |
| Klebsiella 1 | R | R | R | R | R |
| Klebsiella 2 | R | R | R | R | R |
| Klebsiella 22 | S | S | S | S | S |
| Klebsiella 25 | S | S | S | S | S |
| Klebsiella 28 | S | R | R | R | R |
| | | | | | |
| E.coli 2 | S | S | S | S | S |

| | | | | | | | | | |
|---|---|---|---|---|---|---|---|---|---|
| **E.coli 3** | | S | | | S | | | S | |
| **Ecoli 10** | | S | | | S | | | S | |
| **E.coli 28** | | S | | | S | | | S | |
| **E.coli 30** | | S | | | S | | | S | |
| **E.coli 31** | | S | | | S | | | S | |
| **E.coli 34** | | S | | | S | | | S | |

**→ The antibiograms with SERS have been implemented with concentration ciprofloxacin 0.5µg/ml.**

**F. Ceftriaxone**

| MIC (µg/ml) | Interpretation |
|---|---|
| ≤ 8 | Susceptible = S |
| 16-32 | Intermediate = I |
| > 64 | Resistant = R |

| Ceftriaxone (µg/ml) Bacteria | 64 | 32 | 16 | 8 | 4 | Final resistance or susceptibility of bacteria |
|---|---|---|---|---|---|---|
| **Citrobacter 1** | S | S | S | R | R | R |
| **Citrobacter 2** | S | S | S | S | S | S |
| **Citrobacter 3** | | | | | | |
| **Citrobacter 4** | S | S | S | S | S | S |
| **Citrobacter 7** | S | S | S | S | S | S |
| **Citrobacter 8** | S | S | S | S | S | S |
| **Citrobacter 9** | S | S | S | S | S | S |
| **Citrobacter 10** | S | S | S | S | S | S |
| **Citrobacter 11** | S | S | S | S | S | S |
| **Citrobacter 12** | S | S | S | S | S | S |
| **Citrobacter 13** | S | S | S | S | S | S |
| **Citrobacter 14** | S | S | S | S | S | S |
| **Citrobacter 15** | S | S | S | S | S | S |
| **Citrobacter 21** | S | S | S | S | S | S |
| **Citrobacter 22** | S | S | S | S | R | S |
| **Citrobacter 23** | S | S | S | S | S | S |
| **Citrobacter 24** | S | S | S | S | S | S |
| | | | | | | |
| **Proteus 2** | S | S | S | S | S | S |
| **Proteus 3** | S | S | S | S | S | S |
| **Proteus 4** | S | S | S | S | S | S |
| **Proteus 5** | S | S | S | S | S | S |
| **Proteus 6** | S | S | S | S | S | S |
| **Proteus 7** | S | S | S | R | R | S |
| **Proteus 8** | S | S | S | S | S | S |

| | | | | | | |
|---|---|---|---|---|---|---|
| **Proteus 9** | S | S | S | S | S | S |
| **Proteus 10** | S | S | S | S | S | S |
| **Proteus 11** | S | S | S | S | S | S |
| **Proteus 12** | S | S | S | S | S | S |
| **Proteus 13** | S | S | S | S | S | S |
| **Proteus 16** | S | S | S | S | S | S |
| **Proteus 17** | S | S | S | S | S | S |
| **Proteus 18** | S | S | S | S | S | S |
| **Proteus 19** | S | S | S | S | S | S |
| **Proteus 20** | S | S | S | S | S | S |
| **Proteus 21** | S | S | S | S | S | S |
| **Proteus 22** | S | S | S | S | S | S |
| **Proteus 23** | S | S | S | S | S | S |
| | | | | | | |
| **Klebsiella 1** | R | R | R | R | R | R |
| **Klebsiella 2** | S | S | S | S | S | S |
| **Klebsiella 22** | S | S | S | S | S | S |
| **Klebsiella 25** | S | S | S | S | S | S |
| **Klebsiella 28** | S | S | S | S | S | S |
| | | | | | | |
| **E.coli 2** | S | S | S | S | S | S |
| **E.coli 3** | S | S | S | S | S | S |
| **E.coli 4** | S | S | S | S | S | S |
| **E.coli 5** | S | S | S | S | S | S |
| **E.coli 6** | S | S | S | S | S | S |
| **E.coli 10** | S | S | S | S | S | S |
| **E.coli 11** | S | S | S | S | S | S |
| **E.coli 12** | S | S | S | S | S | S |
| **E.coli 13** | S | S | S | S | S | S |
| **E.coli 14** | S | S | S | S | S | S |
| **E.coli 15** | S | S | S | S | S | S |
| **E.coli 20** | S | S | S | S | S | S |
| **E.coli 28** | S | S | S | S | S | S |
| **E.coli 30** | S | S | S | S | S | S |
| **E.coli 31** | S | S | S | S | S | S |
| **E.coli 34** | S | S | S | S | S | S |
| | | | | | | |
| **Enterobacter1** | S | S | R | R | R | R |
| **Enterobacter4** | S | S | S | S | S | S |
| **Enterobacter5** | S | S | S | S | S | S |
| **Enterobacter6** | S | S | S | R | R | R |
| **Enterobacter7** | S | S | S | S | S | S |
| **Enterobacter8** | S | S | S | R | R | R |
| **Enterobacter9** | R | R | R | R | R | R |
| **Enterobacter10** | S | S | S | S | S | S |
| **Enterobacter11** | S | S | S | S | S | S |

| | | | | | | |
|---|---|---|---|---|---|---|
| **Enterobacterur 12** | S | S | S | S | S | S |
| **Enterobacter13** | R | R | R | R | R | R |
| **Enterobacter14** | S | S | S | S | S | S |

| Bacteria | Resistant | Sensitive |
|---|---|---|
| **Citrobacter** | **1** | **15** |
| **Proteus** | **0** | **20** |
| **Klebsiella** | **1** | **4** |
| **E.coli** | **0** | **16** |
| **Enterobacteur** | **5** | **7** |
| **Total** | **7** | **62** |

**→ The antibiograms with SERS have been implemented with concentration ceftriaxone 8µg/ml.**

**G. Cefazolin**

| MIC (µg/ml) | Interpretation |
|---|---|
| ≤ 16 | Susceptible = S |
| 32 | Intermediate = I |
| > 64 | Resistant = R |

| Cefazolin (µg/ml) / Bacteria | 64 | 32 | 16 | 8 | 4 | Final resistance or susceptibility of bacteria |
|---|---|---|---|---|---|---|
| **Citrobacter 7** | S | S | S | S | S | S |
| **Citrobacter 10** | S | S | S | S | S | S |
| **Citrobacter 21** | S | S | S | S | S | S |
| **Citrobacter 22** | S | S | R | R | R | I |
| **Citrobacter 23** | S | S | S | S | S | S |
| | | | | | | |
| **Proteus 4** | S | S | S | R | R | S |
| **Proteus 5** | S | S | S | R | R | S |
| **Proteus 11** | R | R | R | R | R | R |
| **Proteus 12** | R | R | R | R | R | R |
| **Proteus 22** | S | S | S | S | R | S |
| | | | | | | |
| **Klebsiella 1** | R | R | R | R | R | R |
| **Klebsiella 2** | S | S | R | R | R | I |
| **Klebsiella 22** | S | S | S | S | R | S |
| **Klebsiella 25** | S | S | S | S | R | S |
| **Klebsiella 28** | S | S | S | S | R | S |
| | | | | | | |
| **E.coli 2** | S | S | S | S | S | S |

| | | | | | | |
|---|---|---|---|---|---|---|
| **E.coli 3** | S | S | S | S | S | S |
| **Ecoli 10** | S | S | S | S | S | S |
| **E.coli 28** | S | S | S | S | S | S |
| **E.coli 30** | S | S | S | S | S | S |
| **E.coli 31** | S | S | S | S | S | S |
| **E.coli 34** | S | S | S | S | S | S |

**→ The antibiogrmas with SERS have been implemented with concentration cefazolin 16μg/ml.**

**H. Amikasin**

| MIC (μg/ml) | Interpretation |
|---|---|
| ≤ 8 | Susceptible = S |
| > 16 | Resistant = R |

| **Amikasin (μg/ml)** **Bacteria** | **32** | **16** | **8** | **4** | **Final resistance or susceptibility of bacteria** |
|---|---|---|---|---|---|
| **Citrobacter 1** | | | | | |
| **Citrobacter 2** | | | | | |
| **Citrobacter 3** | | | | | |
| **Citrobacter 4** | | | | | |
| **Citrobacter 7** | | | | | |
| **Citrobacter 8** | S | S | S | S | S |
| **Citrobacter 9** | S | S | R | R | R |
| **Citrobacter 10** | S | S | R | R | R |
| **Citrobacter 11** | S | S | S | R | S |
| **Citrobacter 12** | S | S | R | R | R |
| **Citrobacter 13** | S | S | S | S | S |
| **Citrobacter 14** | S | S | S | S | S |
| **Citrobacter 15** | S | S | S | S | S |
| **Citrobacter 21** | S | S | S | S | S |
| **Citrobacter 22** | S | S | S | S | S |
| **Citrobacter 23** | S | S | S | S | S |
| **Citrobacter 24** | S | S | S | S | S |
| | | | | | |
| **Proteus 2** | S | S | S | R | S |
| **Proteus 3** | S | S | S | R | S |
| **Proteus 4** | S | R | R | R | R |
| **Proteus 5** | R | R | R | R | R |
| **Proteus 6** | S | R | R | R | R |
| **Proteus 7** | S | R | R | R | R |
| **Proteus 8** | S | R | R | R | R |
| **Proteus 9** | S | R | R | R | R |
| **Proteus 10** | S | R | R | R | R |

| | | | | | |
|---|---|---|---|---|---|
| **Proteus 11** | S | S | R | R | R |
| **Proteus 12** | S | R | R | R | R |
| **Proteus 13** | R | R | R | R | R |
| **Proteus 16** | S | R | R | R | R |
| **Proteus 17** | S | R | R | R | R |
| **Proteus 18** | S | S | R | R | R |
| **Proteus 19** | S | R | R | R | R |
| **Proteus 20** | S | R | R | R | R |
| **Proteus 21** | S | R | R | R | R |
| **Proteus 22** | | | | | |
| **Proteus 23** | S | R | R | R | R |
| | | | | | |
| **Klebsiella 3** | S | S | S | R | S |
| **Klebsiella 4** | S | S | S | R | S |
| | | | | | |
| **E.coli 4** | S | S | S | R | S |
| **E.coli 5** | S | R | R | R | R |
| **E.coli 6** | S | S | S | R | S |
| **E.coli 11** | S | R | R | R | R |
| **E.coli 12** | S | R | R | R | R |
| **E.coli 13** | S | R | R | R | R |
| **E.coli 14** | S | R | R | R | R |
| **E.coli 15** | S | R | R | R | R |
| | | | | | |
| **Enterobacter1** | S | S | S | S | S |
| **Enterobacter4** | R | R | R | R | R |
| **Enterobacter5** | R | R | R | R | R |
| **Enterobacter6** | S | S | S | S | S |
| **Enterobacter7** | R | R | R | R | R |
| **Enterobacter8** | S | S | S | S | S |
| **Enterobacter9** | R | R | R | R | R |
| **Enterobacter10** | S | S | S | S | S |
| **Enterobacter11** | S | S | S | S | S |
| **Enterobacter12** | S | S | S | S | S |
| **Enterobacter13** | S | S | S | S | S |
| **Enterobacter14** | S | S | S | S | S |

| Bacteria | Resistant | Sensitive |
|---|---|---|
| **Citrobacter** | **3** | **9** |
| **Proteus** | **16** | **2** |
| **Klebsiella** | **0** | **2** |
| **E.coli** | **6** | **2** |
| **Enterobacteur** | **4** | **8** |
| **Total** | **29** | **23** |